

ABSTRACT

Title of Dissertation: Modeling Extended Fluid Objects in General Relativity

Conrad Schiff, Doctor of Philosophy, 2005

Dissertation directed by: Professor Charles W. Misner
Department of Physics

The purpose of this dissertation is to introduce and explore the notion of modeling extended fluid objects in numerical general relativity. These extended fluid objects, called Fat Particles, are proxies for compact hydrodynamic objects. Unlike full hydrodynamic models, we make the approximation that the details of the matter distribution are not as important as the gross motion of the Fat Particles center of mass and its contribution to the gravitational field. Thus we provide a semi-analytic model of matter for numerical simulations of Einstein's equations, which may help in modeling gravitational radiation from candidate sources.

Our approach to carrying out these investigations is to begin with a continuum variational principle, which yields the desired hydrodynamic and gravitational equations for ideal fluids. Following our analysis of the related numerical technique, Smoothed Particle Hydrodynamics (SPH), we apply a set of discretization and smoothing rules to obtain a discrete action. Subsequent variations yield the Fat Particle equations.

Our analysis of a classical ideal fluid demonstrated that a Newtonian Fat Particle is capable of remaining at rest while generating its own gravitational field. We then developed analogous principles for describing relativistic ideal fluids in both covariant

and ADM 3+1 forms. Using these principles, we developed analytic and numerical results from relativistic Fat Particle theory. We began with the Subscribe Only model, in which a Fat Particle of negligible mass moves in a fixed background metric. Corrections to its motion due to the extended nature of the Fat Particle, are obtained by summing metric contributions over its volume. We find a universal scaling law that describes the phase shift, relative to a test particle, that is independent of its size, shape, and distribution. We then show that finite-size effects eventually dominate radiation damping effects in describing the motion of a white dwarf around a more massive black hole. Finally, we derive the Publish and Subscribe model, which comprises a full back-reacting system. Comparison of the Fat Particle equations for a static, symmetric spacetime with their continuum analogs shows that the system supports a consistent density definition and holds promise for future development.

Modeling Extended Fluid Objects in General Relativity

by

Conrad Schiff

Dissertation submitted to the Faculty of the Graduate School of the
University of Maryland, College Park in partial fulfillment
of the requirements for the degree of
Doctor of Philosophy
2005

Advisory Committee:

Professor Charles W. Misner, Chairman/Advisor
Professor Dieter Brill
Professor David Levermore
Professor M. Coleman Miller
Professor Ho Jung Paik

© Copyright by
Conrad Schiff
2005

DEDICATION

This work is dedicated to my family without whose support I would have never been able to finish and above all to the good God for creating such a wonderful world to explore, to the Son for earning our salvation, and to the Spirit for bring understanding and wisdom.

ACKNOWLEDGEMENTS

My time working on this project was divided into two pieces - professional flight dynamicist at Goddard Space Flight Center by day and part-time graduate student by night. Needless to say, it has been a difficult juggling act on both sides. I acknowledge most of all Charlie Misner for his patience through the numerous delays caused by my work on the Microwave Anisotropy Probe (MAP), Global Precipitation Measurement (GPM), Magnetospheric Multi-Scale (MMS), James Webb Space Telescope (JWST) missions, and the MOMS proposal, competition and transition. His kindness and hospitality will always be appreciated. I also acknowledge the kind patience of Bob Sperling at a.i. solutions, Inc. Bob, like Charlie, has had to put up with numerous delays and has been gracious all along.

I would be remiss if I didn't make special mention of Daryl Carrington and Dave Rohrbaugh. The three of us were given MAP a year from launch with little design work done and no documentation. Without their assistance, the daunting task of re-analyzing and re-designing the launch trajectories and then preparing for launch would never have happened.

I would like to thank Ted Einstein for allowing to work with his group for a year - I learned a great deal about physics and computing. I also

thank M.S. Cramer, of Virginia Tech, for numerous emails helping me to gain a better understanding of fluid dynamics. Great appreciation goes out to David Fiske who helped immensely with my understanding of the state of affairs in numerical relativity and who lent much assistance in my struggles with L^AT_EX. Finally, my thanks go to Dave Rand who designed and built the machine on which the majority of the code was developed and run. It really screams Dave - thanks.

TABLE OF CONTENTS

List of Tables		vii
List of Figures		ix
1 Introduction		1
1.1 Introduction		1
1.2 Einstein’s Equations and the Prediction of Gravitational Radiation		4
1.3 Gravitational Wave Detection		7
1.4 Modeling the Inspiral		9
1.5 Notation and Conventions		11
2 Ideal Self-Gravitating Newtonian Fluids		14
2.1 Introduction		14
2.2 Euler’s Equation - Heuristic Derivation		17
2.3 Euler’ Equation - Variational Formalism		23
2.4 Newtonian Gravity		26
2.5 Kernel Estimation Techniques		27
2.6 Smoothed Particle Hydrodynamics		33
2.7 Classical Fat Particle Equations		38
3 ADM Vacuum Equations		41
3.1 Introduction		41
3.2 Spacetime Slicing		42
3.3 Gravitational Action in 3+1		51
3.4 Vacuum ADM Equations		53
4 Ideal Self-Gravitating Relativistic Fluids		60
4.1 Introduction		60
4.2 Point Particle Geodesics - Covariant Formalism		61
4.3 Relativistic Action for an Ideal Fluid - Covariant Formalism		63
4.3.1 Description of the Density		64
4.3.2 Action Principle		66
4.4 Point Particle Geodesics - ADM Formalism		71
4.5 Ideal Fluid - ADM Formalism		73

4.5.1	Density Revisited	73
4.5.2	3+1 Action	74
4.6	Solving the ADM Matter Equations	83
5	Relativistic Fat Particles	86
5.1	Introduction	86
5.2	Development of the Single Fat Particle - Subscribe Only Picture . . .	88
5.2.1	Equations of Motion	89
5.2.2	Numerical Implementation	90
5.2.3	Black Hole Metrics	94
5.2.4	Circular Orbit Initial Conditions	98
5.2.5	Stability	101
5.2.6	Convergence	101
5.2.7	Smoothing Choice - Phase Angle Tests	108
5.3	Finite-Size Corrections to the Motion of a Fat Particle	113
5.4	Fat Particles - Publish and Subscribe	121
6	Conclusion	130
A	Derivatives of Determinants	134
A.1	Variations of a Determinant	134
A.2	Variations of the Metric	136
A.3	Variations of a Jacobian and Other Associated Derivatives	136
	Bibliography	141
	Vita	154

LIST OF TABLES

2.1	Normalization factors and exact smoothed values for x^3 for the Misner n -kernels W_2 , W_3 , W_4 , and the Gaussian kernel W_G as defined in Eq. (2.46). The normalization for the Gaussian kernel is expressed by $\mathcal{N}_G = 3/(\text{erf}(3)\sqrt{\pi})$, where $\text{erf}(x) = 2/\sqrt{\pi} \int_0^x e^{-t^2} dt$ is the Gauss error function (see Section 5.10 of [4]) and $\mathcal{Q} = (1/6 - \exp(-9)\mathcal{N}_G/3)$	29
5.1	Conserved quantities, orbital frequency, and initial values of the four-velocity for a test particle circular orbit with initial position described by $y = z = 0$ and $x = r$ for STD or PG spacetimes and $x = R$ for the ISO spacetime. The parameter $C = \sqrt{4R^2 - 8MR + M^2}$	101
5.2	Estimates of absolute and relative uncertainties in the evaluation of the non-zero components of the right-hand side of the Fat Particle Subscribe Only equations and the energy, evaluated for both kernel and smoothed derivatives. The smoothed derivative (SD) computations introduce noise two orders of magnitude less than those introduced by the kernel derivative (KD) computations.	105
5.3	Estimation of the error between evaluating derivatives of the metric functions for kernel and smoothed derivatives using the R3G smoothing prescription.	107
5.4	A summary of the phase shift computations for ‘targeted’ Fat Particle orbits with smoothed derivatives. The targeting involved varying the in-plane components of the covariant velocity to achieve the exact value for the radius ($r = 18M$ for standard Schwarzschild coordinates and $R = 16.98528M$ for isotropic coordinates) and zero standard deviation.	110
5.5	The phase shift Δ measured as degrees per orbit for the test orbits listed in Table 5.4.	111
5.6	A summary of the phase shift computations for ‘targeted’ Fat Particle orbits with smoothed derivatives. The targeting involved varying the in-plane components of the covariant velocity to achieve the exact value for the radius ($r = 7M$ for standard Schwarzschild coordinates and $R = 5.958040M$ for isotropic coordinates) and zero standard deviation.	111
5.7	The phase shift, Δ , measured as degrees per orbit for the test orbits listed in Table 5.6.	112

5.8	Phase shifts Δ for a W_3 Fat Particle with $h = 1$ using the R3G smoothing prescription in both the STD and ISO metrics. Also shown are the ratios of these phase shifts compared to the ratios of the determinants of the three-metric γ	112
5.9	Value of the dimensionless parameter ξ which satisfies Eq. (5.59).	114

LIST OF FIGURES

1.1	The action of a gravitational wave on a ring of test masses. At t_0 , the wave, which propagates into the page, has not encountered the ring. At later times t_1 and t_2 , the waves passage through the ring has caused the masses to move in the plane perpendicular to the direction of propagation. The top sequence shows the $+$ polarization while the bottom one shows the \times polarization. (Adapted from Figure 9.1 in [110].)	5
1.2	Comparison between the Two Body problem in Newtonian physics and general relativity.	6
2.1	The kinematics of a single fluid element	18
2.2	The free body diagram for a single fluid element showing the net force due to pressure gradients ∇P due to the surrounding fluid	20
2.3	Schematic representation of the trajectory function. A parcel of fluid located at position \vec{a} in the initial data flows along the unique path $\vec{z}(\vec{a}, t)$ as time evolves.	24
2.4	Profiles of the one-dimensional form of the smoothing kernels W_2 , W_3 , W_4 of the Misner n -family of kernels and the Gaussian kernel W_G	30
2.5	Comparisons between exact and numerical estimates of the smoothed function x^3 for sets of points uniformly or random distributed in the interval $[-1, 1]$	31
2.6	The error between the exact and numerically estimated value of the smoothed function x^3 as a function of the number of points used in the computation.	32
2.7	The error between the exact and numerically estimated value of the smoothed function $\frac{\partial x^4}{\partial x}$ as a function of the number of points used in the computation.	33
3.1	The slicing of the spacetime manifold \mathcal{M} by spacelike hypersurfaces Σ_t as described in the text. The curve $\gamma_{\mathcal{P}}$ connects the distinct points \mathcal{P} , \mathcal{P}' , and \mathcal{P}'' in \mathcal{M} since each point shares a common coordinate label in each of the Σ_t , $\Sigma_{t'}$, and $\Sigma_{t''}$	43
5.1	Schematic representation of the data structures used in the Subscribe Only Fat Particle study. A three-dimensional array of pointers to <i>tensor++</i> objects serves as a discrete model of a three-dimensional hypersurface.	92

5.2	Numerical representation of a test particle geodesic in the standard Schwarzschild spacetime for a $r = 16M$ circular orbit; (a) Orbit trace in the $X - Y$ -plane, (b) fractional deviation of the energy H from its initial value, (c) fractional deviation of the z -component of the angular momentum L_z from its initial value, (d) fractional deviation of the orbital radius R from its initial value.	95
5.3	A typical example of a Fat Particle orbital evolution. This case corresponds to a nearly circular orbit at an STD radius of $r = 16M$ (here $M = 1$) integrated for 2.5 orbits: (a) Orbit trace in the $X - Y$ -plane, (b) fractional deviation of the energy H from its initial value, (c) fractional deviation of the z -component of the angular momentum L_z from its initial value, (d) fractional deviation of the orbital radius R from its initial value. Compare with Figure 5.2	102
5.4	The convergence of the right-hand side component for dy/dt for $r = 16$ using kernel derivatives (KD) for the bare smoothing prescription. The vertical line represents the difference between the maximum and minimum points on the curve.	104
5.5	The convergence of the right-hand side component for du/dt for $r = 16$ using kernel derivatives (KD) for the bare smoothing prescription. The vertical line represents the difference between the maximum and minimum points on the curve.	105
5.6	The convergence of the right-hand side component for dy/dt for $r = 16$ using smoothed derivatives (SD). The vertical line represents the difference between the maximum and minimum points on the curve.	106
5.7	The convergence of the right-hand side component for du/dt for $r = 16$ using smoothed derivatives (SD). The vertical line represents the difference between the maximum and minimum points on the curve.	106
5.8	A schematic representation of the expected phase shift between a Fat Particle and a test particle, starting together, each on a circular orbit of the same radius. A secular growth in the phase shift, denoted by Δ , is expected.	108
5.9	Targeting geometry in selecting the Fat Particle initial conditions that yield circular orbits.	109
5.10	Scaling plots for (a) Δ_{STD} (b) Δ_{STD}/h^2 (c) Δ_{ISO} and (d) Δ_{ISO}/h^2	114
5.11	Scaling plots for (a) Δ_{STD} (b) Δ_{STD}/ξ^2 (c) Δ_{ISO} and (d) Δ_{ISO}/ξ^2	115
5.12	Scaling plots for (a) Δ_{STD} (b) $\Delta_{STD}\gamma_{STD}$ (c) Δ_{ISO} and (d) $\Delta_{ISO}\gamma_{ISO}$	116
5.13	Scaling plot for Δ_{unit}	117
5.14	A comparison of the phase shift due to gravitational radiation to those due to finite size affects for the white dwarf/black hole system discussed in the text.	120
A.1	Schematic representation of the flow on the manifold \mathcal{M} due to the vector field \vec{V} . The point \mathcal{P} is mapped downstream an amount λ to the point \mathcal{Q}	138

Chapter 1

Introduction

1.1 Introduction

The purpose of this dissertation is to introduce and explore the notion of modeling extended fluid objects in numerical general relativity. These extended fluid objects, which we affectionately call Fat Particles, are stand-ins or proxies for compact hydrodynamic objects like neutron stars and white dwarfs. Unlike full hydrodynamic models, we make the approximation that the details of how the matter is distributed within the object are not as important as the overall gross motion of the Fat Particle's center of mass and its resulting contribution to the gravitational field. By making this approximation, we provide a semi-analytic model of matter for numerical simulations of Einstein's equations and, in doing so, help obviate some of the difficulties currently encountered in generating theoretical predictions of gravitational radiation from candidate sources such as the inspiral phase of a binary system.

Adding particle-like source terms or analytic prescriptions for the matter to three-dimensional numerical relativity is not a commonly pursued technique. In fact, the only other particle technique, of which I am aware, that attempts to fully model the coupled evolution of the matter and gravitational fields is the work by Mark Dubal [41]. Fortunately, one doesn't need to look far to find a large body of work on classical self-gravitating fluids that employs particle-based techniques. The popular computational approach, called Smoothed Particle Hydrodynamics (SPH), is often used to model Newtonian astrophysical problems. Conceptually, an SPH particle

represents the usual textbook definition of a fluid element - that is to say a parcel of fluid small enough that its thermodynamic properties are constant but large enough so that the details of its internal motion can be ignored. Each center is endowed with a finite size of characteristic length h and a smoothing kernel that allows the particle to communicate with the matter and fields that surround it. Moving from Newtonian SPH to relativistic Fat Particles requires careful investigation. First of all, the consequences of fattening a Newtonian SPH particle must be explored. Second, it must be established how to express a Fat Particle in a covariant way. Finally, since our ultimate goal is the modeling of gravitational radiation, we need to express the coupling between the fluid and the gravitational field in way that ensures that energy losses in one component are accompanied by energy gains elsewhere.

Our approach to carrying out these investigations while maintaining as high degree of rigor as possible is as follows: We begin by developing a continuum variational principle for both classical and relativistic ideal fluids which give the desired hydrodynamic and gravitational equations. We then develop discretization and smoothing rules to arrive at a discrete action. Taking the appropriate variations, we arrive at our Fat Particle equations. Finally, we analyze some analytic and numeric solutions to the resulting equations.

During the pursuit of this program we produced several significant accomplishments. Our development of a coupled approach to Newtonian SPH, where gravity and fluid degrees of freedom are treated on equal footing, yielded from first principles a justification for the standard SPH density expression. This expression has been the subject of some controversy and debate over the inclusion of the self-density contribution. We also demonstrated that the Newtonian Fat Particle is capable of remaining at rest while generating its own gravitational field. Thus the Fat Particle is dynamically immune to its own self-force, an important physical requirement for a feasible theory. With these Newtonian gravity results as a guide, we developed a variational principle for describing ideal fluid flow in the Lagrangian picture in both covariant and 3+1 forms. These principles not only aided us in our Fat Particle analysis but could be potential springboards for other works. We then developed

analytic and numerical results from relativistic Fat Particle theory. We began with the *Subscribe Only* model, in which a Fat Particle of negligible mass moves in a fixed background metric. Corrections to the motion, due to the extended nature of the Fat Particle, are obtained by summing metric contributions over its volume. Imposition of a simple physical requirement selects out a consistent covariant form of the smoothing prescription. Using this model, we were able to numerically estimate the finite-size contribution to the phase shift of a Fat Particle by comparing its motion to a test particle on the same circular orbit. We find a universal scaling law (going as $r^{-7/2}$ where r is the orbital radius) that describes the phase shift that is independent of its size, shape, and distribution. Applying the universal scaling law, we are able to show that finite-size effects eventually dominate radiation damping effects in describing the motion of a white dwarf around a more massive black hole. This result is of much physical interest since such sources will provide frequent signals to the LISA mission. Additionally, we confirmed that finite-size effects are dwarfed in importance to radiation damping in the inspiral of a binary neutron star system. This is the first strong field estimate of the finite-size effects on the motion of compact objects that we know of. Finally, we derive the *Publish and Subscribe* Fat Particle equations in general relativity. These equations comprise a full back-reacting system. Comparison of these equations for a static, symmetric spacetime with their continuum analogs shows that the system supports a consistent density definition that limits the contribution of the matter source in the ADM equations to the compact support of the kernel and which seems to hold promise for future development.

The remainder of this chapter is devoted to placing the material in proper physical and historical context. Section 1.2 provides a brief overview of the structure of Einstein's equations and the predictions of and the indirect observational evidence for gravitational radiation from the Hulse-Taylor Pulsar. Section 1.3 touches upon gravitational wave detection from astrophysical sources, such as a binary systems comprised of black holes, neutron stars, or white dwarfs. Due to the naturally small signals expected from these sources, detectors such as LIGO, LISA, GEO, VIRGO, and TAMA [73, 75, 48, 124, 120] are designed to use matched filtering to augment

observations with theoretical wave templates. In Section 1.4, we discuss some of the approaches that are currently pursued to develop these templates. Section 1.5 covers the notation that I employ. Chapter 2 presents the Fat Particle approach within the context of Newtonian physics. Chapters 3 and 4 deal with the development of the relativistic gravitational and ideal fluid actions, respectively. Chapter 5 covers the Fat Particle formalism, including its application to determining the finite-size corrections to the motion of a low-mass companion object in orbit around a more massive black hole. Chapter 6 brings this dissertation to a close with a conclusion and suggestions for future work. Some mathematical techniques that are used often in Chapters 2 - 5, but whose presentation would have interrupted the flow of the discussion, are covered in Appendix A.

1.2 Einstein's Equations and the Prediction of Gravitational Radiation

Despite the nearly 90 years that have elapsed from the introduction of general relativity by Einstein in 1915 [42], little is known about the totality of behavior that can emerge from his description of gravity. This lack of insight is not a discredit to the great number of people who have invested lifetimes exploring the content of the theory but rather a testament to the difficulties that they faced. The equations of general relativity are among the most difficult in mathematical physics [113], being comprised of 10 non-linear coupled partial differential equations. Each of the 10 functions generically depends on the four coordinates used to describe the spacetime and are subjected to sets of conditions and constraints inter-relating them.

Despite these difficulties, several important exact and approximate solutions exist. Amongst the most important of these are the predictions of the existence of black holes and the gravitational radiation. Gravitational waves are emitted by accelerating masses much in the way that electromagnetic radiation is produced by accelerating charges. Linearized Einstein theory clearly predicts that gravitational radiation propagates as a transverse wave that moves with the speed of light [89].

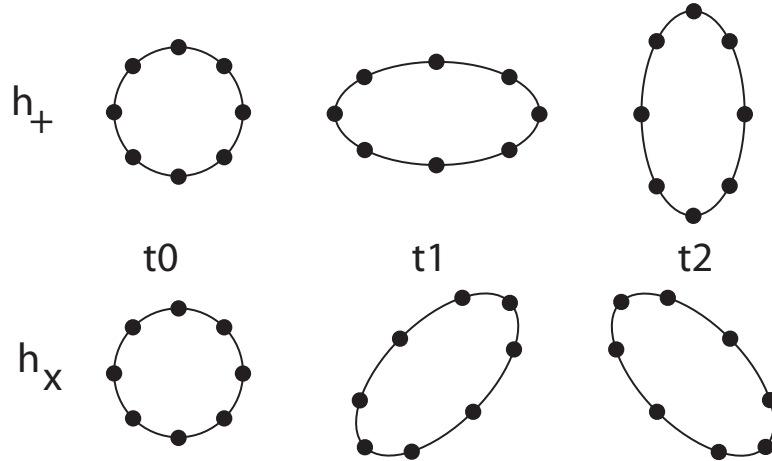


Figure 1.1: The action of a gravitational wave on a ring of test masses. At t_0 , the wave, which propagates into the page, has not encountered the ring. At later times t_1 and t_2 , the waves passage through the ring has caused the masses to move in the plane perpendicular to the direction of propagation. The top sequence shows the + polarization while the bottom one shows the \times polarization. (Adapted from Figure 9.1 in [110].)

The wave possesses two distinct polarizations that exert stretch forces on test masses that encounter the wave. Figure 1.1 shows the disturbances a ring of test particles experiences during the passage of a gravitational wave. The existence of gravitational radiation has many interesting implications. For example, the analog of the Kepler two-body problem has no known analytic solution in general relativity. The fundamental difference between the classical and relativistic descriptions of the two-body problem is that in the Kepler problem, Newtonian space and time comprises a fixed stage for the two bodies to perform their choreography. In Einstein's theory, the spacetime joins in the dynamics, interacting with the two bodies and in most circumstances carrying off energy and angular momentum from the system. Figure 1.2 shows this difference schematically. In the Newtonian case, the mechanical energy of the system is conserved and the bodies continue to orbit their center-of-mass indefinitely. In general relativity, the continuous acceleration of masses produces gravitational radiation that carries energy away causing the bodies to inspiral and eventually merge. This 'strange' aspect of Einstein's theory was seriously doubted

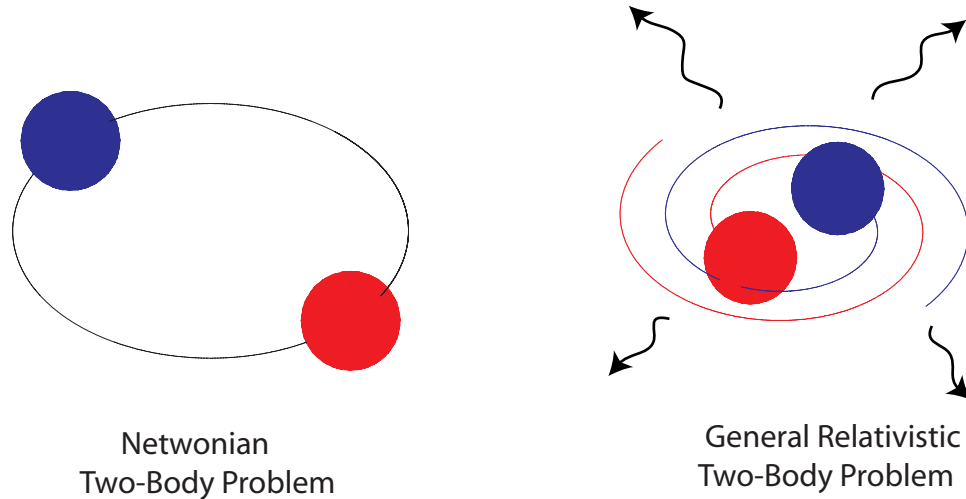


Figure 1.2: Comparison between the Two Body problem in Newtonian physics and general relativity.

decades after its prediction (see, for example, the opening discussion in Will and Wiseman [131]).

The situation changed dramatically in 1974, when Russell Hulse and Joseph Taylor found a binary neutron star system, PSR1913+16, in which one of the members was a pulsar [61, 62, 63]. Using the ‘beat’ of the pulsar as a natural clock to time the orbital motion and collecting data for over many years, they were able to show that the period of the orbit decreased in accordance to with the prediction of general relativity. In particular, they were able to determine the rate of change in the orbital period $\dot{P}_{OBS} = (-2.30 \pm 0.22) \times 10^{-12}$, comparing very well with the rate $\dot{P}_{GRQ} = (-2.403 \pm 0.005) \times 10^{-12}$ predicted by the quadrapole formula of general relativity [121]. The inference being that the loss in mechanical energy from the system is due to the energy carried off by gravitational waves. This result put to rest most doubt in the existence of gravitational waves and netted Taylor and Hulse the 1993 Nobel Prize in Physics.

Since that time, a handful of other binary neutron star systems have been observed, each providing a natural laboratory for testing the predictions of Einstein’s theory. Most recently, the double pulsar system PSR J0737-3039A/B was discovered [79]. Its unique parameters, including its distance from Earth, its orbital plane ori-

entation, and the time scale for geodetic precession of the pulsars' spin axes, require a higher order description of the relativistic effects and thus provide a more stringent test of general relativity.

1.3 Gravitational Wave Detection

Despite the success of Taylor and Hulse in applying general relativity to the pulsar PSR1913+16, direct Earth-bound detection of gravitational radiation has so far been elusive.¹ This is due to the fact that gravitational radiation is relatively weak, carrying off only a small fraction of the energy of a system. For example in the two-body evolution discussed above, the fraction of the ADM mass lost during the inspiral is $0.007 - 0.008M_{ADM}$ [28].

Thus special detectors, like the resonant detectors described by Hamilton [53] or first generation interferometers reviewed by Barish [6] have been built to find direct observational evidence of gravity waves and to begin to harness these waves for scientific research. We will focus on two such systems: the Laser Interferometer Gravitational-Wave Observatory (LIGO) [73]², and the formation-flying Laser Interferometer Space Antenna (LISA) [75].

LIGO is comprised of two separate observing facilities, one in Hanford, Washington and the other in Livingstone, Louisiana. Each facility is equipped with a laser interferometer with two perpendicular arms 4 km in length. Laser light is introduced into each arm from a beam splitter located at the corner where the arms join. Mirrors suspended at both ends of each arm keep light traveling back and forth in such a way that if the distance between each pair of mirrors is the same then all light impinging on the beam-splitter returns to the laser. Differences in the dis-

¹The current situation in gravitational wave detection is analogous to the period of time between Fermi's prediction of the existence of the neutrino and its discovery. While we have excellent inferential proof of the existence of gravitational radiation, direct observation is desired. (The author thanks CWM for this analogy.)

²Similar facilities to LIGO have been built internationally. Namely, the Italian-French VIRGO [124], the English-German GEO600 [48], and the Japanese TAMA [120].

tances between the pair of mirrors in one arm from the other disturb the destructive interference allowing some of the light to make it to a photodetector. Run by over 30 different control systems, LIGO must measure the movements of its mirrors to within one thousandth the diameter of a proton. Currently, the inspiral, merger, and ringdown of a binary compact object (black hole/black hole, black hole/neutron star, or neutron star/neutron star) system is the most promising source of gravitational radiation (see, *e.g.* [86]). Based on the detecting volume of first generation LIGO, the estimated event rates range from on the order of 1 event per year (BH-BH inspiral) to 1 event per millennium (NS-NS inspiral) [86].³ The sensitivity of LIGO (100 Hz - 1000 Hz)⁴, sets a limit on the amount of the inspiral that can be seen. It is expected that the signal from these events will last on the order of minutes.

LISA is made up of three spacecraft flying in formation in heliocentric orbit. The baseline orbit lags the Earth by 20 degrees and the individual spacecraft are spaced about it so that the inter-satellite distances (*i.e.*, the arm lengths of the interferometer) on the order of 4 million km. The frequency range of LISA is in the range of 10^{-4} - 10^{-1} Hz, opening up the possibility of detecting astrophysical sources to which LIGO is blind. In particular, tightly bound binary systems consisting of a compact object of a few solar masses and a supermassive black hole of (10^6 - 10^9) solar masses are very promising sources of gravitational radiation for LISA [47]. These events, termed *extreme mass ratio inspirals* (EMRI), are expected to start with the capture of a small mass object, like a white dwarf, into an eccentric orbit about a black hole [82]. Preferential emission of radiation at the periastron [105, 104] should eventually circularize the orbit followed by an adiabatic inspiral until the companion is swallowed by the black hole.

Despite their violence, the signal from these astrophysical sources will still be very weak upon reaching the Earth. All interferometers (LIGO, LISA, VIRGO, etc.) will require a supply of theoretical templates of expected gravitational radiation

³According to the report by Fritschel [45], second generation LIGO should increase its detecting volume 1000 fold concomitantly increasing the event rate of an inspiral to on the order of 1 per day.

⁴The lower limit on terrestrial observations is set at about 10 HZ due to seismic noise [76].

in order to perform matched filtering. Matched filtering is the technique in which the experimental signal is compared against a series of expected signals. From this comparison, an overlap value indicating the confidence that the signal matches the template is obtained. For an introduction to matched filtering, refer to Section 17 of the book by Wainstein and Zubakov [126].

1.4 Modeling the Inspiral

Since the relativistic description of the inspiral of a binary system evades exact solution, one must resort to either approximation methods, numerical modeling, or some combinations of both. Currently there are two avenues being actively explored. The post-Newtonian (PN) approximation techniques (reviewed in [19]) and numerical relativity (NR) (see, *e.g.*, the review in [71]).

The post-Newtonian (PN) computations, which have been developed to account for relativistic corrections to astrophysical hydrodynamics [31, 32, 35, 34, 33], have at their heart the assumptions that the gravitational fields are not too strong and that the velocities involved are not too fast. Expansions in powers of $1/c^2$, where c is the speed of light, yield perturbative corrections to linearized gravity [19]. Adaptation to the inspiral problem is achieved by essentially taking delta-function sources for the stress-energy tensor and there is a large body of work devoted to extracting field configurations, equations of motion, and radiation-reaction forces during the inspiral of a compact object binary [125, 106, 129, 22, 21, 26, 17, 131, 18, 115, 25, 130, 23, 102, 19, 24, 103, 20, 82]. However, the finite-size effects on the particles are necessarily ignored in this approach. The influence of finite-size effects on the motion of a black hole binary can be rejected immediately. However, this assumption needs more careful scrutiny for binaries involving neutron stars and white dwarfs. Blanchet [19], citing work from both classical and relativistic computations, asserts that finite-size effects, being of order 5PN, are ignorable for neutron star binaries but that in the case of non-compact (or moderately compact) objects like white dwarfs, the finite size effects dominate the radiation damping. Given these assumptions, it

is natural to ask how far these perturbative techniques can be pushed in determining templates for the interferometry observatories.⁵ In some sense, this is still an open question but it is generally believed that PN computations can be trusted at least until the velocities are of the order of $0.25 - 0.3c$ [27] if not further - perhaps even to the beginnings of the merger [20]. Regardless of exactly where these computations ultimately fail, many of the templates that are currently constructed are from direct PN computations [13, 40, 39, 37, 38].

Counterpoint to the post-Newtonian approach is the domain of numerical relativity (NR). This method places no limits on the strength of the fields, on the size of the velocities involved, or on the size of the matter sources (provided they are not point sources). By design, numerical relativity is meant to provide detailed theoretical predictions of the behavior of gravity in a strong-field regime [113, 112, 114, 28, 71]. Lehner marks the beginning of full numerical relativity in 1995 with the first attempts to model gravitational dynamics in three-dimensions without special symmetry. Initial work with gravitational waves [1, 2, 113, 112] was promising. However, progress towards modeling the inspiral and merge of binary systems, with the compact objects as black holes or neutron stars, was not rapid [112]. In 1999, very accurate simulations of binary systems were only possible for fairly short evolution times (less than $50M$, where M is the ADM mass of the system) [112]. By 2002, the length of stable simulations had increased to several $1000M$ [132]. Much of this improvement has come about for several reasons. First, a great deal of effort has been expended to developing improved formulations. The BSSN method achieves greater stability by using a conformal decomposition of the three-metric and by introducing additional variables (connection functions) [8, 132]. Doing so seems to remove much of the instability in the original ADM system by making the Ricci tensor look like an elliptical operator [67]. This success has sparked additional variants, such as the work by Laguna and Shoemaker [70]. Second, the community has gained a much deeper understanding of how to handle the gauge degrees of freedom represented by the

⁵Clearly these assumptions are well met for binaries like the Hulse-Taylor pulsar. However, the signal from these sources is too weak to be directly observed.

lapse and shift. A wide variety of prescriptions have been examined. These include ‘passive’ techniques such as maximal or algebraic slicings (‘1 +log’) [113, 112, 132], minimal distortion shift [28], minimal-strain gauge conditions [117, 122], and ‘active’ techniques like the gamma driver [132] and K-driver [114] controls. While definite strides are being made to increase the stability, there is still a great deal of technical hurdles that must be cleared.

One particular hurdle in the modeling of the NS/NS inspiral occurs when the neutron stars are moderately far separated (say, $20M$). These simulations have two characteristic sizes. On the short scale is the physical extent of each star ($3M$) and on a large scale the wavelength of the gravitational radiation ($90M$). Even assuming that the computational grid can sit fairly close to the source, generally the stars consume at most about 10% of the total volume. Capturing detail on this scale is a challenge to currently available computing resources and techniques like adaptive mesh-refinement [108], which help by lowering the required memory, are no panacea. Thus the probability of obtaining an alternative source of theoretical templates in the near term, even in the absence of the difficulties discussed in the preceding paragraph, is not very high.

It is against this backdrop that we introduce the Fat Particle model. We construct in this model a delta-function-like matter source (the smoothing kernel can be thought of as a member of a δ -sequence) to numerical relativity. Doing so, we are able to perform computations in strong field gravity that can not be attempted in either PN or pure finite-difference techniques.

1.5 Notation and Conventions

On the question of notation, it is probably best to recall Ralph Waldo Emerson when he said “A foolish consistency is the hobgoblin of little minds, adored by little statesmen and philosophers and divines. With consistency a great soul has simply nothing to do.” I have strived to create a consistent set of notation, however, for a variety of reasons, including typographical considerations, the desire to stay true

to the look and feel of various disciplines, and above all else clarity, several different notations co-exist in the text.

Indices for 4-dimensional tensors are always written as with Greek letters, such as μ , and range over the values $(0, 1, 2, 3)$. Correspondingly, 3-dimensional tensors are written with Latin letters, such as i and j , and range over the values $(1, 2, 3)$. Often an object will hold other indices, such as labels for individual fluid elements. When this occurs, these indices ‘bind’ more tightly to the base symbol. For example, a $(0, 2)$ rank tensor defined at a particular spacetime event labeled as A , would be written as $g_{\mu\nu}(x^\alpha(A)) \equiv g_{A\mu\nu}$. I try to avoid this later situation when possible.

The signature of the spacetime and hypersurface three metrics, the sign conventions, and index placement for usual tensors follow the MTW convention. The following notations are equivalent for partial derivatives

$$\frac{\partial f}{\partial \bar{z}} = \frac{\partial f}{\partial z^i} = \partial_{\bar{z}} f = f_{,i} \quad , \quad (1.1)$$

spacetime covariant derivatives

$$\nabla_\mu f = f_{;\mu} \quad , \quad (1.2)$$

and hypersurface covariant derivatives

$$D_i f = f_{|i} \quad . \quad (1.3)$$

The Lie derivative of tensor field $g^{\mu\nu}$ along a vector field v^α is denoted by $\mathcal{L}_{\bar{v}} g^{\mu\nu}$. Finally, the notation I use for variational derivatives is based on a decidedly older vintage. I assume that an action of the form

$$I = \int_{x_1}^{x_2} f(y, y_{,x}, x) dx \quad (1.4)$$

can always be thought of as being parameterized by a α -family of variations

$$y(x, \alpha) = y(x, 0) + \alpha \delta y(x) \quad (1.5)$$

$$\delta y(x_1) = 0 \quad (1.6)$$

$$\delta y(x_2) = 0 \quad (1.7)$$

to give

$$I(\alpha) = \int_{x_1}^{x_2} f [y(x, \alpha), y_{,x}(x, \alpha), x] dx \quad . \quad (1.8)$$

Taking the ordinary derivative of Eq. (1.8) with respect to α and setting $\alpha = 0$ yields the usual Euler-Lagrange equations. Using the δ notation, this is written as

$$\delta I \equiv \left. \frac{dI(\alpha)}{d\alpha} \right|_{\alpha=0} = \int_{x_1}^{x_2} \left(\frac{\partial f}{\partial y} - \frac{d}{dx} \frac{\partial f}{\partial y_{,x}} \right) \delta y \quad . \quad (1.9)$$

In most cases, an action depends on more than one independent function. One could, of course, generalize Eq. (1.8) as

$$I(\alpha, \beta) = \int_{x_1}^{x_2} f [y(x, \alpha), y_{,x}(x, \alpha), z(x, \beta), z_{,x}(x, \beta), x] dx \quad , \quad (1.10)$$

but I prefer a more compact notation in which

$$\delta I|_{y(x)} \equiv \int_{x_1}^{x_2} \left(\frac{\partial f}{\partial y} - \frac{d}{dx} \frac{\partial f}{\partial y_{,x}} \right) \delta y \quad (1.11)$$

and

$$\delta I|_{z(x)} \equiv \int_{x_1}^{x_2} \left(\frac{\partial f}{\partial z} - \frac{d}{dx} \frac{\partial f}{\partial z_{,x}} \right) \delta z \quad . \quad (1.12)$$

Chapter 2

Ideal Self-Gravitating Newtonian Fluids

2.1 Introduction

In this chapter, we develop our Fat Particle method within the context of classical physics. This will allow us to discuss the method in a way which brings the physical ideas to the forefront using a simpler model for self-gravitating fluids than the one needed in Einstein’s theory of gravity. While this ‘toy’ model no doubt possesses properties that are interesting in their own right, we will not dwell on the behavior it exhibits, contenting ourselves instead with the steps we must take to go from a continuum variational principle to a well-defined discrete model suitable for computational work.

Before beginning, we should note that the Fat Particle method is based on a popular computational fluid dynamics (CFD) approach called Smoothed Particle Hydrodynamics (SPH).¹ SPH belongs to a class of methods that describe fluid flow in terms of a ‘disordered’ set of points or particles [9]. The first particle technique, known as the particle in cell (PIC) method, was developed by Harlow [54, 55] to overcome the disadvantages that grid-based Eulerian and Lagrangian methods at that time had [92]. The PIC method simulated advection by moving particles which carried mechanical and thermodynamic properties, such as mass, momentum, in-

¹There is no universal agreement as to whether the ‘S’ in SPH should stand for ‘Smooth’ or ‘Smoothed’ even among the works of a single author. We adopt the term ‘Smoothed’ since it reminds us that we have actively extended an infinitesimal fluid element into a smooth distribution.

ternal energy, entropy, etc.. The remaining nonadvective, physical properties were calculated on an Eulerian grid. In a PIC simulation, the particle properties are interpolated to the grid where the spatial derivatives are calculated and the results subsequently interpolated back to the particles. While the PIC method was relatively successful in describing several problems, it had the disadvantage that the back and forth interpolation introduced large implicit diffusion and required a larger amounts of computational storage [92]. In addition, in some circumstances there were serious problems ensuring numerical stability [94].

SPH was introduced by Lucy [78] and Gingold and Monaghan [49] as an alternative particle method that only needed a grid for the computation of the fluid's self-gravity. In SPH, a fluid is modeled in terms of a finite number of particles with local fluid properties at position \vec{r} determined using a smoothing principle. The smoothing principle is defined in terms of a kernel with compact support over the range h . Since SPH is purely Lagrangian, it is naturally adaptive [58] and, consequently, is useful for modeling astrophysical phenomena with complicated geometries and arbitrarily large density gradients [116].

From its beginning, much of the work employing SPH was concerned with the simulation of the self-gravitating fluids, such as the gravitational collapse of gas clouds [50, 10, 100], stellar collisions between low-mass white dwarfs [12], $n = 3/2$ polytropes [58], and even cosmological hydrodynamics [11, 43]. The pressure forces between the fluid elements arise solely within the compact support of the kernels used to define the SPH particle and thus can be handled locally with straightforward computational techniques. Due to its infinite range, the self-gravity of the fluid is more complex and was originally handled using a three step method. The densities were first interpolated onto a computational grid. This was followed by a solution of Poisson's equation using an elliptic equation solver. The final step involved a second interpolation to determine the gravitational force at a given SPH particle's position. This method has the disadvantage that the performance of the algorithm goes as $O(N^2)$, where N is the number of grid points [12]. As a result, the modeling of self-gravity in Newtonian cases now uses point-wise interactions over nearby fluid

elements. A hierarchical tree data structure provides the means for tracking nearest neighbors efficiently, and the resulting algorithm performs to $O(N \log N)$ [59]. Despite this obvious advantage, we will not cast the Fat Particle formalism in terms of point-wise interactions since fluid self-gravity cannot be treated as a particle-particle interaction in general relativity. Rather, we will use the older methods of interpolating to and from the grid, which we term *Publish* (for interpolation to the grid) and *Subscribe* (for interpolation from the grid), respectively.

Another significant modification of the original SPH algorithm involves allowing the smoothing length h to change as both a function of space and time. The use of variable smoothing lengths improves the fidelity of the modeling by adapting the size of each fluid element’s kernel to accommodate the spatial and temporal variations in the density. This change is not without a price, however, as so-called ‘grad-h’ terms must be included to ensure the expected conservation laws, such as energy conservation [43]. Hernquist [58] points out that the handling of the ‘grad-h’ terms is not as simple as originally thought and that the SPH formalism should be examined to determine the best way. There are several ways of formalizing or justifying the SPH equations. For example, Benz [10] starts with the continuum equations, multiplies each term by a smoothing kernel, and integrates over space. However, Nelson and Papaloizou [101] point out that this approach cannot accommodate the ‘grad-h’ terms. More rigorous approaches use variational principles [50, 93, 100].

While we will not include ‘grad-h’ terms in our models, we will nonetheless start from a variational principle. For computational purposes, we envision that the gravitational degrees of freedom (the Newtonian potential in the context of the present chapter) live on a discrete grid and that in general the position of the SPH (or Fat) Particles, defined to be the center of the kernel’s support, will generally not coincide with a grid point. Using these concepts, we will take a continuum action and discretize it using a simple rule. From this technique, we will find that to be consistent with Poisson’s equation, we will have to adopt a specific form for the density and that this form is exactly the standard SPH expression. We will also see that with this form energy and momentum are exactly conserved. The goal of making and

combining these two discretization approximations makes it important that a clear distinction be kept in mind between the particle trajectories \vec{z} and the field points \vec{x} , even though the equation $\vec{x} = \vec{z}(\vec{a}, t)$ embeds a particle trajectory within the grid where field values will be known.

The remainder of the chapter details this approach as follows. Section 2.2 presents a brief heuristic summary of the continuum fluid equations for a compressible ideal fluid in the Lagrangian viewpoint. These equations, known as Euler’s equations, can be derived from the variational principle of Mittag, Stephen, and Yourgrau (MSY) as demonstrated in Section 2.3. In Section 2.4, we show how the corresponding equations for a self-gravitating fluid arise from a straightforward modification of the MSY continuum action. In Section 2.5, we present the rule by which we interpolate between particle and particle or particle and grid. We follow this with Section 2.6, in which we discretize the continuum action of Section 2.3 and Section 2.4 to arrive at a set of discrete equations that can be identified as the standard SPH equations for an ideal fluid. Finally in Section 2.7, we recast the standard SPH equations to the corresponding Fat Particle equations. This transformation is essentially conceptual and we will explore it in terms of a single self-gravitating star.

2.2 Euler’s Equation - Heuristic Derivation

In this section we derive Euler’s equation for a compressible ideal fluid using a heuristic method that focuses on the physics of a single fluid element. Our treatment is an adaptation of the discussion found in Chapter 8 of Symon [119].

Any fluid quantity, such as the pressure P , will generally depend on both the location of the fluid element, described here by the spatial coordinates x, y, z , and on the time t . The change in the pressure as the fluid moves from position x, y, z at time t to position $x + dx, y + dy, z + dz$ at time $t + dt$ will be

$$\begin{aligned} dP &= P(x + dx, y + dy, z + dz, t + dt) - P(x, y, z, t) \\ &\approx \frac{\partial P}{\partial x} dx + \frac{\partial P}{\partial y} dy + \frac{\partial P}{\partial z} dz + \frac{\partial P}{\partial t} dt \quad . \end{aligned} \tag{2.1}$$

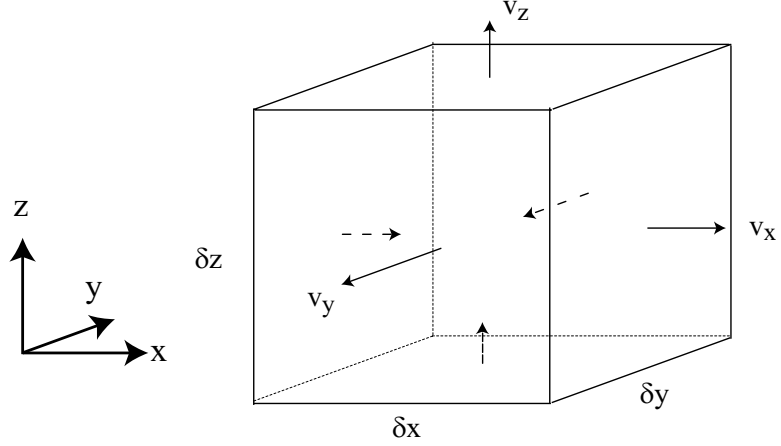


Figure 2.1: The kinematics of a single fluid element

As we take the limit $dt \rightarrow 0$, the total rate of change in the pressure becomes

$$\begin{aligned} \frac{dP}{dt} &= \frac{\partial P}{\partial x}v_x + \frac{\partial P}{\partial y}v_y + \frac{\partial P}{\partial z}v_z + \frac{\partial P}{\partial t} \\ &= \vec{v} \cdot \nabla P + \frac{\partial P}{\partial t} \quad , \end{aligned} \quad (2.2)$$

where $dx/dt, dy/dt, dz/dt$ are the components of the fluid's velocity \vec{v} . Generalizing the above argument leads to the total time derivative defined by

$$\frac{d}{dt} = \vec{v} \cdot \nabla + \frac{\partial}{\partial t} \quad . \quad (2.3)$$

The total time derivative, which is known also as the *convective* or *material* derivative, is useful in translating from the Lagrangian to the Eulerian viewpoint.

Now consider the volume of a rectangular fluid element, denoted by δV . Referring to Figure 2.1, we can see that the volume $\delta V = \delta x \delta y \delta z$ will change if the velocities on any two opposite faces are different.

To determine the precise way in which the volume changes during the flow, first consider how its extent along the x -direction changes. If we denote the position of the right and left faces of the fluid element in Figure 2.1 as x^+ and x^- respectively, then the element's length along the x -direction at time t is

$$\delta x = x^+ - x^- \quad . \quad (2.4)$$

Defining the x -component of velocity of the right and left faces analogously as v_x^+ and v_x^- then the value of δx at time $t + dt$ is

$$\delta x = (x^+ + v_x^+ dt) - (x^- + v_x^- dt) \quad . \quad (2.5)$$

The change in δx between times t and $t + dt$ is obtained by subtracting Eq. (2.4) from Eq. (2.5) to yield

$$\begin{aligned} d(\delta x) &= (v_x^+ - v_x^-) dt \\ &\approx \frac{\partial v_x}{\partial x} \delta x dt \quad . \end{aligned} \quad (2.6)$$

Dividing Eq. (2.6) by dt and taking the usual limit gives

$$\frac{d}{dt} \delta x = \frac{\partial v_x}{\partial x} \delta x \quad (2.7)$$

as the time rate of change for the δx . Similar results hold for the other lengths δy and δz . Combining these tells us that the volume of the fluid element changes according to

$$\frac{d}{dt} \delta V = (\nabla \cdot \vec{v}) \delta V \quad . \quad (2.8)$$

Using Eq. (2.8) we can derive the mass continuity equation as follows. Mass conservation for the fluid element implies that

$$\frac{d}{dt} \delta m = \frac{d}{dt} (\rho \delta V) = 0 \quad . \quad (2.9)$$

Substituting Eq. (2.8) into Eq. (2.9) results in

$$\frac{d}{dt} \rho + \rho \nabla \cdot \vec{v} = 0 \quad , \quad (2.10)$$

which is the mass continuity equation in the Lagrange viewpoint. Using the definition of the total derivative in Eq. (2.3), we can also obtain

$$\frac{\partial \rho}{\partial t} + \nabla \cdot (\rho \vec{v}) = 0 \quad , \quad (2.11)$$

which is the mass continuity equation in the more familiar Eulerian viewpoint. We will not employ the Eulerian viewpoint any further.

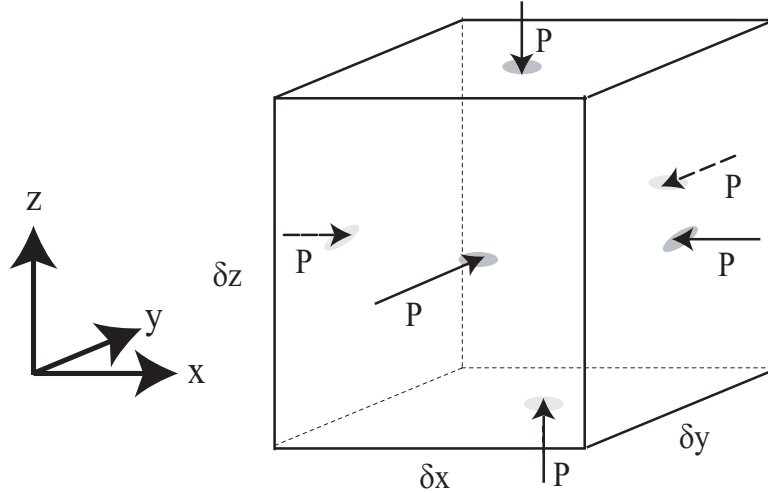


Figure 2.2: The free body diagram for a single fluid element showing the net force due to pressure gradients ∇P due to the surrounding fluid

Having the kinematics of our fluid element well in hand, we can now turn our attention to its dynamics. We will characterize the forces on our fluid element as arising from three sources. The first is the contact force $\vec{F}_{pressure}$ acting perpendicular to the boundary due to the pressure of the surrounding fluid. The second will be the body force \vec{F}_{body} arising from the fluids gravitational interaction with either an external agency (*e.g.*, a star or planet) or itself - the latter being referred to as self-gravity. Into the third category will go all of the other contact forces $\vec{F}_{viscous}$ that arise due to stresses that act parallel to the boundary of the fluid element. These forces, which act to shear the fluid element rather than to compress it, arise due to the fluid's viscosity.

Applying Newton's second law to the element is straightforward and following our method above we will first start with the pressure forces in the x -direction. Figure 2.2 shows the corresponding free body diagram for the pressure forces.

The net force from the pressure difference between the right and left faces is

$$\left[\vec{F}_{pressure} \right]_x = \left(-\frac{\partial P}{\partial x} \delta x \right) \delta y \delta z \quad . \quad (2.12)$$

Similar result hold for the other directions and they can be combined with Eq. (2.12)

to give

$$\vec{F}_{pressure} = -\nabla P \delta V \quad (2.13)$$

Newton's second law now takes the form

$$m \frac{d\vec{v}}{dt} = \rho \delta V \frac{d\vec{v}}{dt} = -\nabla P \delta V + \vec{F}_{body} + \vec{F}_{viscous} \quad (2.14)$$

If the fluid is self-gravitating, which we will assume for the remainder of this section, the body force is derivable from a potential Φ and can be written as

$$\vec{F}_{body} = -\rho \delta V \nabla \Phi \quad (2.15)$$

where the potential must obey Poisson's equation

$$\nabla^2 \Phi = 4\pi G \rho \quad (2.16)$$

Substituting Eq. (2.15) into Eq. (2.14), gathering all of the terms to the left-hand-side, and dividing by $\rho \delta V$ gives the momentum equation for our fluid

$$\frac{d\vec{v}}{dt} + \frac{1}{\rho} \nabla P + \nabla \Phi - \frac{\vec{F}_{viscous}}{\delta m} = 0 \quad (2.17)$$

It remains for us to model the changes in the internal stresses as the fluid evolves. To accomplish this, we assume the existence of an internal energy function $e(\rho, s)$, which is a function of the density ρ and the specific entropy s [30] and which obeys the first law of thermodynamics

$$de = T ds + \frac{P}{\rho^2} d\rho \quad (2.18)$$

Dividing Eq. (2.18) by dt and taking the limit as $dt \rightarrow 0$ gives an evolution equation for the energy

$$\frac{de}{dt} = T \frac{ds}{dt} + \frac{P}{\rho^2} \frac{d\rho}{dt} \quad (2.19)$$

which can be simplified using the continuity equation Eq. (2.10) to be

$$\frac{de}{dt} = T \frac{ds}{dt} - \frac{P}{\rho} \nabla \cdot \vec{v} \quad (2.20)$$

Entropy changes in the fluid, given by the first term in Eq. (2.20), are caused by two mechanisms; either from heat flow between the fluid element and its surroundings or

from viscous dissipation (see, *e.g.*, page 44 of [60]).² The second term in Eq. (2.20) accounts for the rate of work performed. In most of this work, we will limit our scope to ideal fluids. Ideal fluids are characterized by the absence of shearing stresses even when the fluid is in motion. This requires that the fluid have no viscosity (*i.e.*, $\vec{F}_{viscous} = 0$). This in turn implies that there is no mechanism for the transfer of heat and as a consequence the entropy of any fluid element is constant

$$\frac{ds}{dt} = 0 \quad . \quad (2.21)$$

Such a flow is termed isentropic.

Since the flow is isentropic, Eq. (2.18) tells us that changes in the internal energy are caused only by work performed on the fluid. The rate of change for the internal energy is thus

$$\frac{de}{dt} = -\frac{P}{\rho} \nabla \cdot \vec{v} \quad . \quad (2.22)$$

The time evolution of the fluid can thus be summarized by the set of first-order evolution equations

$$\frac{d}{dt} \begin{pmatrix} \rho \\ e \\ \vec{v} \end{pmatrix} = \begin{pmatrix} \rho \nabla \cdot \vec{v} \\ -\frac{P}{\rho} \nabla \cdot \vec{v} \\ \frac{-\nabla P}{\rho} - \nabla \Phi \end{pmatrix} \quad , \quad (2.23)$$

with the auxiliary equation $\nabla^2 \Phi = 4\pi G \rho$. Equivalently, this set can be written in the energy representation (see [30] for a comparison of the energy and entropy representations) as

$$\frac{d}{dt} \begin{pmatrix} \rho \\ s \\ \vec{v} \end{pmatrix} = \begin{pmatrix} \rho \nabla \cdot \vec{v} \\ 0 \\ \frac{-\nabla P}{\rho} + \nabla \Phi \end{pmatrix} \quad . \quad (2.24)$$

In either case, the resulting momentum equation for isentropic flow is known as Euler's equation. To close this set, we will employ the usual polytropic equation of state [49, 95, 12, 116]

$$P = A(s_0) \rho^\gamma \quad , \quad (2.25)$$

²Note that we are assuming that there is no heat production, say from chemical means, within the fluid element and no heating due to radiation. Nor do we consider shocks.

where $A(s_0)$ is a constant related to the initial specific entropy of the fluid element and γ is the ratio of the fluid's specific heat at constant pressure to its specific heat at constant volume. Typical values of γ for an ideal gas range between 1.7 and 1.3 [52]. This equation of state is often expressed in the entropy representation as $P = (\gamma - 1)\rho e$ [59, 58, 57, 118].

Since we are explicitly accounting for the constancy of the specific entropy along the fluid's path in our form of the equation of state Eq. (2.25), we can drop the entropy evolution equation from Eq. (2.24) reducing the equations to a system of four equations in four unknowns. This set, solved in conjunction with Poisson's equation Eq. (2.16) and supplemented with the equation of state Eq. (2.25), constitutes a complete description of our ideal fluid.

2.3 Euler' Equation - Variational Formalism

In this section, we demonstrate how Euler's momentum equation derived in Section 2.2 can be obtained from a variational approach. In the subsequent section, we will extend this action principle to account for the self-gravity of the fluid. At this stage, this technique is merely a recapitulation of previous results. However, following this path will provide us with a springboard for obtaining the FP equations.

Our approach is based on the work of Mittag, Stephen, and Yourgrau (MSY) [90], in which they constructed an action that yielded continuum equations for the motion of an ideal fluid.

Start with an initial distribution of fluid with each element labeled by its position \vec{a} at the time $t = 0$. Following MSY, we then introduce what we call the trajectory function $\vec{z}(\vec{a}, t)$ which gives any fluid element's position \vec{x} at some later time t by

$$\vec{x} = \vec{z}(\vec{a}, t) \quad . \quad (2.26)$$

The trajectory function has the obvious boundary condition $\vec{z}(\vec{a}, 0) = \vec{a}$. Figure 2.3 shows a schematic representation of the trajectory function for a two-dimensional fluid.

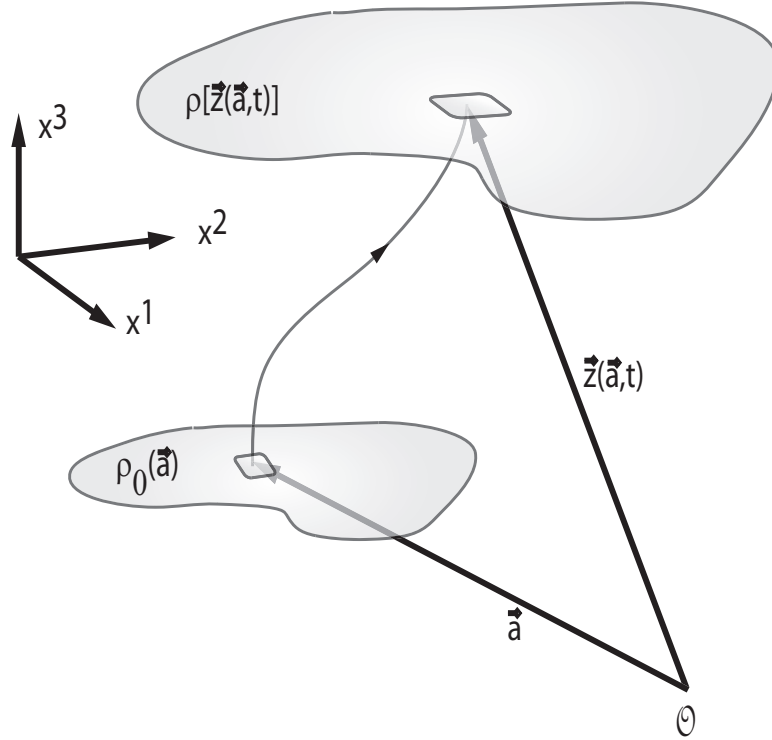


Figure 2.3: Schematic representation of the trajectory function. A parcel of fluid located at position \vec{a} in the initial data flows along the unique path $\vec{z}(\vec{a}, t)$ as time evolves.

Assuming the fluid to be ideal, its motion is subject to two constraints. The first is the conservation of mass (see Eq. (2.10)), which takes the form

$$\rho(\vec{z}, t) d^3z = \rho(\vec{a}, 0) d^3a \quad . \quad (2.27)$$

Introducing the Jacobian determinant $J = \det\left(\frac{\partial z^i}{\partial a^j}\right)$ allows the conservation of mass equation to be given by

$$\rho(\vec{z}, t) J(\vec{z}, t) = \rho_0(\vec{a}) \quad . \quad (2.28)$$

Thus ρ depends on the family of trajectories $\vec{z}(\vec{a}, t)$ under consideration, and is entirely determined by it. The second constraint is the conservation of entropy (see Eq. (2.21)) which takes on the form

$$s(\vec{a}, t) = s(\vec{a}, 0) \quad . \quad (2.29)$$

Although MSY incorporate these constraints in a variational principle by the use

of Lagrange multipliers, we find the equations shorter and easier to read if one takes ρ and s to be defined by Eq. (2.28) and Eq. (2.29) and to take only those variations which respect these relations. The modified MSY action then is

$$I = \int d^3a dt \left[\frac{\rho_0}{2} \left(\frac{\partial z^i}{\partial t} \right)^2 - \rho_0 (e + \Phi) \right] , \quad (2.30)$$

where $e(\rho, s)$ is the specific internal energy and $\Phi(\vec{z}(\vec{a}, t), t)$ is the gravitational potential energy per unit mass at the position of particle \vec{a} . In this formalism, $\vec{z}(\vec{a}, t)$ are the dynamical variables that are varied to produce the equations of motion.

The variation of the action with respect to the trajectory function \vec{z} requires the various properties of the Jacobian that MSY employ in their formulation and which are summarized in Appendix A. We must remember that since ρ is defined by Eq. (2.28) both ρ and $e(\rho, s)$ will vary when \vec{z} is varied. Thus we find

$$\delta I|_{\delta \vec{z}} = \int d^3a dt \left[\rho_0 \frac{\partial z^i}{\partial t} \delta \left(\frac{\partial z^i}{\partial t} \right) - \rho_0 \frac{P}{\rho^2} \delta \rho - \rho_0 \frac{\partial \Phi}{\partial z^i} \delta z^i \right] . \quad (2.31)$$

Here we have used the thermodynamic relationship $de = Tds - Pd(1/\rho)$ in the form $(\partial e/\partial \rho)_s = P/\rho^2$ in evaluating how the internal energy e changes when the trajectory variations cause changes in ρ but not in s at a particular fluid element.³ The problematic term here is that containing $\delta \rho$. But from $\rho J = \rho_0$, where the right hand side is independent of \vec{z} , one has $J\delta\rho + \rho\delta J = 0$. Thus the term $-(\rho_0 P/\rho^2)\delta\rho$ becomes $-(P/\rho)J\delta\rho = +P\delta J$. Employing Eq. (A.13), we can write $\delta J = (\partial J/\partial z^i{}_{,j})\delta z^i{}_{,j} = J_i{}^j\delta z_{i,j}$, where $z^i{}_{,j} = \partial z^i/\partial a^j$ and $J_i{}^j$ is the (i, j) minor of the Jacobian. Substituting $-(\rho_0 P/\rho^2)\delta\rho = PJ_i{}^j\delta z^i{}_{,j}$ into Eq. (2.31), results in the first and second terms being proportional to derivatives of δz^i . Exchanging the order of the variation and the partial differentiation in these terms and integrating them by parts gives

$$\delta I|_{\delta z^i} = - \int d^3a dt \left[\rho_0 \left(\frac{\partial^2 z^i}{\partial t^2} \right) + \frac{\partial}{\partial a^j} (PJ_i{}^j) + \rho_0 \frac{\partial \Phi}{\partial z^i} \right] \delta z^i . \quad (2.32)$$

Setting this variation to zero leads to the partial differential equation

³Recall that the specific entropy s is constant for each fluid element. Thus we have used the constancy of the specific entropy to select a set of allowable variations.

$$\rho_0 \left(\frac{\partial^2 z^i}{\partial t^2} \right) + \rho_0 \frac{\partial \Phi}{\partial z^i} + \frac{\partial}{\partial a^j} (P J_i^j) = 0 \quad . \quad (2.33)$$

From the relations $\partial J_{ij}/\partial a_j = 0$ (see the discussion leading up to Eq. (A.15)), the last term becomes

$$\frac{\partial}{\partial a^j} (P J_i^j) = \frac{\partial P}{\partial a^j} J_i^j = \frac{\partial P}{\partial z^k} \frac{\partial z^k}{\partial a^j} J_i^j \quad . \quad (2.34)$$

Finally, by using $(\partial z^k/\partial a^j) J_i^j = J$ (see Eq. (A.4)) and $J = \rho_0/\rho$, we put Eq. (2.33) into the form

$$\left(\frac{\partial^2 z^i}{\partial t^2} \right) + \frac{\partial \Phi}{\partial z^i} + \frac{1}{\rho} \frac{\partial P}{\partial z^i} = 0 \quad . \quad (2.35)$$

The set of Eqs. (2.28), (2.29), and (2.35), supplemented with the equation of state Eq. (2.25), are equivalent to the set in Eq. (2.24).

2.4 Newtonian Gravity

In the preceding section, Newtonian gravity was included as a potential Φ due to external masses. When the self-gravitation of the fluid is to be included more care is needed. Unlike the usual Newtonian SPH applications, we do not want to think of gravitation as a mutual interaction of the smoothed particles—this viewpoint, effective in Newtonian problems, will not provide guidance for the relativistic problems we aim to formulate. Instead we write a field theory.

A variational principle which gives rise to Poisson's equation is $\delta I_G = 0$ with

$$I_G = - \int d^3x dt \left[(1/8\pi G)(\nabla\Phi(\vec{x}, t))^2 + \rho(\vec{x}, t)\Phi(\vec{x}, t) \right] \quad . \quad (2.36)$$

Varying Φ here gives

$$\nabla^2\Phi = 4\pi G\rho \quad , \quad (2.37)$$

with solutions such as $\Phi = -GM/r$.

A continuum variational principle extending that of Section 2.3 to include the field dynamics is $\delta I = 0$ with $I = \int L dt$ and

$$I = \int d^3 a dt \left[\frac{\rho_0}{2} \left(\frac{\partial z^i}{\partial t} \right)^2 - \rho_0 e(\rho, s_0) - \rho_0 \Phi(\vec{z}(\vec{a}, t)) \right] - (1/8\pi G) \int d^3 x dt (\nabla \Phi(\vec{x}, t))^2 . \quad (2.38)$$

The terms here containing $\vec{z}(\vec{a}, t)$ are exactly those considered in Section 2.3, so the fluid equations are just Eq. (2.35). But to see that Eq. (2.37) also results, we need to rewrite the $\rho_0 \Phi$ term to see that it is the same as in Eq. (2.36). This we do by invoking the definition of ρ in a change of variables $\rho_0 d^3 a = \rho d^3 z$ in the integral

$$\begin{aligned} \int d^3 a dt \rho_0(\vec{a}) \Phi(\vec{z}(\vec{a}, t)) &= \int d^3 z dt \rho(\vec{z}, t) \Phi(\vec{z}, t) \\ &= \int d^3 x dt \rho(\vec{x}, t) \Phi(\vec{x}, t) , \end{aligned} \quad (2.39)$$

where the last step is a notational change of the dummy variable of integration. Thus Eq. (2.37) also results by varying $\Phi(\vec{x})$ in this combined Lagrangian Eq. (2.38).

It is important to note that only the first form of the interaction term in Eq. (2.39), as given in Eq. (2.38), is acceptable in the fundamental Lagrangian. For in making the change of variables from \vec{a} to \vec{z} in Eq. (2.39) one has assumed a definite fluid motion $\vec{z}(\vec{a}, t)$. Since reference to this particular motion disappears in the $\int d^3 x dt \rho(\vec{x}, t) \Phi(\vec{x}, t)$ form of this term, it would not be possible to carry out the $\delta \vec{z}$ variations were this form to be stated as part of the basic Lagrangian. We have used it here only to carry out a variation of Φ while holding the fluid motion $\vec{z}(\vec{a}, t)$ unchanged.

2.5 Kernel Estimation Techniques

In this section we present the basic ideas behind the kernel estimation technique that is the main numerical method used throughout the text. Assume that we have at our disposal a smooth, differentiable function $f(\vec{x})$, defined over some domain. The kernel estimate of this function is defined through the integral relation

$$\langle f \rangle(\vec{z}) = \frac{\int d^3 x W(\vec{z} - \vec{x}; h) f(\vec{x})}{\int d^3 x W(\vec{z} - \vec{x}; h)} . \quad (2.40)$$

The *smoothing kernel* $W(\vec{z} - \vec{x})$ weights the contribution of the function across its domain according to the distance between the *source* point \vec{x} and the *observation* point \vec{z} . The kernel is defined over a compact support limited in distance to the *smoothing length* h about the observation point. As our smoothing length will always be constant for a given simulation, we will usually suppress the h , referring to the kernel as $W(\vec{z} - \vec{x})$ ([101] discusses variable smoothing lengths).

The essential properties of the smoothing kernel W are that it is normalized.

$$\int d^3z W(\vec{z}) = \mathcal{N} = 1 \quad (2.41)$$

and that it has a delta-function limit

$$\lim_{h \rightarrow 0} W(\vec{z} - \vec{x}; h) = \delta(\vec{z} - \vec{x}) \quad . \quad (2.42)$$

Note that we will explicitly keep the denominator in Eq. (2.40) since we will eventually estimate the integrals numerically. However, we can dispense with it, when desired, in the continuum discussion which follows.

In addition, we assume that we are using a symmetric, even, non-negative kernel. Expanding $f(\vec{x}) \equiv f(\vec{z} + \vec{q})$ in Eq. (2.40) around \vec{z} yields

$$\begin{aligned} \langle f(\vec{z}) \rangle &= \mathcal{N}^{-1} \int d^3q f(\vec{z} + \vec{q}) W(\vec{q}) \\ &= \mathcal{N}^{-1} \int d^3q \left(f(\vec{z}) + \frac{\partial f}{\partial z^i} q^i + \frac{1}{2!} \frac{\partial^2 f}{\partial z^i \partial z^j} q^i q^j + \dots \right) W(\vec{q}) \quad . \quad (2.43) \end{aligned}$$

Since the kernel is even, only the even powers of q^i survive. Define a scaling variable $\vec{y} = \vec{q}/h$ and Eq. (2.43) becomes

$$\langle f(\vec{z}) \rangle = \tilde{\mathcal{N}}^{-1} \left(f(\vec{z}) + \frac{1}{2!} \frac{\partial^2 f}{\partial z^i \partial z^j} h^2 \int_{|\vec{y}| \leq 1} d^3y W(\vec{y}) y^i y^j + O(h^4) \right) \quad (2.44)$$

where $\tilde{\mathcal{N}} = \int d^3y W(\vec{y})$. Note that the integrals over d^3y in Eq. (2.44) are independent of h .

We will illustrate these ideas using a one-dimensional estimation of the function $f(\vec{x}) = x^3$. To perform the estimation, we employ the Misner n -family of kernels (which are a generalization of the kernel used in [87])

$$W_n(\vec{z} - \vec{x}) \equiv \begin{cases} N_n \left(1 - \frac{|\vec{z} - \vec{x}|^2}{h^2} \right)^n & |\vec{z} - \vec{x}| < h \\ 0 & |\vec{z} - \vec{x}| \geq h \end{cases} \quad (2.45)$$

Kernel	N_n	$\langle x^3 \rangle (z)$
W_2	$15/(16h)$	$z^3 + (3/7)zh^2$
W_3	$35/(32h)$	$z^3 + (1/3)zh^2$
W_4	$315/(256h)$	$z^3 + (3/11)zh^2$
W_G	\mathcal{N}_G/h	$z^3 + \mathcal{Q}zh^2$

Table 2.1: Normalization factors and exact smoothed values for x^3 for the Misner n -kernels W_2 , W_3 , W_4 , and the Gaussian kernel W_G as defined in Eq. (2.46). The normalization for the Gaussian kernel is expressed by $\mathcal{N}_G = 3/(\text{erf}(3)\sqrt{\pi})$, where $\text{erf}(x) = 2/\sqrt{\pi} \int_0^x e^{-t^2} dt$ is the Gauss error function (see Section 5.10 of [4]) and $\mathcal{Q} = (1/6 - \exp(-9)\mathcal{N}_G/3)$.

and a Gaussian kernel W_G defined as

$$W_G(\vec{z} - \vec{x}) \equiv \begin{cases} N_n \exp\left(-9\frac{|\vec{z}-\vec{x}|^2}{h^2}\right) & |\vec{z} - \vec{x}| < h \\ 0 & |\vec{z} - \vec{x}| \geq h \end{cases}. \quad (2.46)$$

Note that Faulk [46] presents an extensive investigation of the characteristics of other classes of kernels in the one-dimensional problem. Table 2.1 shows the values of N_n and $\langle x^3 \rangle (z)$ for the kernels W_2 , W_3 , W_4 , and W_G . Figure 2.4 shows the corresponding profiles of each kernel.

Generally, we won't be able to evaluate the integral in the numerator of Eq. (2.40) analytically but we will instead have to resort to a numerical computation of the form

$$\langle f \rangle (\vec{z}) = \frac{\sum_{\ell=1}^N f(\vec{x}_\ell) W(\vec{z} - \vec{x}_\ell)}{\sum_{\ell=1}^N W(\vec{z} - \vec{x}_\ell)}, \quad (2.47)$$

where the point-index ℓ takes the place of the continuous index \vec{x} in the integral. To bound the errors that one may expect in computing the estimate in Eq. (2.47), we examined two options, either estimating the integrals over a uniformly-spaced grid or over a randomly distributed set of points.

For our test case smoothing of x^3 at the observation point $z = 1$, we constructed two point sets spanning the range from $[0, 2]$. The first set comprised a uniform grid and the second a random group of points sampled from a uniform distribution defined over the same interval. In this latter case, the sums in Eq. (2.47) become

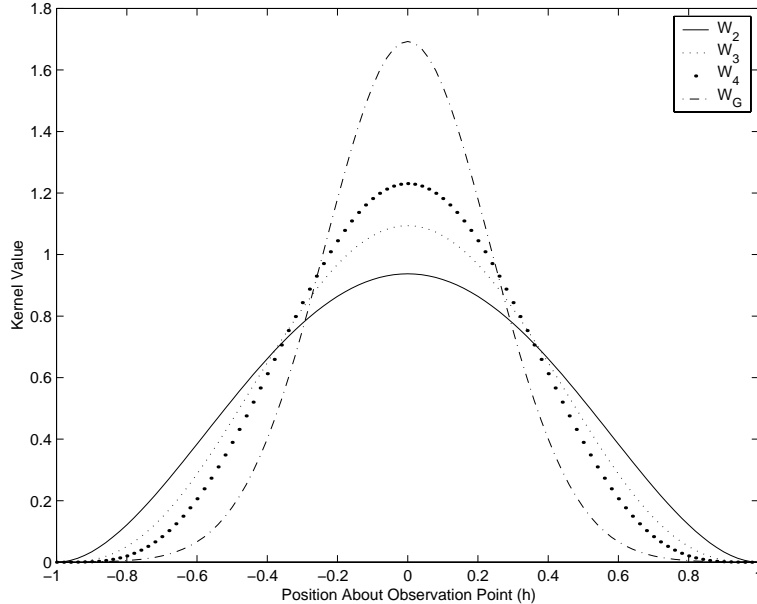


Figure 2.4: Profiles of the one-dimensional form of the smoothing kernels W_2 , W_3 , W_4 of the Misner n -family of kernels and the Gaussian kernel W_G .

Monte Carlo estimates of the integrals in Eq. (2.40) [51]. We then carried out the corresponding sums for a varying number of points in the sets and compared the exact answer, $\langle x^3 \rangle_{exact}$ to the numerical estimates $\langle x^3 \rangle_{uniform}$ and $\langle x^3 \rangle_{random}$. The results are shown in Figure 2.5 for the four kernels considered.

Clearly the results for $\langle x^3 \rangle_{uniform}$ are better behaved than those from $\langle x^3 \rangle_{random}$.⁴

Figure 2.6 shows the error for the uniform smoothing defined as $\epsilon = |\langle x^3 \rangle_{exact} - \langle x^3 \rangle_{uniform}|$ as a function of the number of points in the estimate. The rapid convergence of the numerical estimate to the exact value is clear. Although we do not have an explanation for the difference in slopes, experiments with other functional forms suggest that it is related to the form of the kernel rather than the power of the function being smoothed.

It is often the case that the derivative of a smoothed function with respect to the

⁴Note that the results displayed for the random smoothing depend not only on the number of points in set but also the particular sample obtained from the pseudo-random number generator. No attempt was made to improve the Monte Carlo estimate using techniques such as binning or importance sampling [51, 65].

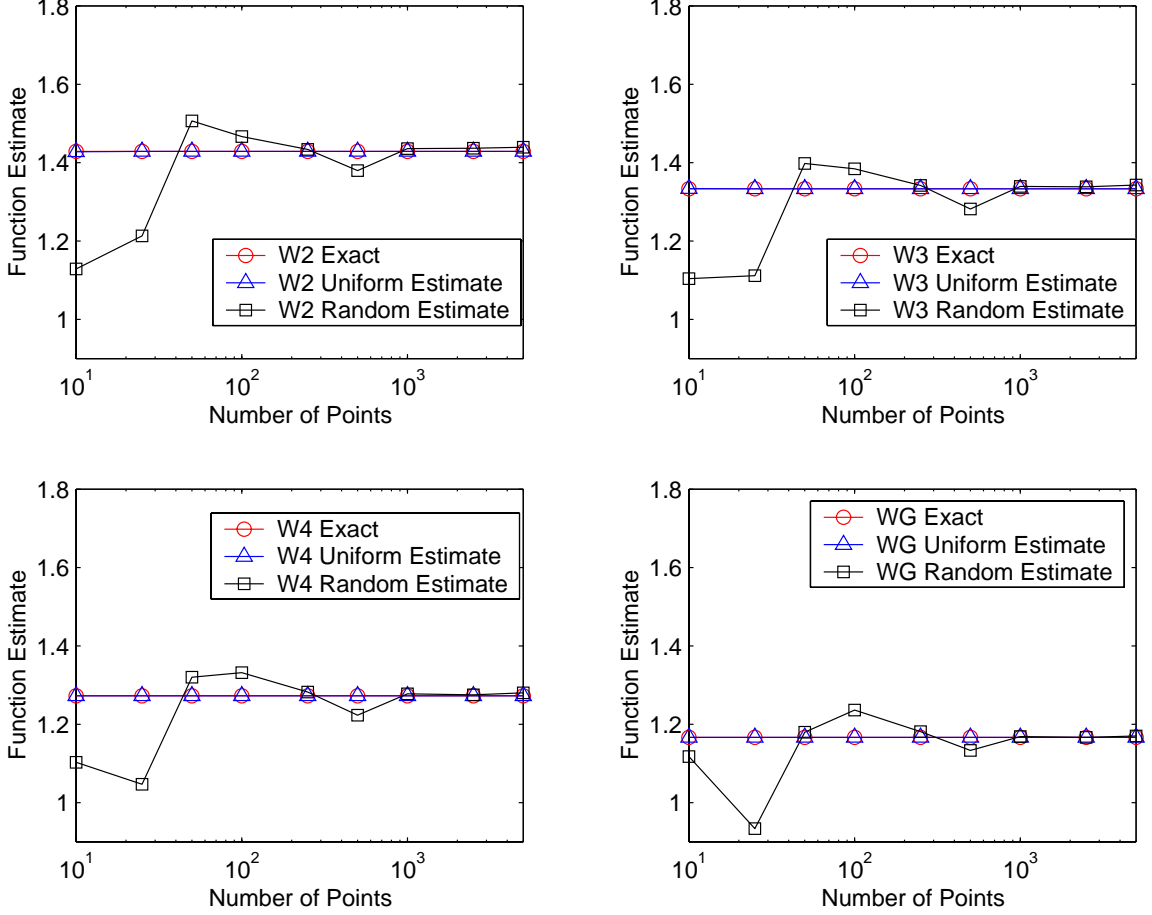


Figure 2.5: Comparisons between exact and numerical estimates of the smoothed function x^3 for sets of points uniformly or random distributed in the interval $[-1, 1]$.

observation point is needed. In this case, we can simply differentiate Eq. (2.40) with respect to \vec{z} to obtain

$$\frac{\partial}{\partial \vec{z}} \langle f \rangle = \frac{\int d^3x \frac{\partial}{\partial \vec{z}} W(\vec{z} - \vec{x}) f(\vec{x})}{\int d^3x W(\vec{z} - \vec{x})} - \langle f \rangle \frac{\int d^3x \frac{\partial}{\partial \vec{z}} W(\vec{z} - \vec{x})}{\int d^3x W(\vec{z} - \vec{x})} . \quad (2.48)$$

In the continuum case, the last term in Eq. (2.48) can be omitted since the derivative of an even kernel produces an odd function, which when integrated over an even range results in zero. However, we include this term for the cases when the integrals are approximated as sums over a discrete set of points. Using the symmetric property of the kernel, we can switch the differentiation from \vec{z} to \vec{x} in the first term in Eq. (2.48).

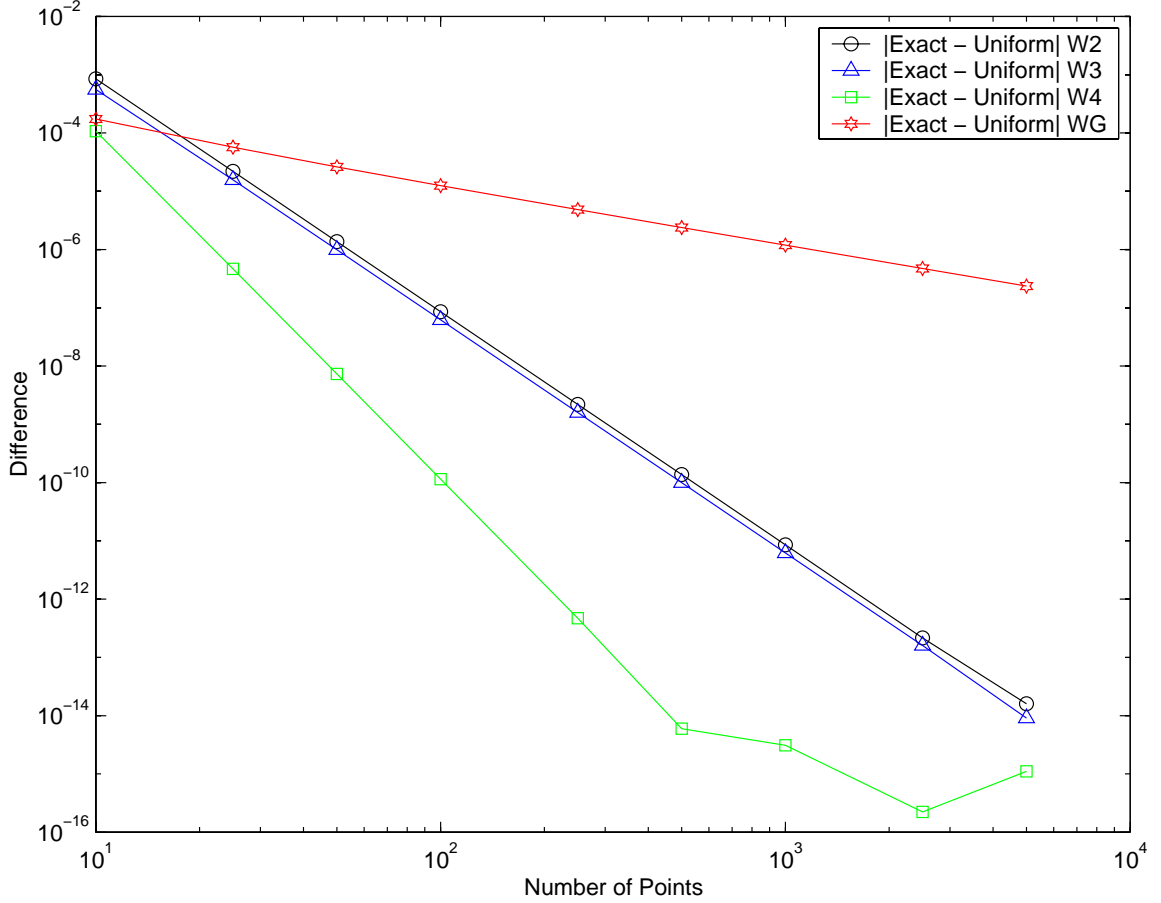


Figure 2.6: The error between the exact and numerically estimated value of the smoothed function x^3 as a function of the number of points used in the computation.

A subsequent integration by parts yields the alternative formula

$$\frac{\partial}{\partial \vec{z}} \langle f \rangle = \left\langle \frac{\partial}{\partial \vec{x}} f \right\rangle - \langle f \rangle \frac{\int d^3x \frac{\partial}{\partial \vec{z}} W(\vec{z} - \vec{x})}{\int d^3x W(\vec{z} - \vec{x})} . \quad (2.49)$$

We refer to the derivative calculated in Eq. (2.48) as a *kernel derivative* and the derivative calculated via Eq. (2.49) as a *smoothed derivative*. As a test case, we considered numerically calculating the derivative of $\langle x^4 \rangle$ using the W_3 kernel over a uniform grid. The exact value of this derivative is

$$\frac{\partial}{\partial z} \langle x^4 \rangle (z) = 4z^3 + \frac{4}{3}zh^2 . \quad (2.50)$$

Figure 2.7 shows the error $\epsilon = |\partial_z \langle x^4 \rangle_{exact} - \partial_z \langle x^4 \rangle_{uniform}|$ of the numerical approximations of both the kernel and smoothed derivative methods as a function of the number of points used in the uniform grid.

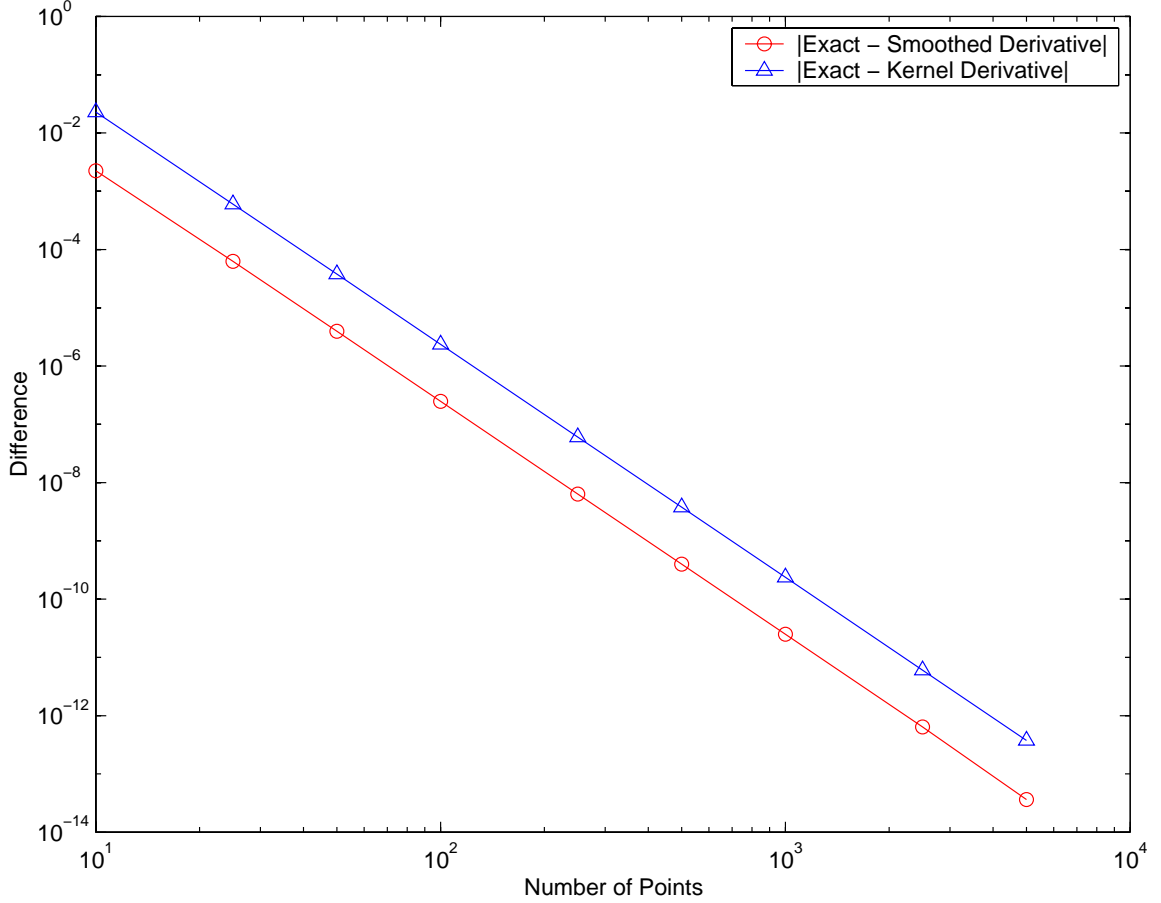


Figure 2.7: The error between the exact and numerically estimated value of the smoothed function $\frac{\partial x^4}{\partial x}$ as a function of the number of points used in the computation.

The error in the smoothed derivative method is always an order of magnitude less than the kernel derivative method. The reason for this is that the kernel derivative method depends on the cancelation of relatively large terms that appear in the sum with opposite signs. Small numerical errors in the individual terms are more apt to be significant. This is analogous to the errors that arise in the classical theory of computing numerical derivatives [68].

2.6 Smoothed Particle Hydrodynamics

In this section, we derive a version of the SPH equations for an ideal fluid using a discretized form of our continuum action and the smoothing techniques discussed in

Section 2.5. Our aim is to demonstrate that the variational principle employed yields ‘good’ equations by comparing what we obtain against the generally accepted forms found in the literature.

Starting a fashion similar to Bicknell [15], we define the initial density of the fluid as a sum of delta functions

$$\rho_0 = \sum_A m_A \delta(\vec{a} - \vec{r}_A) \quad . \quad (2.51)$$

Substituting this relation into Eq. (2.36) yields the discrete variational principle

$$I = \sum_A m_A \int dt \left[\left(\frac{\partial \vec{z}_A}{\partial t} \right)^2 - e_A(\rho) - \Phi_A \right] - \frac{1}{8\pi G} \int d^3x dt (\nabla \Phi(\vec{x}, t))^2 \quad , \quad (2.52)$$

where the gravitational potential at the particle’s location is given by the smoothed form

$$\Phi_A \equiv \Phi(\vec{z}_A, t) = \frac{\int d^3x W(\vec{z}_A - \vec{x}) \Phi(\vec{x})}{\mathcal{N}_A} \quad , \quad (2.53)$$

where $\mathcal{N}_A = \int d^3x W(\vec{z}_A - \vec{x})$. Taking the variation of Eq. (2.52) with respect to the gravitational potential Φ yields

$$\begin{aligned} \delta I|_{\Phi(\vec{x}, t)} &= - \sum_A m_A \int d^3x dt \frac{W(\vec{z}_A - \vec{x}) \delta \Phi(\vec{x}, t)}{\mathcal{N}_A} \\ &\quad - \frac{1}{4\pi G} \int d^3x dt \nabla \Phi(\vec{x}, t) \nabla \delta \Phi(\vec{x}, t) \quad . \end{aligned} \quad (2.54)$$

Setting the integrand equal to zero gives a smoothed form of Poisson’s equation

$$\nabla^2 \Phi(\vec{x}, t) = 4\pi G \left\{ \sum_A \frac{m_A}{\mathcal{N}_A} W(\vec{z}_A - \vec{x}) \right\} \quad (2.55)$$

and interpreting the term in the braces in the usual way gives our ‘SPH’ definition of the density

$$\rho(\vec{x}) = \sum_B \frac{m_B}{\mathcal{N}_B} W(\vec{z}_B - \vec{x}) \quad . \quad (2.56)$$

That Eq. (2.56) is an adequate definition of density is immediately seen by integrating over all space

$$\int d^3x \rho(\vec{x}) = \sum_A m_A \frac{\mathcal{N}_A}{\mathcal{N}_A} = \sum_A m_A \quad (2.57)$$

and seeing that the total mass is conserved. To show that this definition is ‘good’ according to the criterion discussed above, consider the density, given in Eq. (2.56), evaluated at a particle position \vec{z}_A

$$\rho(\vec{z}_A) = \sum_B \frac{m_B}{\mathcal{N}_B} W(\vec{z}_B - \vec{z}_A) \quad , \quad (2.58)$$

which we write in the more compact notation

$$\rho_A \equiv \sum_B \frac{m_B}{\mathcal{N}_B} W_{AB} \quad . \quad (2.59)$$

If we recall that the denominator is exactly unity in the continuum case (and nearly so when discretely computed), this definition is identical to the one used in the vast majority of the literature.⁵ Next we take the variation of Eq. (2.52) with respect to changes in the particle trajectories and equating the variation to zero yields

$$m_A \frac{\partial^2 \vec{z}_A}{\partial t^2} + \sum_B m_B \frac{P_B}{\rho_B^2} \frac{\partial \rho_B}{\partial \vec{z}_A} + m_A \frac{\partial \Phi_A}{\partial \vec{z}_A} = 0 \quad . \quad (2.60)$$

Using the density definition in Eq. (2.58), we obtain

$$\begin{aligned} \frac{\partial \rho_B}{\partial \vec{z}_A} &= \sum_C \frac{m_C}{\mathcal{N}_C} \nabla_B W_{BC} \{ \delta_{BA} - \delta_{CA} \} \\ &\quad - \frac{m_A}{\mathcal{N}_A^2} W_{BA} \mathcal{N}_A' \quad , \end{aligned} \quad (2.61)$$

where the short-hand notation $\nabla_A W_{BC} = \frac{\partial W(\vec{z}_B - \vec{z}_C)}{\partial \vec{z}_A}$ and $\mathcal{N}_A' = \int d^3x \frac{\partial W(\vec{z}_A - \vec{x})}{\partial \vec{z}_A}$ will be used frequently hereafter for convenience. Substituting Eq. (2.61) into Eq. (2.60) results in the *symmetric additive* momentum equation

$$\begin{aligned} m_A \frac{d^2 \vec{z}_A}{dt^2} + \sum_B m_A m_B \left(\frac{P_B}{\mathcal{N}_A \rho_B^2} + \frac{P_A}{\mathcal{N}_B \rho_A^2} \right) \nabla_A W_{AB} \\ - \frac{m_A}{\mathcal{N}_A^2} \mathcal{N}_A' \sum_B m_B W_{AB} + m_A \frac{\partial \Phi_A}{\partial \vec{z}_A} = 0 \quad , \end{aligned} \quad (2.62)$$

where the derivative of the gravitational potential is computed either via the kernel derivative formula in Eq. (2.48) or from the smoothed derivative formula of Eq. (2.49).

⁵Note that this definition includes the ‘self-density’ of the particle located at \vec{z}_A . Even though the inclusion of this term has been the subject of some controversy in the literature [44, 128], it is widely accepted that the self-density is needed.

To see that the symmetric additive momentum equation is ‘good’ in the sense of the criterion employed before, we again consider the continuum case where $\mathcal{N}_A = 1$ and $\mathcal{N}'_A = 0$ and we also ignore the self gravity of the fluid. Doing so yields

$$m_A \frac{d^2 \vec{z}_A}{dt^2} + \sum_B m_A m_B \left(\frac{P_B}{\rho_B^2} + \frac{P_A}{\rho_A^2} \right) \nabla_A W_{AB} = 0 \quad , \quad (2.63)$$

which is the equation advocated by many authors for its ability to conserve linear and angular momentum [12, 91, 93, 10]. To see why this equation conserves linear momentum, we follow Benz [10] by considering the force on m_A due solely to m_B from Eq. (2.63)

$$\begin{aligned} m_A \frac{d^2 \vec{z}_A}{dt^2} \Big|_{m_B} &= m_A m_B \left(\frac{P_B}{\rho_B^2} + \frac{P_A}{\rho_A^2} \right) \nabla_A W_{AB} \\ &= -m_A m_B \left(\frac{P_B}{\rho_B^2} + \frac{P_A}{\rho_A^2} \right) \nabla_B W_{BA} \\ &= -m_B \frac{d^2 \vec{z}_B}{dt^2} \Big|_{m_A} \end{aligned} \quad (2.64)$$

and we see that the forces between the particles cancel pair-wise. A similar argument holds for the conservation of angular momentum. Other ‘symmetric’ forms are possible [50, 91, 59, 57] but as pointed out by Monaghan [92] none of these other forms seem to offer any advantages over Eq. (2.63).

The SPH set comprised of Eq. (2.55), Eq. (2.56), and Eq. (2.62), supplemented by the equation of state Eq. (2.25), is a complete description of a self-gravitating fluid. Since the SPH form of the density automatically satisfies the continuity equation, it need not be explicitly computed [58]. Also, we have accounted for the constancy of the specific entropy in the form we’ve adopted for the equation of state. Thus, given an initial distribution of SPH particles, we can simulate the fluid’s behavior as follows. First we lay out a computational grid to be used in numerically solving the SPH Poisson’s equation Eq. (2.55).⁶ Next we compute the density at the grid points according to Eq. (2.56) and solve Poisson’s equation using standard elliptical

⁶Despite the appearance of a grid, this technique is authentically an SPH application. In fact, as discussed in the introduction, the early SPH applications used a computational grid to determine the gravitational forces on a given element [92].

equation solution techniques such as successive over-relaxation (see [108, 68]). Next we estimate the gradients of the gravitational potential at each particle’s location using Eq. (2.53) and Eq. (2.48). This completes the computation of the gravitational force at the particle. Next we calculate the density at each particle according to Eq. (2.58) and using the equation of state we now have the corresponding pressures. The gradients of the kernel are easily obtained and once calculated we have the pressure forces as well. With these data, we have a complete characterization of the forces in Eq. (2.62) and can take a time step forward for each particle using, for example, the staggered leap-frog method.

While we can employ this algorithm in principle, we will not do so. There are two reasons for doing so. First, our primary purpose for the above derivation was to develop our Fat Particle method within a known context so that we would have a guide for our relativistic explorations. Second, the state-of-the-art in SPH is quite advanced and there exist a host of commonly accepted modifications which we have ignored. Probably the most important of these is the inclusion of artificial viscosity to control particle penetration. SPH does not require that the velocity field be single valued. Two or more particles, with different velocities, may occupy the same positions. This leads to the problem of particle penetration, which at low Mach number simulations is not expected to be a problem but which must be addressed otherwise [94]. To address this problem, artificial viscosity is introduced (see *e.g.*, [43]) into the symmetric additive momentum equation using the form developed by Gingold and Monaghan [50]. The inclusion of this term, which is equivalent to the addition of a ‘viscous pressure’, adds a heat source that must be accounted for in the energy balance. Thus we need to solve either the evolution for the specific entropy or the specific internal energy. Since the artificial viscosity has to be added in by hand, it is not derivable from our variational computation and we are faced with constructing the appropriate energy equation. Starting from the symmetric additive momentum equation, Benz [10] demonstrates how to derive one form of the energy equation. Unfortunately, others are also possible and the interested reader is directed to the many of the references cited already for lively discussions of the pros

and cons of different forms. Another important modification is the use of variable smoothing lengths to ensure that each smoothing kernel samples approximately the same number of nearby particles. This is particularly important when high density gradients are present or in the case of gravitational collapse. Adopting a variable smoothing length violates energy conservation unless additional terms are added to the energy equation. These ‘grad-h’ terms are discussed in detail in [91, 59, 15, 101]. Nothing prevents us from adopting a variable smoothing length in our variational principle. Doing so ensures that we will automatically include these terms in the momentum and energy equations. Since their inclusion only complicates an already complex discussion and are not needed for the applications we will be pursuing, this modification is left for a later analysis. Finally, accurate modeling of astrophysical phenomena often require modeling of additional physics, such as magnetic fields, radiation heating, nucleosynthesis and the like. The inclusion of these terms is possible in SPH and is discussed in the review by Benz [10]. Again, the inclusion of these effects falls outside of the scope here and will be left for a sequel.

2.7 Classical Fat Particle Equations

In this section, we adapt the formalism we derived in the previous section to the case where we have a small number of fluid elements, most often one or two. To distinguish from the SPH case, with generally 10^3 - 10^5 particles, we will refer to these elements as Fat Particles. Conceptually, we imagine a Fat Particle as a single compact object such as a main sequence star, a white dwarf, a neutron star, etc. It may seem unusual to do so since the regular interpretation of a fluid element is that it is a parcel large enough so that we can ignore the internal motions on the molecular scale but small enough such that its physical properties are constant across its extent. However, it is also common to think of a variety of fluids as single entities. When describing a swimming pool, we don’t specify individual fluid elements. We comfortably talk about the pressure or temperature of the pool, noting, where needed, how they vary

with depth. The fact that the swimming pool is moving inertially as the Earth rotates and revolves plays no role in our planning on a warm summer's day. Likewise, we often talk about the density and pressure profiles of the Earth's atmosphere or the solar interior.⁷ As long as the internal degrees of freedom are effectively isolated from the overall motion of the center-of-mass, our viewpoint is valid. What is ignored is the possible excitation of hydrodynamical modes due to the forces confronted by the center-of-mass. This is an approximation that we are content to employ with this understanding.

To illustrate our point-of-view, consider a single self-gravitating Fat Particle. We will demand that the solution of Poisson's equation be well defined and that the momentum equation have a solution that leave an initial stationary Fat Particle at rest. This last requirement ensures that the Fat Particle does not move due to the pressure or gravitational forces it generates. The pressure required to keep the Fat Particle from collapsing will not be explicitly calculated but will be consistent with the barotropic equation of state Eq. (2.2) that we have employed above. Furthermore, as we will not be approximating our integrals numerically, we will drop the awkward normalization terms \mathcal{N} without loss of generality. Note that the steps we follow below are in direct correspondence with the algorithm outlined at the end of Section 2.6.

The density profile of our Fat Particle

$$\rho(\vec{x}) = mW(\vec{x} - \vec{z}) \tag{2.65}$$

is obtained from Eq. (2.56). The solution to Poisson's equation

$$\Phi(\vec{x}) = \int d^3x' \frac{mW(\vec{x}' - \vec{z})}{|\vec{x} - \vec{x}'|} \tag{2.66}$$

follows immediately from elementary considerations. This solution, which is of the type usually discussed in intermediate mechanics, is perfectly well defined. Our Fat Particle viewpoint has passed its first test. Next we examine the momentum equation

⁷It is interesting to find a density profile for a star in the work by Prialnik [109] that can be described by the Misner n -family kernel for $n = 1$

Eq. (2.63). We need not calculate the density at the Fat Particle since the $\nabla_A W_{AB}$ term is identically zero. The resulting momentum equation becomes

$$\frac{d^2 \vec{z}}{dt^2} = -\frac{\partial \Phi}{\partial \vec{z}} \quad . \quad (2.67)$$

To determine the right hand side, we first need to compute the gravitational potential at the Fat Particle's position according to the smoothing relation Eq. (2.55)

$$\Phi(\vec{z}) = \int d^3 x d^3 x' \frac{m W(\vec{z} - \vec{x}) W(\vec{x}' - \vec{z})}{|\vec{x} - \vec{x}'|} \quad . \quad (2.68)$$

From this expression, we can calculate the gradient as

$$\begin{aligned} \frac{\partial \Phi(\vec{z})}{\partial \vec{z}} &= \int d^3 x d^3 x' \frac{m}{|\vec{x} - \vec{x}'|} \\ &\quad \left(\frac{\partial W(\vec{z} - \vec{x})}{\partial \vec{z}} W(\vec{x}' - \vec{z}) + W(\vec{z} - \vec{x}) \frac{\partial W(\vec{x}' - \vec{z})}{\partial \vec{z}} \right) \quad . \quad (2.69) \end{aligned}$$

Switching the variable of differentiation in each of the terms from \vec{z} to \vec{x} and \vec{x}' , respectively, and integrating by parts yields

$$\begin{aligned} \frac{\partial \Phi(\vec{z})}{\partial \vec{z}} &= \int d^3 x d^3 x' m W(\vec{z} - \vec{x}) W(\vec{x}' - \vec{z}) \\ &\quad \left(\frac{\partial}{\partial \vec{x}} + \frac{\partial}{\partial \vec{x}'} \right) \frac{1}{|\vec{x} - \vec{x}'|} \quad , \quad (2.70) \end{aligned}$$

from which we can immediately conclude

$$\frac{\partial \Phi(\vec{z})}{\partial \vec{z}} = 0 \quad . \quad (2.71)$$

Thus a single Fat Particle is a valid representation for a self-gravitating fluid, given the caveats discussed above.

Chapter 3

ADM Vacuum Equations

3.1 Introduction

Einstein's equations

$$G_{\mu\nu} = 8\pi T_{\mu\nu} \tag{3.1}$$

comprise 10 non-linear coupled partial differential equations that depend on the four spacetime variables. That is to say, we are required to specify a spacetime manifold \mathcal{M} and equip it with a metric $g_{\mu\nu}$. Solutions to the Einstein equations, in either the presence or absence of matter (*i.e.*, $T_{\mu\nu} \neq 0$ or $T_{\mu\nu} = 0$, respectively), then give the form of the metric functions. A simple analysis of these equations (see *e.g.* Chapter 8 of Schutz [110] within the context of linearized gravity) demonstrates that not all of the 10 degrees of freedom are dynamic. In fact, 4 of the degrees of freedom connect the mass-energy at a given time to the curvature at that time (refer to the discussion in Section 21.1 of [89]). The other 6 degrees of freedom govern how the metric functions evolve as the time progresses. In order to better understand the physical content on Einstein's equations and to pave the way for numerical solution of these equations, we would like to have a general prescription for separating the 'constraint' equations from the 'dynamic' equations.

To accomplish this separation, we follow the approach of Arnowitt, Deser and Misner (ADM) that they explored in the late 1950's and early 1960's (see [5] for a summary of their work and the references to the original articles). In their approach, spacetime is subjected to a '3+1' splitting that automatically separates Einstein's

equations into a set of constraint and evolution equations. Excellent reviews of the ADM formalism are available [89, 133, 127, 107] and the results presented below are a synthesis of those cited.

In the remainder of this chapter, we present the ADM approach in a form suitable for the discretization we employed in Chapter 2. We first summarize the 3+1 decomposition in Section 3.2. This section borrows heavily from material in Chapters 3 and 4 of Poisson [107]. In Section 3.3, we transform the Einstein-Hilbert action to construct, as Arnowitt, Deser, and Misner did, a corresponding variational principle. Section 3.3 is based on Chapter 21 of MTW [89]. The resulting ADM action is analogous to the Newtonian one I_G employed in Chapter 2. Subsequent variations, performed in Section 3.4, provide the constraint and dynamical equations for vacuum solutions. This section is based partially on Appendix E of Wald [127] but much of the notation and organization of the variations are my own. In the next chapter, we will extend this principle to include an ideal fluid as a source.

3.2 Spacetime Slicing

To accomplish the ADM 3+1 decomposition, introduce a scalar field $t(x^\alpha)$ such that $t = \text{constant}$ describes a family of non-intersecting spacelike hypersurfaces Σ_t . This “time-function” is completely arbitrary; the only requirements are that t be a single-valued function of the coordinates x^α and that the normal to the hypersurface

$$n_\alpha = \frac{-t_{,\alpha}}{|g^{\mu\nu}t_{,\mu}t_{,\nu}|^{1/2}} \quad (3.2)$$

be future pointing.

On each hypersurface, we install coordinates y^i . We connect the coordinates on one hypersurface with the others by constructing a congruence of curves $\gamma_{\mathcal{P}}$ that intersects each hypersurface, doing so at a point \mathcal{P} on Σ_t , at point \mathcal{P}' on $\Sigma_{t'}$, and so on, as shown in Figure 3.1.

These curves need not be geodesics nor do they need to intersect the hypersurfaces orthogonally. We use t as a parameter for these curves and the vector $t^\alpha = dx^\alpha/dt$

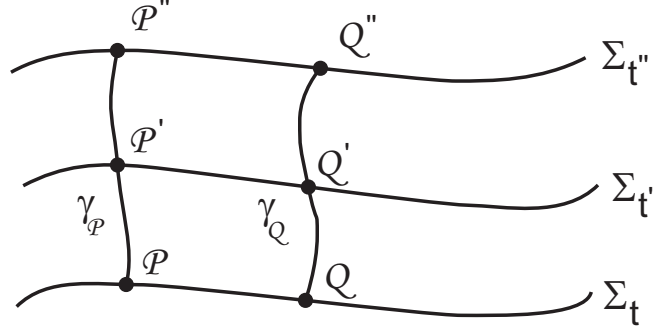


Figure 3.1: The slicing of the spacetime manifold \mathcal{M} by spacelike hypersurfaces Σ_t as described in the text. The curve $\gamma_{\mathcal{P}}$ connects the distinct points \mathcal{P} , \mathcal{P}' , and \mathcal{P}'' in \mathcal{M} since each point shares a common coordinate label in each of the Σ_t , $\Sigma_{t'}$, and $\Sigma_{t''}$.

is thus tangent to the curves. It is easy to see that $t^\alpha \partial_\alpha t = 1$, which assures us that n_α is future pointing. Now, if we specify that the hypersurface coordinates of \mathcal{P} are given by $y^i(\mathcal{P})$ we can naturally specify the coordinates of \mathcal{P}' as $y^i(\mathcal{P}) = y^i(\mathcal{P}')$. That is to say that y^i is held constant along each curve. In this fashion, we have constructed a coordinate system (t, y^i) for our spacetime.

As a consequence, the original spacetime coordinates can be defined in terms of (t, y^i) . A new set of basis vectors in the spacetime can be defined as

$$t^\alpha = \left(\frac{\partial x^\alpha}{\partial t} \right)_{y^i} , \quad (3.3)$$

where t^α points along the direction of increasing t , and

$$e_i^\alpha = \left(\frac{\partial x^\alpha}{\partial y^i} \right)_t \quad (3.4)$$

are vectors lying within Σ_t .

The set of vectors $\{\bar{t}, \bar{e}_i\}$, as defined in Eqs. (3.3) and (3.4), form a coordinate basis. As a consequence, the set is Lie transported by itself

$$\begin{aligned} \mathcal{L}_{\bar{t}} \bar{e}_i &= 0 \quad , \\ \mathcal{L}_{\bar{e}_i} \bar{t} &= 0 \quad , \\ \mathcal{L}_{\bar{e}_i} \bar{e}_j &= 0 \quad . \end{aligned} \quad (3.5)$$

Also, since the congruence $\gamma_{\mathcal{P}}$ was not required to be perpendicular to Σ_t , the vector \bar{t} will not coincide with the normal \bar{n} . Taking the normalization in Eq. (3.2) to be defined such that

$$n_\beta \equiv -\alpha \partial_\beta t \quad , \quad (3.6)$$

where the quantity α is called the lapse. The vector \bar{t} can be expressed in terms of the set $\{\bar{n}, \bar{e}_i\}$ as

$$\bar{t} = \alpha \bar{n} + \beta^i \bar{e}_i \quad , \quad (3.7)$$

which meets the requirement, $t^\alpha \partial_\alpha t = 1$ along \bar{t} . Note that each \bar{e}_i are orthogonal to the normal since

$$e_i^\alpha n_\alpha = -\alpha \frac{\partial x^\alpha}{\partial y^i} \frac{\partial t}{\partial x^\alpha} = \frac{\partial t}{\partial y^i} = 0 \quad . \quad (3.8)$$

A displacement dy^i within Σ_t corresponds to a constrained displacement $dx^\alpha = (\partial x^\alpha / \partial y^i) dy^i$ in \mathcal{M} . Thus the line element within Σ_t is given by

$$\begin{aligned} ds_\Sigma^2 &= g_{\alpha\beta} dx^\alpha dx^\beta \\ &= g_{\alpha\beta} e_i^\alpha e_j^\beta dy^i dy^j \\ &= \gamma_{ij} dy^i dy^j \quad , \end{aligned} \quad (3.9)$$

where γ_{ij} is termed the induced metric on Σ_t . The hypersurface is now equipped with a metric tensor γ_{ij} defined naturally in terms of the inner product

$$\gamma_{ij} = \bar{e}_i \cdot \bar{e}_j \quad (3.10)$$

of the spatial vectors spanning it.

The usual rules attach and we can construct and decompose vectors lying in the hypersurface using

$$\bar{A} = A^i \bar{e}_i \quad . \quad (3.11)$$

Taking the inner product of Eq. (3.11) with \bar{e}_j yields

$$\begin{aligned} \bar{A} \cdot \bar{e}_j &= A^i \bar{e}_i \cdot \bar{e}_j \\ &= A^i \gamma_{ij} \\ &= A_j \quad , \end{aligned} \quad (3.12)$$

from which we get the rule

$$A_j = A_\alpha e_j^\alpha \quad (3.13)$$

by writing the inner product in Eq. (3.12) out explicitly. Note that the A_j are space-time scalars, which is to say that they are invariant under coordinate transformations of the spacetime manifold \mathcal{M} .

We can also take an arbitrary spacetime tensor $T^{\mu\nu}$ and project it to the hypersurface using the projection operator

$$h_{\mu\nu} = g_{\mu\nu} + n_\mu n_\nu \quad . \quad (3.14)$$

It is obvious from the definition Eq. (3.14) that $h_{\mu\nu}$ lies entirely in the hypersurface. Contracting $h_{\mu\nu}$ on both indices with e_i^μ and e_j^ν yields

$$h_{\mu\nu} e_i^\mu e_j^\nu = g_{\mu\nu} e_i^\mu e_j^\nu = \gamma_{ij} \quad (3.15)$$

since $e_i^\alpha n_\alpha = 0$. The projection tensor is the spacetime version of the induced metric of the hypersurface.

A similar procedure can be done with tensors with covariant components, such as $T^\mu{}_\nu$. We can see that the tensor algebra on the hypersurface is well-defined and complete, allowing us to move tensors back and forth between the hypersurface and spacetime representations. As an example, we derive an expression that will be useful latter.

Consider Eq. (3.14) with both indices raised and arranged so that the spacetime metric is isolated on the left-hand side

$$g^{\mu\nu} = h^{\mu\nu} - n^\mu n^\nu \quad . \quad (3.16)$$

Since $h^{\mu\nu}$ lies within Σ_t , it admits the representation

$$h^{\mu\nu} = h^{ij} e_i^\mu e_j^\nu \quad . \quad (3.17)$$

Substituting Eq. (3.17) into Eq. (3.16), yields

$$g^{\mu\nu} = h^{ij} e_i^\mu e_j^\nu - n^\mu n^\nu \quad (3.18)$$

or using Eq. (3.15)

$$g^{\mu\nu} = \gamma^{ij} e_i^\mu e_j^\nu - n^\mu n^\nu \quad . \quad (3.19)$$

This result will come in handy when we derive the Gauss-Weingarten equation below.

Next, we express the spacetime metric in its hypersurface representation. To do so, consider a displacement dx^α , which now is not restricted to Σ_t , as

$$\begin{aligned} dx^\alpha &= \frac{\partial x^\alpha}{\partial t} dt + \frac{\partial x^\alpha}{\partial y^i} dy^i \\ &= t^\alpha dt + e_j^\alpha dy^j \\ &= (\alpha n^\alpha + \beta^i e_i^\alpha dt) dt + e_i^\alpha dy^i \\ &= \alpha n^\alpha dt + e_i^\alpha (dy^i + \beta^i dt) \quad . \end{aligned} \quad (3.20)$$

Substituting Eq. (3.20) into $ds^2 = g_{\alpha\beta} dx^\alpha dx^\beta$ yields

$$ds^2 = -\alpha^2 dt^2 + \gamma_{ij} (dy^i + \beta^i dt) (dy^j + \beta^j dt) \quad . \quad (3.21)$$

In matrix form, the metric is represented as

$$g_{\mu\nu} = \begin{pmatrix} \beta^\ell \beta_\ell - \alpha^2 & \beta_i \\ \beta_j & \gamma_{ij} \end{pmatrix} \quad , \quad (3.22)$$

where $\beta^\ell \beta_\ell = \beta^k \beta^\ell \gamma_{k\ell}$. The inverse metric $g^{\mu\nu}$ can be determined by inverting the 4×4 matrix in Eq. (3.22). However, before proceeding, consider the component g^{tt} of the inverse metric. Using Eq. (A.7), it can be expressed as

$$g^{tt} = \text{cofactor}(g_{tt}) / \det g_{\mu\nu} \equiv \text{cofactor}(g_{tt}) / g \quad . \quad (3.23)$$

Using Eq. (A.4), $\text{cofactor}(g_{tt}) = \det \gamma_{ij} \equiv \gamma$. Since g^{tt} is defined as

$$\begin{aligned} g^{tt} &= \tilde{d}t \cdot \tilde{d}t \\ &= \tilde{d}x^\alpha \cdot \tilde{d}x^\beta \frac{\partial t}{\partial x^\alpha} \frac{\partial t}{\partial x^\beta} \\ &= g^{\alpha\beta} t_{,\alpha} t_{,\beta} \\ &= g^{\alpha\beta} \frac{n_\alpha n_\beta}{\alpha^2} \\ &= -\frac{1}{\alpha^2} \quad . \end{aligned} \quad (3.24)$$

Combining Eq. (3.23) with Eq. (3.24), we arrive at the simple result

$$\sqrt{-g} = \alpha \sqrt{\gamma} \quad . \quad (3.25)$$

With the forms of the metric (Eq. (3.22)) and g^{tt} (Eq. (3.24)), it is straightforward to compute the inverse by constructing $h^\mu{}_\nu$ in two separate ways. First, $h_{\mu\nu}$ can be determined. Second, $h^\mu{}_\nu$ can be constructed directly from $h^\mu{}_\nu = \delta^\mu{}_\nu + n^\mu n_\nu$ and then its index can be lowered. Equating the two, one arrives at

$$g^{\mu\nu} = \begin{pmatrix} \frac{-1}{\alpha^2} & \frac{\beta^i}{\alpha^2} \\ \frac{\beta^j}{\alpha^2} & \gamma^{ij} - \frac{\beta^i \beta^j}{\alpha^2} \end{pmatrix} \quad . \quad (3.26)$$

Next, we turn to defining a covariant derivative intrinsic to the hypersurface. We take as our definition

$$D_j A_i = A_{i|j} \equiv A_{\alpha;\beta} e_i^\alpha e_j^\beta \quad , \quad (3.27)$$

where A^α lies within Σ_t (*i.e.*, $A^\alpha = A^i e_i^\alpha$ and $A^\alpha n_\alpha = 0$). We start by expanding the right-hand side of Eq. (3.27)

$$\begin{aligned} A_{\alpha;\beta} e_i^\alpha e_j^\beta &= (A_\alpha e_i^\alpha)_{;\beta} e_j^\beta - A_\alpha e_i^\alpha{}_{;\beta} e_j^\beta \\ &= (A_i)_{;\beta} e_j^\beta - A^k e_{k\alpha} e_i^\alpha{}_{;\beta} e_j^\beta \\ &= A_{i,\beta} e_j^\beta - A^k e_k^\alpha e_{i\alpha;\beta} e_j^\beta \\ &= \frac{\partial A_i}{\partial x^\beta} \frac{\partial x^\beta}{\partial y^j} - A^k \Gamma_{kij} \\ &= A_{i,j} - A^k \Gamma_{kij} \quad , \end{aligned} \quad (3.28)$$

where we have defined

$$\Gamma_{kij} = e_k^\alpha e_{i\alpha;\beta} e_j^\beta \quad . \quad (3.29)$$

The definition in Eq. (3.27) will yield a valid covariant derivative provided that

$$\Gamma_{kij} = \frac{1}{2} (\gamma_{ki,j} + \gamma_{kj,i} - \gamma_{ij,k}) \quad . \quad (3.30)$$

Expanding the right-hand side of Eq. (3.29) yields

$$\begin{aligned} \Gamma_{kij} &= e_k^\alpha e_{i\alpha;\beta} e_j^\beta \\ &= e_k^\alpha g_{\alpha\gamma} e_i^\gamma{}_{;\beta} e_j^\beta \\ &= g_{\alpha\gamma} e_k^\alpha e_j^\beta (e_i^\gamma{}_{,\beta} + \Gamma^\gamma{}_{\sigma\beta} e_i^\sigma) \\ &= g_{\alpha\gamma} e_k^\alpha e_j^\beta e_i^\gamma{}_{,\beta} + \Gamma_{\gamma\alpha\beta} e_i^\alpha e_j^\beta e_k^\gamma \end{aligned} \quad (3.31)$$

Using Eq. (3.15) in expanding the right-hand side of Eq. (3.30), we get

$$\begin{aligned} \frac{1}{2}(\gamma_{ki,j} + \gamma_{kj,i} - \gamma_{ij,k}) &= \frac{1}{2}(g_{\gamma\alpha,\beta} + g_{\gamma\beta,\alpha} - g_{\alpha\beta,\gamma}) e_i^\alpha e_j^\beta e_k^\gamma \\ &\quad + g_{\alpha\gamma} e_k^\alpha e_i^\gamma{}_{,j} \quad . \end{aligned} \quad (3.32)$$

Since, by the chain rule, $e_i^\gamma{}_{,j} = e_i^\gamma{}_{,\beta} e_j^\beta$, the two expressions match and our definition of the covariant derivative is valid.

Now, consider the vector $A^\alpha{}_{;\beta} e_j^\beta$, which is the directional derivative of the spatial vector A^γ along the direction \bar{e}_j . Despite the fact that \bar{A} and \bar{e}_j are both contained in the hypersurface, $A^\alpha{}_{;\beta} e_j^\beta$ will generically have a normal component. To see this, write $A^\alpha{}_{;\beta} e_j^\beta$ as $g^\alpha{}_\mu A^\mu{}_{;\beta} e_j^\beta$ and use Eq. (3.19)

$$\begin{aligned} A^\alpha{}_{;\beta} e_j^\beta &= (\gamma^{k\ell} e_k^\alpha e_{\ell\mu} - n^\alpha n_\mu) A^\mu{}_{;\beta} e_j^\beta \\ &= (A^\mu{}_{;\beta} e_j^\beta e_{\ell\mu}) \gamma^{k\ell} e_k^\alpha - (n_\mu A^\mu{}_{;\beta} e_j^\beta) n^\alpha \quad . \end{aligned} \quad (3.33)$$

Since $A^\mu n_\mu = 0$, we can switch the covariant derivative from A^μ to n_μ at the cost of a sign. Then, using Eqs. (3.11) and (3.27), we can write Eq. (3.33) as

$$A^\alpha{}_{;\beta} e_j^\beta = A^k{}_{|j} e_k^\alpha + A^k (n_{\mu;\beta} e_j^\beta e_k^\mu) n^\alpha \quad . \quad (3.34)$$

If we define the extrinsic curvature tensor as

$$K_{kj} = -n_{\mu;\beta} e_j^\beta e_k^\mu \quad , \quad (3.35)$$

then we can write Eq. (3.34) as

$$A^\alpha{}_{;\beta} e_j^\beta = A^k{}_{|j} e_k^\alpha - A^k K_{kj} n^\alpha \quad . \quad (3.36)$$

Before moving on, we can prove two useful facts concerning the extrinsic curvature. First, it is a symmetric tensor as can be seen by

$$\begin{aligned} n_{\alpha;\beta} e_i^\alpha e_j^\beta &= -n_\alpha e_i^\alpha{}_{;\beta} e_j^\beta \\ &= -n_\alpha e_j^\alpha{}_{;\beta} e_i^\beta \\ &= n_{\alpha;\beta} e_j^\alpha e_i^\beta \quad , \end{aligned} \quad (3.37)$$

where we have used the orthogonality between n_α and e_i^α and the fact that, by construction, the basis vectors in the hypersurface Lie transport each other, so that

Eq. (3.5) can be used. Second, from its symmetry, the extrinsic curvature can be expressed as

$$K_{ij} = -n_{(\alpha;\beta)} e_i^\alpha e_j^\beta = -\frac{1}{2} (\mathcal{L}_{\bar{n}} g_{\alpha\beta}) e_i^\alpha e_j^\beta \quad . \quad (3.38)$$

Now, returning to Eq. (3.36), if we substitute e_i^α for A^α , which by Eq. (3.11) implies $A^j = \delta^j_i$, we get

$$e_i^\alpha{}_{;\beta} e_j^\beta = \Gamma^k_{ij} e_k^\alpha - K_{ij} n^\alpha \quad , \quad (3.39)$$

which is known as the Gauss-Weingarten equation.

Now, we turn to a characterization of the intrinsic curvature defined on the hypersurface in terms of the spacetime curvature. The intrinsic curvature is defined by

$$A^i{}_{|jk} - A^i{}_{|kj} = -R^i{}_{\ell jk} A^\ell \quad . \quad (3.40)$$

To relate $R^i{}_{\ell jk}$ to $R^\mu{}_{\nu\alpha\beta}$, we start with the Gauss-Weingarten equation expressed as

$$(e_i^\alpha{}_{;\beta} e_j^\beta)_{;\gamma} e_\ell^\gamma = (\Gamma^k_{ij} e_k^\alpha - K_{ij} n^\alpha)_{;\gamma} e_\ell^\gamma \quad . \quad (3.41)$$

Expanding both sides and solving for $e_i^\alpha{}_{;\beta\gamma} e_j^\beta e_k^\gamma$ yields

$$\begin{aligned} e_i^\alpha{}_{;\beta\gamma} e_j^\beta e_k^\gamma &= \Gamma^\ell_{ij,k} e_\ell^\alpha + \Gamma^\ell_{ij} (\Gamma^m_{lk} e_m^\alpha - K_{lk} n^\alpha) \\ &\quad - K_{ij,k} n^\alpha - K_{ij} n^\alpha{}_{;\gamma} e_k^\gamma \\ &\quad - \Gamma^\ell_{jk} (\Gamma^m_{i\ell} e_m^\alpha - K_{i\ell} n^\alpha) + K_{jk} e_i^\alpha{}_{;\beta} n^\beta \quad . \end{aligned} \quad (3.42)$$

Repeating for $e_i^\alpha{}_{;\gamma\beta} e_j^\beta e_k^\gamma$ and subtracting gives

$$\begin{aligned} R^\mu{}_{\alpha\beta\gamma} e_i^\alpha e_j^\beta e_k^\gamma &= R^m{}_{ijk} e_m^\mu + (K_{ij|k} - K_{ik|j}) n^\mu \\ &\quad + K_{ij} n^\mu{}_{;\gamma} e_k^\gamma - K_{ik} n^\mu{}_{;\beta} e_j^\beta \quad . \end{aligned} \quad (3.43)$$

Contracting with e_ℓ^μ gives

$$R_{\mu\alpha\beta\gamma} e_i^\alpha e_j^\beta e_k^\gamma e_\ell^\mu = R_{\ell ijk} - K_{ij} K_{\ell k} + K_{ik} K_{\ell j} \quad , \quad (3.44)$$

which is one of the Gauss-Codazzi equations. The other is obtained by projecting Eq. (3.43) along n_μ ; however, this is not needed for our purposes.

Finally, we want to compute the Ricci scalar. From the definition of the Einstein tensor, the Ricci scalar can be isolated by contractions on both its indices with the unit normal to give

$$R = 2 (G_{\alpha\beta} n^\alpha n^\beta - R_{\alpha\beta} n^\alpha n^\beta) \quad . \quad (3.45)$$

The term involving the Einstein tensor in Eq. (3.45) can be related to contractions on the Riemann tensor through an equivalent route. Starting from

$$R_{\alpha\beta\gamma\delta} h^{\alpha\gamma} h^{\beta\delta} = R + 2R_{\alpha\beta} n^\alpha n^\beta = 2G_{\alpha\beta} n^\alpha n^\beta \quad , \quad (3.46)$$

where we used Eq. (3.16) and the fact that $R_{\alpha\beta\gamma\delta} n^\alpha n^\beta n^\gamma n^\delta = 0$ due to the symmetry of Riemann. Using Eq. (3.17), the left-hand side of Eq. (3.46) can be expressed as

$$R_{\alpha\beta\gamma\delta} h^{\alpha\gamma} h^{\beta\delta} = \gamma^{ij} \gamma^{kl} R_{\alpha\beta\gamma\delta} e_i^\alpha e_j^\beta e_k^\gamma e_l^\delta \quad . \quad (3.47)$$

Combining Eqs. (3.44) and (3.47) yields

$$\begin{aligned} R_{\alpha\beta\gamma\delta} h^{\alpha\gamma} h^{\beta\delta} &= \gamma^{ij} \gamma^{kl} (R_{ijkl} - K_{kj} K_{il} + K_{kl} K_{ij}) \\ &= {}^{(3)}R + Tr(K)^2 - Tr(K^2) \quad , \end{aligned} \quad (3.48)$$

where ${}^{(3)}R$ is the intrinsic Ricci scalar on Σ_t , $Tr(K) = K_{kl} \gamma^{kl} = K^\ell_\ell$, and $Tr(K^2) = K^{ik} K_{ik}$. Combining Eqs. (3.46) and (3.48) gives

$${}^{(3)}R + Tr(K)^2 - Tr(K^2) = R + 2R_{\alpha\beta} n^\alpha n^\beta \quad . \quad (3.49)$$

The last term to be expanded is $R_{\alpha\beta} n^\alpha n^\beta$. Using the definition of the Riemann tensor, we get

$$\begin{aligned} R_{\alpha\beta} n^\alpha n^\beta &= R^\gamma_{\alpha\gamma\beta} n^\alpha n^\beta \\ &= n^\beta (\nabla_\gamma \nabla_\beta - \nabla_\beta \nabla_\gamma) n^\gamma \\ &= +n^\beta_{;\beta} n^\gamma_{;\gamma} - n^\beta_{;\gamma} n^\gamma_{;\beta} \\ &\quad + (n^\beta n^\gamma_{;\beta})_{;\gamma} - (n^\beta n^\gamma_{;\gamma})_{;\beta} \end{aligned} \quad (3.50)$$

The first two terms of Eq. (3.50) can be simplified using Eq. (3.17) and Eq. (3.19)

$$\begin{aligned} n^\beta_{;\gamma} n^\gamma_{;\beta} &= g^{\beta\delta} n_{\delta;\gamma} g^{\gamma\tau} n_{\tau;\beta} \\ &= Tr(K^2) \end{aligned} \quad (3.51)$$

and

$$n^\alpha{}_{;\alpha} = g^{\alpha\beta} n_{\alpha;\beta} = -Tr(K) \quad (3.52)$$

where we used Eqs. (3.17) and (3.19), and the fact that $(n^\alpha n_\alpha)_{;\beta} = n^\alpha n_{\alpha;\beta} = 0$. Thus we arrive at

$$R = {}^{(3)}R + Tr(K^2) - Tr(K)^2 - 2 \left[(n^\beta n^\gamma{}_{;\beta})_{;\gamma} - (n^\beta n^\gamma{}_{;\gamma})_{;\beta} \right] \quad . \quad (3.53)$$

3.3 Gravitational Action in 3+1

In this section, we want to perform the spacetime splitting of the previous section on the Einstein-Hilbert action

$$I_g = \frac{1}{16\pi} \int d^4x \sqrt{-g} R \quad . \quad (3.54)$$

In our treatment, we will ignore all boundary terms and the corresponding boundary actions that are added to Eq. (3.54). We direct the reader to [127] and [107] for further discussions of these terms. Also, we will drop the ‘(3)’ notation and hereafter will refer to the Ricci scalar intrinsic to Σ_t as simply R .

Using Eqs. (3.25) and (3.53), we obtain

$$I_g = \frac{1}{16\pi} \int d^3y dt \mathcal{L} \quad , \quad (3.55)$$

where $\mathcal{L} = \alpha \sqrt{\gamma} (R + Tr(K^2) - Tr K^2)$ and where we have discarded the total divergence terms.

Now, we wish to transform to the Hamiltonian viewpoint in which I_g is expressed in terms of the time derivative $\partial_t \gamma_{ij}$ defined as

$$\partial_t \gamma_{ij} = \mathcal{L}_{\bar{t}} \gamma_{ij} \quad . \quad (3.56)$$

Expanding the right-hand side of Eq. (3.56) yields

$$\begin{aligned} \partial_t \gamma_{ij} &= \mathcal{L}_{\bar{t}} (g_{\mu\nu} e_i^\mu e_j^\nu) \\ &= (\mathcal{L}_{\bar{t}} g_{\mu\nu}) e_i^\mu e_j^\nu \\ &= (t_{\mu;\nu} + t_{\nu;\mu}) e_i^\mu e_j^\nu \end{aligned} \quad (3.57)$$

where Eq. (3.5) and Eq. (A.26) were used.

Substituting Eqs. (3.7), (3.35), and (3.41) into Eq. (3.57) and after a little algebra, we get

$$\partial_t \gamma_{ij} = -2\alpha K_{ij} + D_j \beta_i + D_i \beta_j \quad , \quad (3.58)$$

where Eqs. (3.27) and (3.37) were used.

We define the conjugate momentum as

$$\pi^{ij} = \frac{\partial \mathcal{L}}{\partial (\partial_t \gamma_{ij})} = \frac{\partial \mathcal{L}}{\partial K_{ij}} \frac{\partial K_{ij}}{\partial (\partial_t \gamma_{ij})} \quad (3.59)$$

and use Eq. (3.38) to arrive at

$$\pi^{ij} = \sqrt{\gamma} [\gamma^{ij} \text{Tr}(K) - K^{ij}] \quad . \quad (3.60)$$

The Hamiltonian density is defined as

$$\mathcal{H} = \pi^{ij} \partial_t \gamma_{ij} - \mathcal{L} \quad . \quad (3.61)$$

Contracting Eq. (3.60) with γ_{ij} gives

$$\pi^{ij} \gamma_{ij} = \text{Tr}(\pi) = 2\sqrt{\gamma} \text{Tr}(K) \quad (3.62)$$

and using Eq. (3.62) allows Eq. (3.60) to be inverted, giving K^{ij} in terms of π^{ij} as

$$K^{ij} = \frac{\text{Tr}(\pi)}{2\sqrt{\gamma}} \gamma^{ij} - \frac{\pi^{ij}}{\sqrt{\gamma}} \quad . \quad (3.63)$$

Using Eq. (3.63) in Eq. (3.55) gives the Hamiltonian density as

$$\mathcal{H} = \alpha \sqrt{\gamma} \left[\frac{\text{Tr}(\pi^2)}{\gamma} - \frac{\text{Tr}(\pi)^2}{2\gamma} - R \right] - 2\beta_i \pi^{ij}{}_{|j} + 2(\beta_i \pi^{ij})_{|j} \quad . \quad (3.64)$$

Since the last term in Eq. (3.64) is a total divergence, it will be ignored. Inverting Eq. (3.61) gives the Lagrangian density as

$$\mathcal{L} = \pi^{ij} \partial_t \gamma_{ij} - \alpha R^0 - \beta_i R^i \quad , \quad (3.65)$$

where

$$R^0 = \sqrt{\gamma} \left[\frac{\text{Tr}(\pi^2)}{\gamma} - \frac{\text{Tr}(\pi)^2}{2\gamma} - R \right] \quad (3.66)$$

and

$$R^i = -2\pi^{ij}{}_{|j} \quad . \quad (3.67)$$

Thus we finally arrive at the ADM action

$$I_{ADM} = \frac{1}{16\pi} \int d^3y dt [\pi^{ij} \partial \gamma_{ij} - \alpha R^0 - \beta_k R^k] \quad , \quad (3.68)$$

(compare *e.g.* Eq. (21.95) of MTW [89]).

3.4 Vacuum ADM Equations

To obtain the ADM system of equations in a vacuum, we must take variations of Eq. (3.68) with respect to the lapse α , the shift β_k , the conjugate momentum π^{ij} , and the three metric γ_{ij} .

We first consider the variation with respect to the lapse. Since the lapse enters into the action in a non-dynamical way this variation will yield a constraint equation that the initial value data must satisfy and which will remain satisfied at each subsequent time.

The variation is easy to carry out yielding

$$\delta I_{ADM}|_{\delta\alpha} = \frac{1}{16\pi} \int d^3y dt (-R^0) \delta\alpha \quad . \quad (3.69)$$

Setting the variation equal to zero and substituting in the definition of R^0 found in Eq. (3.66) results in

$$\sqrt{\gamma} \left(\frac{Tr(\pi^2)}{\gamma} - \frac{Tr(\pi)^2}{2\gamma} - R \right) = 0 \quad . \quad (3.70)$$

This relation, which is known as the Hamiltonian constraint, is in the standard form for the (γ, π) system (see *e.g.* Eq. 7-3.14a in [5].)

We next consider the variation with respect to the shift. Like the lapse, the shift enters into the action in a non-dynamical way. Subsequent variation will also yield a set of constraint equations that must be satisfied by the initial value data and which will remain satisfied as the system evolves.

The variation is easy to carry out yielding

$$\delta I_{ADM}|_{\delta\beta_i} = \frac{1}{16\pi} \int d^3y dt (-R^i) \delta\beta_i \quad . \quad (3.71)$$

Setting the variation equal to zero and substituting in the definition of R^i found in Eq. (3.67) results in

$$D_j \pi^{ij} = 0 \quad . \quad (3.72)$$

These relations, which are known as the momentum constraints, are in the standard form for the (γ, π) system [5].

We next consider the variation of the ADM action with respect to the conjugate momentum, π^{ij} . We require that we obtain the relationship in Eq. (3.58), defining the time derivative of the 3-metric in terms of the conjugate momentum rather than the extrinsic curvature.

This variation is somewhat more complex than the variations with respect to either the lapse or the shift. Taking the variation symbolically yields

$$\delta I_{ADM}|_{\delta\pi^{ij}} = \frac{1}{16\pi} \int d^3y dt [\partial_t \gamma_{ij} \delta\pi^{ij} - \delta(\alpha R^0)|_{\delta\pi^{ij}} - \delta(\beta_k R^k)|_{\delta\pi^{ij}}] \quad . \quad (3.73)$$

We will handle each of the latter two terms in Eq. (3.73) separately, starting with the term involving R^0 . Since no derivatives of the conjugate momentum appear in the definition of R^0 , the corresponding variation is easy to take:

$$\begin{aligned} \int d^3y dt \delta(\alpha R^0)|_{\delta\pi^{ij}} &= \int d^3y dt \alpha \delta R^0 \\ &= \int d^3y dt \alpha \delta \left[\frac{Tr(\pi^2)}{\sqrt{\gamma}} - \frac{Tr(\pi)^2}{2\sqrt{\gamma}} - R \right] \\ &= \int d^3y dt \frac{1}{\sqrt{\gamma}} (2\pi_{ij} - Tr(\pi)\gamma_{ij}) \delta\pi^{ij} \quad . \quad (3.74) \end{aligned}$$

Thus the functional variation of αR^0 as the conjugate momentum is varied can be written as

$$\delta(\alpha R^0)|_{\delta\pi^{ij}} = \frac{\alpha}{\sqrt{\gamma}} (2\pi_{ij} - Tr(\pi)\gamma_{ij}) \delta\pi^{ij} \quad . \quad (3.75)$$

The variation of the next term, involving R^i is a bit more involved since the definition of R^i contains a spatial derivative of π^{ij} . Carrying out the variation results

in

$$\begin{aligned} \int d^3y dt \delta (\beta_k R^k) |_{\delta\pi^{ij}} &= \int d^3y dt \beta_k \delta (-2D_\ell \pi^{k\ell}) \\ &= -2 \int d^3y dt \beta_k (\partial_\ell \delta\pi^{k\ell} + \delta\pi^{\ell j} \Gamma^k_{\ell j}) \quad , \quad (3.76) \end{aligned}$$

where the symmetry of the connection coefficients was used to simplify last line of Eq. (3.76).¹ Integrating Eq. (3.76) once by parts to move the spatial derivative from to the shift and noting that π^{ij} is symmetric in its indices yields

$$\int d^3y dt \delta (\beta_k R^k) |_{\delta\pi^{ij}} = \int d^3y dt 2 [\partial_{(i} \beta_{j)} - \beta_k \Gamma^k_{ij}] \delta\pi^{ij} \quad . \quad (3.77)$$

Recognizing the form of the three-dimensional covariant derivative in Eq. (3.77) allows us to write the functional variation of $\beta_k R^k$ as the conjugate momentum is varied as

$$\delta (\beta_k R^k) |_{\delta\pi^{ij}} = 2D_{(i} \beta_{j)} \delta\pi^{ij} \quad . \quad (3.78)$$

Substituting the results from Eq. (3.75) and Eq. (3.78) into Eq. (3.73) and setting the variation equal to zero yields

$$\partial_t \gamma_{ij} = \frac{\alpha}{\sqrt{\gamma}} (2\pi_{ij} - Tr(\pi)\gamma_{ij}) + 2D_{(i} \beta_{j)} \quad , \quad (3.79)$$

which is just Eq. (3.58) with the extrinsic curvature eliminated in favor of the conjugate momentum by using Eqs. (3.60) and (3.62).

Finally, we consider the variation of the ADM action with respect to the 3-metric. The computation is lengthy and our approach to managing the complexity will be to tackle each term in the action separately. Liberal use of Riemann normal coordinates will also be employed to express covariant derivatives in terms of partial derivatives. Subsequent integration by parts will be used to move the partial derivatives from the variations of the 3-metric, $\delta\gamma_{ij}$. At the end, we re-interpret the partial derivatives as covariant derivatives using a ‘comma goes to semi-colon’ rule.

The payoff of this approach will more than compensate us for our investment. First the basic structure will carry over directly in both the continuum and Fat

¹Note that by its definition, π^{ij} is a tensor density and its covariant derivative is given by Eq. (A.25).

Particle hydrodynamic actions dealt with latter, allowing us to concentrate on the new features introduced. Second, the compact structure derived here makes it easy to ensure the quality of our computations.

With these encouraging and cautionary remarks under our belt, we can now turn to the desired variation. Symbolically, the variation becomes

$$\delta I_{ADM}|_{\delta\gamma_{ij}} = \int d^3x dt \left[\delta (\partial_t \gamma_{km}) \pi^{km} - \delta (\alpha R^0)|_{\delta\gamma_{ij}} - \delta (\beta_k R^k)|_{\delta\gamma_{ij}} \right] . \quad (3.80)$$

An integration by parts of the first term on the left-hand-side of Eq. (3.80) yields

$$\delta I_{ADM}|_{\delta\gamma_{ij}} = \int d^3x dt \left[-\partial_t \pi^{ij} \delta\gamma_{ij} - \delta (\alpha R^0)|_{\delta\gamma_{ij}} - \delta (\beta_k R^k)|_{\delta\gamma_{ij}} \right] . \quad (3.81)$$

Now we can examine the second term on Eq. (3.80), the term involving the variation of αR^0 as the three-metric is varied,

$$\int d^3x dt \delta (\alpha R^0)|_{\delta\gamma_{ij}} = \int d^3x dt \alpha \delta R^0|_{\delta\gamma_{ij}} . \quad (3.82)$$

Note that since there is no chance for confusion, we will usually drop the explicit indication that the variation is taken with respect to the three-metric.

Begin by expanding the integrand on the right-hand-side of Eq. (3.82) using the definition Eq. (3.66) of R^0 to get

$$\begin{aligned} \int d^3x dt \alpha \delta R^0|_{\delta\gamma_{ij}} &= \int d^3x dt \alpha \sqrt{\gamma} \frac{R^0}{2} \gamma^{ij} \delta\gamma_{ij} \\ &+ \int d^3x dt \alpha \sqrt{\gamma} \delta \left[\frac{Tr(\pi^2)}{\gamma} - \frac{Tr(\pi)^2}{2\gamma} \right] \\ &- \int d^3x dt \alpha \sqrt{\gamma} \delta R \quad , \end{aligned} \quad (3.83)$$

where the formula for the derivative of the determinant of the metric Eq. (A.9) was used for the first term in the last line of Eq. (3.83) and where $R = R^i_i = R^{ij} \gamma_{ij}$. After some straightforward manipulations of the second term in Eq. (3.83) one arrives at

the relationship

$$\delta \left[\frac{Tr(\pi^2)}{\gamma} - \frac{Tr(\pi)^2}{2\gamma} \right] = \left[\frac{2\pi^i_n \pi^{nj}}{\gamma} - \frac{Tr(\pi)\pi^{ij}}{\gamma} + \left(\frac{Tr(\pi)^2}{\gamma} - \frac{Tr(\pi^2)}{\gamma} \right) \gamma^{ij} \right] \delta\gamma_{ij} \quad . \quad (3.84)$$

Next we can deal with the last term in Eq. (3.83) by expanding

$$\begin{aligned} \int d^3x dt \alpha \sqrt{\gamma} \delta R &= \int d^3x dt \alpha \sqrt{\gamma} \delta (R_{kl} \gamma^{kl}) \\ &= \int d^3x dt \alpha \sqrt{\gamma} (\gamma^{ij} \delta R_{ij} - R^{ij} \delta\gamma_{ij}) \quad , \end{aligned} \quad (3.85)$$

and then simplifying the term involving δR_{ij} by using Riemann normal coordinates. First we expand the variation of the three-dimensional Ricci tensor (see Eq. (20) p. 580 of [72])

$$\int d^3x dt \alpha \sqrt{\gamma} \gamma^{kl} \delta R_{kl} = \int d^3x dt \alpha \sqrt{\gamma} \gamma^{kl} (\delta\Gamma^i_{kl,i} - \delta\Gamma^i_{ki,l}) \quad . \quad (3.86)$$

Integrating once by parts removes the partial derivatives from the variations in the connection coefficients to the lapse

$$\int d^3x dt \alpha \sqrt{\gamma} \gamma^{kl} \delta R_{kl} = - \int d^3x dt \sqrt{\gamma} \gamma^{kl} (\alpha_{,i} \delta\Gamma^i_{kl} - \alpha_{,l} \delta\Gamma^i_{ki}) \quad . \quad (3.87)$$

In normal coordinates, the variations in the connection coefficients can be expressed as

$$\delta\Gamma^i_{kl} = \frac{1}{2} \gamma^{im} \delta (\gamma_{mk,l} + \gamma_{ml,k} - \gamma_{kl,m}) \quad (3.88)$$

and

$$\delta\Gamma^i_{ki} = \frac{1}{2} \gamma^{im} \delta (\gamma_{mk,i} + \gamma_{mi,k} - \gamma_{ki,m}) \quad . \quad (3.89)$$

Substituting these relationships into Eq. (3.87) and performing additional integrations by parts to move the derivatives from the variations in the 3-metric to the lapse yields

$$\begin{aligned} \int d^3x dt \alpha \sqrt{\gamma} \gamma^{kl} \delta R_{kl} &= \int d^3x dt \sqrt{\gamma} \\ &\quad (D^i D^j \alpha - \gamma^{ij} D^\ell D_\ell \alpha) \delta\gamma_{ij} \quad , \end{aligned} \quad (3.90)$$

where we have employed the ‘comma goes to semi-colon rule’ to reinterpret the partial derivatives as spatial covariant derivatives. Combining Eqs. (3.91) and (3.85) and then substituting this result along with Eq. (3.84) into Eq. (3.83) yields

$$\int d^3x dt \alpha \delta R^0 = \int d^3x dt (\sqrt{\gamma} A^{ij} + \sqrt{\gamma} B \gamma^{ij}) \delta \gamma_{ij} \quad , \quad (3.91)$$

where

$$A^{ij} = \alpha \left(\frac{2\pi^i_n \pi^{nj}}{\gamma} - \frac{Tr(\pi)\pi^{ij}}{\gamma} + R^{ij} \right) - D^i D^j \alpha \quad (3.92)$$

and

$$B = \alpha \left(\frac{Tr(\pi)^2}{4\gamma} - \frac{Tr(\pi^2)}{2\gamma} - \frac{1}{2}R \right) + D^\ell D_\ell \alpha \quad . \quad (3.93)$$

Thus the functional variation of variations of the three-metric can be written as

$$\delta (\alpha R^0) |_{\delta \gamma_{ij}} = \sqrt{\gamma} (A^{ij} + B \gamma^{ij}) \quad , \quad (3.94)$$

with A^{ij} and B defined as above.

Next we turn to the variation of the third term of Eq. (3.80) in which $\beta_k R^k$ is varied as the 3-metric is varied

$$\int d^3x dt \delta (\beta_k R^k) |_{\delta \gamma_{ij}} = \int d^3x dt \beta_k (\delta R^k) |_{\delta \gamma_{ij}} \quad . \quad (3.95)$$

Expanding the right-hand side yields

$$\begin{aligned} \int d^3x dt \beta_k \delta R^k &= \int d^3x dt \beta_k \delta (-2D_m \pi^{km}) \\ &= -2 \int d^3x dt \beta_k \delta (\pi^{km}_{,m} + \pi^{mn} \Gamma^k_{mn}) \\ &= -2 \int d^3x dt \beta_k \pi^{mn} \delta \Gamma^k_{mn} \quad , \end{aligned} \quad (3.96)$$

where the symmetry of the conjugate momentum and the connection coefficients was used in simplifying the second line of Eq. (3.96). As before, we will continue to use Riemann normal coordinates and take any appropriate integration by parts to move derivatives from the terms involving the metric. After some straightforward algebra and accounting for the symmetry of the three-metric we arrive at

$$\begin{aligned} \int d^3x dt \beta_k \delta R^k &= \int d^3x dt [\beta^i \pi^{jk}_{,k} + \beta^j \pi^{ik}_{,k} \\ &\quad - (\pi^{ij}_{,k} \beta^k - \beta^i_{,k} \pi^{jk} - \beta^j_{,k} \pi^{ik} + \beta^k_{,k} \pi^{ij})] \delta \gamma_{ij} \\ &= \int d^3x dt \left(2\beta^{(i} \pi^{j)k}_{,k} - \mathcal{L}_{\vec{\beta}} \pi^{ij} \right) \delta \gamma_{ij} \quad , \end{aligned} \quad (3.97)$$

where the definition of the Lie derivative of a tensor density of weight one Eq. (A.24) was used to compactly write the last line. Thus the functional variation of $\beta_k R^k$ with respect to variations of the 3-metric can be written as

$$\delta (\beta_k R^k) \Big|_{\delta\gamma_{ij}} = 2\beta^{(i}\pi^{j)k} \Big|_k - \mathcal{L}_{\bar{\beta}}\pi^{ij} \quad , \quad (3.98)$$

where again we have used the ‘comma goes to semi-colon rule’ to convert from partial to covariant derivatives.²

Finally we return to Eq. (3.81) . Setting the variation equal to zero and taking the variation of 3-metric $\delta\gamma_{ij}$ as arbitrary leads to

$$\partial_t \pi^{ij} = - \delta (\alpha R^0) \Big|_{\delta\gamma_{ij}} - \delta (\beta_k R^k) \Big|_{\delta\gamma_{ij}} \quad (3.99)$$

for the matter-free evolution equation for the conjugate momentum. Substituting in the relations from Eq. (3.94) and Eq. (3.98) into Eq. (3.99) yields

$$\begin{aligned} \partial_t \pi^{ij} &= -\sqrt{\gamma} A^{ij} - \sqrt{\gamma} B \gamma^{ij} + \mathcal{L}_{\bar{\beta}}\pi^{ij} - 2\beta^{(i}\pi^{j)k} \Big|_k \\ &= -\sqrt{\gamma} \left[\alpha \left(\frac{2\pi^i{}_m \pi^{mj}}{\sqrt{\gamma}} - \frac{\pi^{ij} Tr(\pi)}{\sqrt{\gamma}} \right) - D^i D^j \alpha \right] \\ &\quad - \sqrt{\gamma} \left[\alpha \left(\frac{Tr(\pi^2)}{4\sqrt{\gamma}} - \frac{Tr(\pi^2)}{2\sqrt{\gamma}} - \frac{1}{2} R \right) + D^\ell D_\ell \alpha \right] \gamma^{ij} \\ &\quad + \mathcal{L}_{\bar{\beta}}\pi^{ij} - 2\beta^{(i}\pi^{j)k} \Big|_k \end{aligned} \quad (3.100)$$

Re-arranging the terms a bit yields the final form of the matter-free evolution equation for the conjugate momentum

$$\begin{aligned} \partial_t \pi^{ij} &= -\alpha \sqrt{\gamma} \left(R^{ij} - \frac{1}{2} R \right) - \frac{\alpha}{\sqrt{\gamma}} (2\pi^i{}_m \pi^{mj} - \pi^{ij} Tr(\pi)) \\ &\quad + \sqrt{\gamma} (D^i D^j \alpha - \gamma^{ij} D^\ell D_\ell \alpha) \\ &\quad - \frac{\alpha}{2\sqrt{\gamma}} \gamma^{ij} \left(\frac{Tr(\pi)^2}{2} - Tr(\pi^2) \right) + \mathcal{L}_{\bar{\beta}}\pi^{ij} - 2\beta^{(i}\pi^{j)k} \Big|_k \quad , \quad (3.101) \end{aligned}$$

which is the standard form (see specifically Eq. 4.17 of [64])

²From the momentum constraint equation $\pi^{jk} \Big|_k = 0$ we can eliminate (as is done in [5, 89]) the divergence equation in Eq. (3.98). However, since this term is not zero in the presence of matter, we will carry it in our equations knowing that we can eliminate it latter by invoking the momentum constraint.

Chapter 4

Ideal Self-Gravitating Relativistic Fluids

4.1 Introduction

In this chapter we relax the source-free condition imposed previously, developing matter action principles for use in conjunction with either the Einstein-Hilbert or ADM gravitational actions. We will apply this analysis to an ideal fluid¹, requiring that the appropriate variations generate the expected equations for the fluid motion and the expected source for the gravitational equations of motion.

In Section 4.2, we first examine a super-Hamiltonian action I_{pp} that produces geodesic motion of a single point particle. By taking the appropriate variations we demonstrate that the usual geodesic equations result. Building on this action principle, Section 4.3 shows that two simple modifications lead to an action I_f that produces the expected form for the motion of the ideal fluid in the Lagrange viewpoint. This action principle, which uses the same general approach as the MSY method [90] used in Chapter 2, has its genesis in the earlier work of Misner [88], but is more readily adapted to the spacetime splitting needed for computational considerations. We also demonstrate that a variation of I_f with respect to the metric $g_{\mu\nu}$ yields the usual stress energy tensor $T_{\mu\nu} = \rho(1 + e + P/\rho)u_\mu u_\nu + Pg_{\mu\nu}$ as the source for the Einstein equations.

¹An ideal fluid is often referred to as a perfect fluid in General Relativity. However, in keeping with the terminology adopted in Chapter 2, we will continue to use the term ideal fluid here as well.

Having established that these covariant actions (point-particle and fluid) yield desired results, we then perform a 3+1 split to produce their ‘ADM’ equivalents. In Section 4.4, we return to the action for point-particle motion. This action serves as the basis for our analysis of the finite-size effects on the orbit of a low-mass compact object in Chapter 5. Continuing on in Section 4.5, we construct the 3+1 form of I_f and subsequently show that it leads to the desired fluid equations of motion in Lagrangian form and the proper source terms for the ADM equations Eq. (3.101). We conclude in Section 4.6 by showing that the ADM-matter equations in a static, spherically symmetric spacetime result in the usual interior solution for a star in terms of the mass and Oppenheimer-Volkov (OV) equations and the familiar exterior solution originally derived by Schwarzschild [111].

4.2 Point Particle Geodesics - Covariant Formalism

The proposed super-Hamiltonian variational principle for a point particle is given by

$$I_{pp} = m \int d\lambda (\dot{z}^\mu u_\mu - \Lambda \mathcal{H}) \quad , \quad (4.1)$$

where m is the particle’s mass, $z^\mu(\lambda)$ is the particle’s worldline as a function of the path parameter λ and $\dot{z}^\mu \equiv \frac{dz^\mu}{d\lambda}$. In this context, the particle’s worldline is analogous to the classical trajectory function introduced in Eq. (2.26) as a way of tracking the motion of a given fluid element. The 4-velocity is given by u_μ and the Hamiltonian \mathcal{H} takes the form

$$\mathcal{H} = \frac{1}{2} (g^{\mu\nu} u_\mu u_\nu + 1) \quad . \quad (4.2)$$

As can be seen in Eq. (4.1), I_{pp} is invariant under changes to the path parameter λ with Λ , which acts as a Lagrange multiplier that enforces 4-velocity normalization, adjusting under each re-parametrization. Thus we can pick $d\lambda$ to be whatever we choose, including, as will be shown below, coordinate time.

There are 9 independent variations of I_{pp} , corresponding to variations in Λ , u_μ , and z^μ . We will take these in turn below.

To begin, we consider the variation of I_{pp} with respect to the Lagrange multiplier Λ

$$\delta I_{pp}|_{\delta\Lambda} = m \int d\lambda \mathcal{H} \delta\Lambda \quad . \quad (4.3)$$

Since $\delta\Lambda$ is arbitrary this leads immediately to the equation

$$\mathcal{H} = g^{\mu\nu} u_\mu u_\nu + 1 = 0 \quad (4.4)$$

which guarantees the normalization of the 4-velocity.

Next, we consider the variation of I_{pp} with respect to u_α

$$\delta I_{pp}|_{\delta u_\alpha} = \int d\lambda (\dot{z}^\alpha - \Lambda g^{\alpha\mu} u_\mu) \delta u_\alpha \quad . \quad (4.5)$$

Setting the variation equal to zero yields

$$\dot{z}^\alpha = \Lambda g^{\alpha\mu} u_\mu \quad , \quad (4.6)$$

which relates the coordinate velocity \dot{z}^μ to the covariant components of the 4-velocity u_μ .

Finally, we consider the variation of I_{pp} with respect to the particle position z^μ

$$\delta I_{pp}|_{\delta z^\alpha} = m \int d\lambda \left(u_\alpha \delta \dot{z}^\alpha - \frac{\Lambda}{2} \delta g^{\mu\nu}|_{\delta z^\alpha} u_\mu u_\nu \right) \quad . \quad (4.7)$$

Since the metric $g^{\mu\nu}$ depends only on the particle position z^α , the corresponding variational derivative is related to the partial derivative by $\frac{\partial g^{\mu\nu}}{\partial z^\alpha} \delta z^\alpha$.

The next step is to integrate the first term by parts which yields

$$\delta I_{pp}|_{\delta z^\alpha} = -m \int d\lambda \left(\frac{d}{d\lambda} u_\alpha + \frac{\Lambda}{2} \frac{\partial g^{\mu\nu}}{\partial z^\alpha} u_\mu u_\nu \right) \delta z^\alpha \quad . \quad (4.8)$$

Since the variation δz^α is arbitrary, its coefficient must be zero, which results in

$$\frac{d}{d\lambda} u_\alpha + \frac{\Lambda}{2} \frac{\partial g^{\mu\nu}}{\partial z^\alpha} u_\mu u_\nu = 0 \quad . \quad (4.9)$$

Solving Eq. (4.6) for Λ and using Eq. (4.4), we obtain

$$\Lambda = \sqrt{-g_{\mu\nu} \dot{z}^\mu \dot{z}^\nu} = \frac{d\tau}{d\lambda} \quad , \quad (4.10)$$

where the last relation follows from the usual definition of the interval. Using the chain rule, we can write Eq. (4.9) as

$$\frac{d\tau}{d\lambda} \frac{d}{d\tau} u_\sigma + \frac{\Lambda}{2} \frac{\partial g^{\mu\nu}}{\partial z^\sigma} u_\mu u_\nu = 0 \quad . \quad (4.11)$$

Dividing out $d\tau/d\lambda$ yields

$$\frac{d}{d\tau} u_\sigma + \frac{1}{2} \frac{\partial g^{\mu\nu}}{\partial z^\sigma} u_\mu u_\nu = 0 \quad , \quad (4.12)$$

which is the usual geodesic equation for the covariant form of the 4-velocity (*e.g.*, see Eq. (7.29) of [110] with identification $g_{\nu\alpha,\beta} u^\nu u^\alpha = -g^{\nu\alpha}{}_{,\beta} u_\nu u_\alpha$). Finally, we can derive the useful relation

$$\dot{z}^\mu u_\mu = \Lambda g^{\mu\nu} u_\mu u_\nu = -\Lambda \quad , \quad (4.13)$$

where the 4-velocity normalization Eq. (4.4) was used in the last step.

4.3 Relativistic Action for an Ideal Fluid - Covariant Formalism

In this section, we modify the point-particle action I_{pp} to arrive at the covariant action I_f which generates the desired fluid equations of motion and which provides the expected source terms to Einstein equations.

We adopt the usual continuum approach, envisioning our fluid as being comprised of numerous elements, each with its own worldline describing its motion. We know that our action must be of the form $I = \int d\lambda L(\lambda)$, where, in this case, the Lagrangian is an integral (sum) over these fluid elements: $L(\lambda) = \int d^3a \mathcal{L}(\lambda, a^{\bar{i}})$, giving the total action as a four dimensional integral $I = \int d^4a \mathcal{L}$. Like the point-particle, each fluid element is described by a worldline that depends on the path parameter λ , which we will now refer to as $a^{\bar{0}}$, and is ‘labeled’ by its initial location, $a^{\bar{i}}$, in spacetime. Taken together, $a^{\bar{0}}$ and $a^{\bar{i}}$ form a natural set of comoving coordinates. The Lagrangian density \mathcal{L} depends on the fluid worldlines z^μ , the spacetime metric $g_{\mu\nu}$, and the auxiliary functions u_μ and Λ .

If our fluid were comprised of a pressureless dust, the previous modification would be all that is required. To account for pressure forces in an ideal fluid, we need to turn to a thermodynamic analysis of the kind employed in Section 2.2 and Section 2.3. We first need to determine to what thermodynamics constraints we will subject our action. These constraints encode the properties of the ideal fluid and are given *a priori* by a fundamental thermodynamical function $e(\rho, s)$ specifying the (specific) internal energy per particle (or per unit mass, or per mole of baryons) as a function of the rest mass density ρ and the specific entropy s . From this and the first law of thermodynamics

$$de = Tds + (P/\rho^2) d\rho \quad , \quad (4.14)$$

one obtains the temperature and the entropy. As discussed in Chapter 2, the specific entropy s of an ideal fluid, will be constant along each fluid worldline. We therefore omit any explicit mention of s in the variational principles that follow.

The rest mass density ρ can be specified arbitrarily at some initial time; thereafter it is fixed by a conservation law. This will cause its distribution to vary as the fluid flow worldline $z^\mu(a^{\bar{\nu}})$ and/or the metric $g^{\mu\nu}$ are varied. We derive below a specific form of the density conservation law, suitable for use in our variational principle. Once obtained, we then perform the required variations and note the resulting equations. We will find that the our covariant action principle yields exactly the equations desired.

4.3.1 Description of the Density

Our aim here is to derive relativistic analogs of Eq. (2.27) and Eq. (2.28), which we used in the classical setting to constrain the variations in the density to respect the continuity equation.

The desired relation is obtained by starting from the differential form of the baryon rest-mass conservation law

$$(\rho u^\mu)_{;\mu} = 0 \quad , \quad (4.15)$$

where ρ is the baryon rest mass energy and u^μ is the four-velocity of the fluid element

we are following. Using $V^\mu{}_{;\mu} = (\sqrt{-g} V^\mu)_{,\mu} / \sqrt{-g}$, we write Eq. (4.15) as

$$\frac{\partial}{\partial z^\mu} \left(\sqrt{-g} \rho \frac{dz^\mu}{d\tau} \right) = 0 \quad , \quad (4.16)$$

Here $d/d\tau$ is an abbreviation for the proper time derivative along the fluid world line:

$$\frac{d}{d\tau} = \frac{1}{\sqrt{-g_{\mu\nu} \dot{z}^\mu \dot{z}^\nu}} \left(\frac{\partial}{\partial a^0} \right) \quad (4.17)$$

where

$$\dot{z}^\mu \equiv \frac{\partial z^\mu}{\partial a^0} \quad (4.18)$$

and the partial derivatives are taken at constant $a^{\bar{k}}$. In $a^{\bar{\mu}}$ coordinates where $\dot{a}^{\bar{0}} = 1$ and $\dot{a}^{\bar{k}} = 0$, Eq. (4.17) reads

$$\frac{\partial}{\partial a^{\bar{0}}} \left(\rho \frac{\sqrt{-\bar{g}}}{\sqrt{-g_{\bar{0}\bar{0}}}} \right) = 0 \quad . \quad (4.19)$$

Thus ρ at an arbitrary point $a^{\bar{\mu}}$ is defined by

$$\rho(a^{\bar{\mu}}) \frac{\sqrt{-\bar{g}}(a^{\bar{\mu}})}{\sqrt{-g_{\bar{0}\bar{0}}}(a^{\bar{\mu}})} = \rho(0, a^{\bar{k}}) \frac{\sqrt{-\bar{g}}(0, a^{\bar{k}})}{\sqrt{-g_{\bar{0}\bar{0}}}(0, a^{\bar{k}})} \equiv \tilde{\rho}_0 \quad . \quad (4.20)$$

Converting Eq. (4.15) to integral form gives the conservation law

$$\int d^3z \rho u^0 \sqrt{-g} = \text{constant} \quad , \quad (4.21)$$

where the constant value on the right-hand side is the total rest mass energy due to the baryons, whose configuration we will assume is specified in the initial data.

Like our approach in the single particle case, we will require that the action be invariant to reparametrizations of the path parameter. The left-hand side of Eq. (4.21) can be expressed in an arbitrary parametrization as follows

$$\begin{aligned} \int d^3z \rho u^0 \sqrt{-g} &= \int d^3z \rho \frac{dz^0}{d\tau} \sqrt{-g} \\ &= \int d^3z \rho \frac{dz^0}{\sqrt{-g_{\mu\nu} dz^\mu dz^\nu}} \sqrt{-g} \\ &= \int d^3z \rho \frac{dz^0}{da^{\bar{0}}} \frac{\sqrt{-g}}{\sqrt{-g_{\mu\nu} \dot{z}^\mu \dot{z}^\nu}} \quad . \end{aligned} \quad (4.22)$$

Eq. (4.22) can be expressed in differential form as

$$d^3 z \rho \frac{dz^0}{da^0} \frac{\sqrt{-g}}{\sqrt{-g_{\mu\nu} dz^\mu dz^\nu}} = d^3 a \tilde{\rho}_0 \quad (4.23)$$

or equivalently

$$\rho J \frac{\sqrt{-g}}{\sqrt{-g_{\mu\nu} dz^\mu dz^\nu}} = \tilde{\rho}_0 \quad , \quad (4.24)$$

where $J = \frac{\partial(z^0, z^1, z^2, z^3)}{\partial(a^0, a^1, a^2, a^3)}$ is the determinant of the Jacobian matrix of the transformation from $a^{\bar{\nu}}$ to z^μ coordinates.

4.3.2 Action Principle

At this point we are able to make our final modification to I_{pp} to arrive at the fluid action. We generalize the mass that appears in Eq. (4.1) to be the product $\tilde{\rho}_0 (1 + e)$. That this choice is correct becomes manifest when we arrive at the usual equations for an relativistic ideal fluid. With this choice, the fluid action is

$$I_f = \int d^4 a \tilde{\rho}_0 (1 + e) (\dot{z}^\mu u_\mu - \Lambda \mathcal{H}) \quad (4.25)$$

with \mathcal{H} , as in Eq. (4.2), given by

$$\mathcal{H} = \frac{1}{2} (g^{\mu\nu}(z) u_\mu u_\nu + 1) \quad (4.26)$$

and $\dot{z}^\mu \equiv \partial z^\mu / \partial a^{\bar{0}}$. The total action for gravitational and matter fields is

$$\begin{aligned} I &= I_{EH} + I_f \\ &= \frac{1}{16\pi} \int d^4 x \sqrt{-g} R + I_f \quad , \end{aligned} \quad (4.27)$$

where I_{EH} is the Einstein-Hilbert action.

We will perform the variations in the same order that we performed them for the point particle. Variations of the Lagrange multiplier Λ yields $\mathcal{H} = 0$, which is interpreted, as before, as the normalization condition

$$g^{\mu\nu}(z) u_\mu u_\nu = -1 \quad (4.28)$$

on the fluid's four velocity. Likewise, the variation with respect to u_μ yields

$$\dot{z}^\mu = \Lambda g^{\mu\nu} u_\nu \quad . \quad (4.29)$$

Combining Eq. (4.28) and Eq. (4.29) leads to

$$\Lambda = \frac{d\tau}{d\alpha^0} = \sqrt{-g_{\mu\nu}(z)\dot{z}^\mu\dot{z}^\nu} \quad . \quad (4.30)$$

To obtain the stress energy tensor associated with our action, we next take a variation of I_f with respect to the four metric and use $2\delta I_f = \int d^4z \sqrt{-g} T^{\mu\nu} \delta g_{\mu\nu}$ (see p. 125 of [72]). For convenience, we actually will take the variation with respect to $g^{\mu\nu}$, with the two related by $\delta g^{\mu\nu} = -g^{\mu\alpha} \delta g_{\alpha\beta} g^{\beta\nu}$. Taking the variation gives

$$\delta I_f|_{\delta g^{\mu\nu}} = \int d^4a \tilde{\rho}_0 \left[\frac{\partial e}{\partial \rho} \delta \rho|_{\delta g^{\mu\nu}} (\dot{z}^\mu u_\mu - \Lambda \mathcal{H}) - (1+e) \Lambda \delta \mathcal{H}|_{\delta g^{\mu\nu}} \right] \quad . \quad (4.31)$$

Now that the variation has been taken, we can employ $\mathcal{H} = 0$, $\dot{z}^\mu u_\mu = -\Lambda$, and $\frac{\partial e}{\partial \rho} = P/\rho^2$. Doing so, we arrive at

$$\delta I_f|_{\delta g^{\mu\nu}} = - \int d^4a \tilde{\rho}_0 \Lambda \left[\frac{P}{\rho^2} \delta \rho + (1+e) \delta \mathcal{H} \right] \quad , \quad (4.32)$$

where we have dropped the explicit reference that we are taking a variation with respect to $g^{\mu\nu}$. The relation $\delta \mathcal{H} = \frac{1}{2} u_\mu u_\nu \delta g^{\mu\nu}$ follows from Eq. (4.26) and since ρ does not depend on derivatives of $g^{\mu\nu}$ its variation can be written as $\delta \rho = \frac{\partial \rho}{\partial g^{\mu\nu}} \delta g^{\mu\nu}$. Thus

$$- 2\delta I_f|_{\delta g^{\mu\nu}} = \int d^4a \tilde{\rho}_0 2\Lambda \left[\frac{P}{\rho^2} \frac{\partial \rho}{\partial g^{\mu\nu}} + \frac{1}{2} (1+e) u_\nu u_\mu \right] \delta g^{\mu\nu} \quad . \quad (4.33)$$

Using Eq. (4.24) in conjunction with Eq. (4.30), we replace $\tilde{\rho}_0$ in Eq. (4.33) with $\rho\sqrt{-g}/\Lambda J$, leading to

$$\begin{aligned} - 2\delta I_f|_{\delta g^{\mu\nu}} &= \int d^4a \rho \sqrt{-g} J \left[2 \frac{P}{\rho^2} \frac{\partial \rho}{\partial g^{\mu\nu}} + (1+e) u_\mu u_\nu \right] \delta g^{\mu\nu} \\ &= \int d^4z \sqrt{-g} \left[2 \frac{P}{\rho} \frac{\partial \rho}{\partial g^{\mu\nu}} + \rho (1+e) u_\mu u_\nu \right] \delta g^{\mu\nu} \quad , \end{aligned} \quad (4.34)$$

where we used $d^4a J = d^4z$. We read off $T_{\mu\nu}$ from Eq. (4.34) as

$$T_{\mu\nu} = \rho (1+e) u_\mu u_\nu + 2 \frac{P}{\rho} \frac{\partial \rho}{\partial g^{\mu\nu}} \quad . \quad (4.35)$$

Taking the variation of Eq. (4.24), we find

$$\delta \left(\frac{\rho \sqrt{-g}}{\sqrt{-g_{\mu\nu} \dot{z}^\mu \dot{z}^\nu}} \right) = 0 \quad (4.36)$$

since variations on the initial boundary are zero and the Jacobian has no dependence on the metric. Carrying out the variation of the left hand side (done for its logarithm) then gives

$$\frac{\delta\rho}{\rho} + \frac{1}{2} \frac{\delta g}{g} + \frac{\delta\sqrt{-g_{\mu\nu}\dot{z}^\mu\dot{z}^\nu}}{\sqrt{-g_{\mu\nu}\dot{z}^\mu\dot{z}^\nu}} = 0 \quad . \quad (4.37)$$

Next, we can expand the variation $\delta\sqrt{-g_{\mu\nu}\dot{z}^\mu\dot{z}^\nu}$ to $-\frac{1}{2}\dot{z}^\mu\dot{z}^\nu\delta g_{\mu\nu}/\sqrt{-g_{\mu\nu}\dot{z}^\mu\dot{z}^\nu} = -\frac{1}{2}u^\mu\dot{z}^\nu\delta g^{\mu\nu}$, which allows us to simplify the last term of Eq. (4.37) to the form

$$\frac{\delta\sqrt{-g_{\mu\nu}\dot{z}^\mu\dot{z}^\nu}}{\sqrt{-g_{\mu\nu}\dot{z}^\mu\dot{z}^\nu}} = -\frac{1}{2}u^\mu u^\nu\delta g_{\mu\nu} = +\frac{1}{2}u_\mu u_\nu\delta g^{\mu\nu} \quad . \quad (4.38)$$

Using Eq. (A.9) to obtain $\delta g = -g g_{\mu\nu}\delta g^{\mu\nu}$ and combining this with Eq. (4.38), we find

$$2\frac{\delta\rho}{\rho} = (g_{\mu\nu} + u_\mu u_\nu)\delta g^{\mu\nu} \quad . \quad (4.39)$$

From Eq. (4.39), we immediately obtain $\frac{\partial\rho}{\partial g^{\mu\nu}} = \frac{1}{2}\rho(g_{\mu\nu} + u_\mu u_\nu)$ and from this the stress energy tensor

$$\begin{aligned} T_{\mu\nu} &= \rho(1+e)u_\mu u_\nu + P(g_{\mu\nu} + u_\mu u_\nu) \\ &= \rho\left(1+e + \frac{P}{\rho}\right)u_\mu u_\nu + P g_{\mu\nu} \end{aligned} \quad (4.40)$$

that arises from our variational principle.

The final variation of I_f we must perform is with respect to variations in the worldlines of each fluid element. Taking this variation yields

$$\delta I_f|_{\delta z^\mu} = \int d^4a \tilde{\rho}_0 \left\{ -\Lambda \frac{P}{\rho} \delta\rho|_{\delta z^\mu} + (1+e)u_\mu \delta\dot{z}^\mu - \Lambda(1+e)\delta\mathcal{H}|_{\delta z^\mu} \right\} \quad . \quad (4.41)$$

Since the density (see Eq. (4.24)) depends on both z^μ and on \dot{z}^μ , its variation can be written as

$$\delta\rho|_{\delta z^\mu} = \frac{\partial\rho}{\partial z^\mu}\delta z^\mu + \frac{\partial\rho}{\partial z^\mu{}_{,\lambda}}\delta z^\mu{}_{,\lambda} \quad (4.42)$$

and likewise, since the Hamiltonian depends only on z^μ , its variation becomes

$$\delta\mathcal{H}|_{\delta z^\mu} = \frac{\partial\mathcal{H}}{\partial z^\mu}\delta z^\mu \quad . \quad (4.43)$$

Substituting Eqs. (4.42) and (4.43) into Eq. (4.40) and then integrating each term involving a partial derivative of a variation by parts (discarding the boundary terms

in the process) leads us to

$$\begin{aligned} \delta I_f|_{\delta z^\mu} &= - \int d^4 a \tilde{\rho}_0 \left\{ \frac{P}{\rho^2} \Lambda \frac{\partial \rho}{\partial z^\mu} - \frac{\partial}{\partial a^\lambda} \left[\frac{P}{\rho^2} \Lambda \frac{\partial \rho}{\partial z^\mu, \lambda} \right] \right. \\ &\quad \left. + \frac{\partial}{\partial a^0} [(1+e)u_\mu] + \Lambda(1+e) \frac{\partial \mathcal{H}}{\partial z^\mu} \right\} \delta z^\mu \quad . \end{aligned} \quad (4.44)$$

It is easier to break Eq. (4.44) apart and then to handle each integral separately. Doing so we define the integrals:

$$A = \int d^4 a \tilde{\rho}_0 \frac{P}{\rho^2} \Lambda \frac{\partial \rho}{\partial z^\mu} \quad , \quad (4.45)$$

$$B = - \int d^4 a \tilde{\rho}_0 \frac{\partial}{\partial a^\lambda} \left[\frac{P}{\rho^2} \Lambda \frac{\partial \rho}{\partial z^\mu, \lambda} \right] \quad , \quad (4.46)$$

$$C = \int d^4 a \tilde{\rho}_0 \frac{\partial}{\partial a^0} [(1+e)u_\mu] \quad , \quad (4.47)$$

and

$$D = \int d^4 a \tilde{\rho}_0 \Lambda (1+e) \frac{\partial \mathcal{H}}{\partial z^\mu} \quad . \quad (4.48)$$

In each of these terms we will be repeatedly substituting in Eq. (4.24) for $\tilde{\rho}_0$ and manipulating the terms in a similar fashion to the way we manipulated the variational principles in Chapter 2. Our aim will be to arrive at a set of integrals over $d^4 z$ ($= d^4 x$ when the dummy variable of integration is relabeled).

For term A , we first need to evaluate $\frac{\partial \rho}{\partial z^\mu}$. Taking the derivative of both sides of Eq. (4.24) with respect to z^μ and using the fact that neither J nor $\tilde{\rho}_0$ depend on z^μ , we get

$$\frac{\partial \rho}{\partial z^\mu} = -\frac{\rho}{2} [g^{\alpha\beta} + u_\alpha u_\beta] \frac{\partial g_{\alpha\beta}}{\partial z^\mu} \quad . \quad (4.49)$$

Substitution of this result into Eq. (4.45) leads immediately to

$$A = - \int d^4 z \sqrt{-g} \frac{P}{2} [g^{\alpha\beta} + u^\alpha u^\beta] \frac{\partial g_{\alpha\beta}}{\partial z^\mu} \delta z^\mu \quad . \quad (4.50)$$

The manipulations involving B are somewhat more involved. We start by determining $\frac{\partial \rho}{\partial z^\mu, \lambda}$. We take the derivative $\frac{\partial}{\partial z^\mu, \lambda}$ of both sides of Eq. (4.24) to arrive at

$$\frac{\partial}{\partial z^\mu, \lambda} \left[\frac{\rho J \sqrt{-g}}{\sqrt{-g_{\mu\nu} \dot{z}^\mu \dot{z}^\nu}} \right] = 0 \quad , \quad (4.51)$$

since $\tilde{\rho}_0$ had no dependence on z^μ or its derivatives. Expanding Eq. (4.51) and solving for $\frac{\partial \rho}{\partial z^\mu, \lambda}$ yields

$$\frac{\partial \rho}{\partial z^\mu, \lambda} = -\rho \left[\frac{1}{J} \frac{\partial}{\partial z^\mu, \lambda} J + \frac{u_\mu \delta^{\lambda 0}}{\sqrt{-g_{\mu\nu} \dot{z}^\mu \dot{z}^\nu}} \right] . \quad (4.52)$$

Substituting Eq. (4.52) into Eq. (4.46), we arrive at

$$B = \int d^4 a \tilde{\rho}_0 \frac{\partial}{\partial a^0} \left(\frac{P}{\rho} u_u \right) + \int d^4 a \tilde{\rho}_0 \frac{\partial}{\partial a^\lambda} \left(\frac{P \sqrt{-g}}{\tilde{\rho}_0} \frac{\partial}{\partial z^\mu, \lambda} J \right) , \quad (4.53)$$

where we have used Eq. (4.24) to eliminate ρ in favor of $\tilde{\rho}_0$ in the last term. The partial derivative of the Jacobian in the last term in Eq. (4.53) can be written in terms of the cofactors of the Jacobian matrix J^λ_μ using Eq. (A.13). Expanding the derivative $\frac{\partial}{\partial a^0} \left(\frac{P}{\rho u_\mu} \right)$ as $\frac{\partial}{\partial z^\sigma} \left(\frac{P}{\rho u_\mu} \right) \frac{\partial z^\sigma}{\partial a^0}$, using Eq. (4.29) that relates $\frac{\partial z^\sigma}{\partial a^0}$ to u_σ , noting that $\frac{\partial}{\partial a^\lambda} J^\lambda_\mu = 0$ (see Eq. (A.15) in Appendix A), and using $d^4 z J = d^4 a$, we get

$$\begin{aligned} B &= \int d^4 z \sqrt{-g} \left[\frac{\partial P}{\partial z^\sigma} u^\sigma u_\mu + P \frac{\partial u_u}{\partial z^\sigma} u^\sigma \right] - \int d^4 a \tilde{\rho}_0 \frac{P}{\rho^2} u_\mu \frac{\partial \rho}{\partial a^0} \\ &\quad + \int d^4 z \frac{\partial P}{\partial z^\sigma} \sqrt{-g} + \int d^4 z \frac{P}{2} \sqrt{-g} \frac{\partial g_{\alpha\beta}}{\partial z^\sigma} . \end{aligned} \quad (4.54)$$

We next turn to the C term. Expanding the derivative with respect to a^0 results in two terms. We again use Eq. (4.24) for $\tilde{\rho}_0$ and we convert one of the integrals over $d^4 a$ to $d^4 z$, arriving at

$$\begin{aligned} C &= \int d^4 a \tilde{\rho}_0 \left(\frac{P}{\rho^2} \right) u_\mu \frac{\partial \rho}{\partial a^0} + \int d^4 a \tilde{\rho}_0 (1+e) \frac{\partial u_\mu}{\partial z^\sigma} \frac{\partial z^\sigma}{\partial a^0} \\ &= \int d^4 a \tilde{\rho}_0 \left(\frac{P}{\rho^2} \right) u_\mu \frac{\partial \rho}{\partial a^0} + \int d^4 z \rho (1+e) \sqrt{-g} \frac{\partial u_\mu}{\partial z^\sigma} u^\sigma . \end{aligned} \quad (4.55)$$

Finally, we evaluate the D term. Like the term involving A , a simple substitution for $\tilde{\rho}_0$ is all that is required for us to get

$$D = - \int d^4 z \rho \sqrt{-g} (1+e) \frac{1}{2} \frac{\partial g_{\alpha\beta}}{\partial z^\mu} u^\alpha u^\beta . \quad (4.56)$$

We can now combine the four terms, noting that the second term in B exactly cancels the first term in C . If we subsequently use $\frac{\partial g^{\mu\nu}}{\partial z^\sigma} = -g^{\mu\alpha} \frac{\partial g_{\alpha\beta}}{\partial z^\sigma} g^{\nu\beta}$ on what remains, we arrive at

$$\begin{aligned} \delta I_f|_{\delta z^\mu} &= \int d^4 z \sqrt{-g} \delta z^\sigma \left\{ -\rho \left(1+e + \frac{P}{\rho} \right) \frac{\partial u_\alpha}{\partial z^\beta} u^\beta \right. \\ &\quad \left. + \rho \left(1+e + \frac{P}{\rho} \right) \frac{\partial g_{\mu\nu}}{\partial z^\beta} u_\mu u_\nu - \frac{\partial P}{\partial z^\beta} g_{\alpha\nu} u^\nu u^\beta - \frac{\partial P}{\partial z^\alpha} \right\} . \end{aligned} \quad (4.57)$$

Organizing Eq. (4.57), using $\Gamma_{\mu\nu\alpha}u^\mu u^\nu = \frac{1}{2}\frac{\partial g_{\mu\nu}}{\partial z^\alpha}u^\mu u^\nu$, and using the definition of the covariant derivative and the geodesic equation, we obtain

$$\rho \left(1 + e + \frac{P}{\rho}\right) u_{\alpha;\beta}u^\beta = -(\delta_\alpha^\beta + u_\alpha u^\beta) \frac{\partial P}{\partial z^\beta} \quad , \quad (4.58)$$

which is precisely the Euler equation (22.13) in MTW [89] for relativistic hydrodynamic flow of an ideal fluid when identifying $\rho_{MTW} = \rho(1 + e)$.

4.4 Point Particle Geodesics - ADM Formalism

In this section, we turn from the covariant formalism used above to the ADM formalism, which, as mentioned, is better adapted to a computational approach. Start with the covariant point particle action I_{pp} from Eq. (4.1), take the coordinate time $z^0 \equiv t$ as the scalar field used to label the spatial hypersurfaces Σ_t , and exploit the gauge freedom of the action by identifying the path parameter λ with t . With this identification $\dot{z}^0 = 1$ and I_{pp} becomes

$$I_{pp} = m \int dt (u_0 + u_i \dot{z}^i - \Lambda \mathcal{H}) \quad . \quad (4.59)$$

Using the 3+1 form of the inverse metric from Eq. (3.26), the Hamiltonian is written as

$$\mathcal{H} = \frac{1}{2} \left[\gamma^{ij} u_i u_j - \frac{(u_0 - \beta^i u_i)^2}{\alpha^2} + 1 \right] \quad . \quad (4.60)$$

The equations of motion are obtained by varying the four functions Λ , u_0 , u_i , and z^i in turn. ²

The variation of the Lagrange multiplier Λ results again in the normalization condition $\mathcal{H} = 0$ from which we obtain the relation

$$u_0 = \beta^i u_i - \alpha \sqrt{1 + ||u||^2} \quad , \quad (4.61)$$

where $||u||^2 = \gamma^{ij} u_i u_j$ and the sign has been chosen so that correspondence with special relativity results in the limit as the metric approaches Minkowski form.

²Variations of the matter action with respect to the metric functions determine the source (*i.e.*, the stress-energy tensor) for the Einstein equations. We postpone examining these variations until we've introduced the 3+1 form of the ideal fluid action in the next section.

The variation with respect to u_0 yields

$$\delta I_{PP}|_{\delta u_0} = m \int dt \left[1 + \Lambda \frac{u_0 + \beta^i u_i}{\alpha^2} \right] \delta u_0 \quad (4.62)$$

from which we express Λ as

$$\Lambda = \frac{\alpha^2}{\beta^i u_i - u_0} \quad (4.63)$$

or, using Eq. (4.61), alternatively as

$$\Lambda = \frac{\alpha}{\sqrt{1 + ||u||^2}} \quad (4.64)$$

The next variation, with respect to u_i , yields

$$\delta I_{PP}|_{\delta u_i} = m \int dt \left[\dot{z}^i - \Lambda \frac{\partial \mathcal{H}}{\partial u_i} \right] \delta u_i \quad (4.65)$$

Setting the variation equal to zero results in

$$\dot{z}^i = -\beta^i + \frac{\alpha \gamma^{ij} u_j}{\sqrt{1 + ||u||^2}} \quad (4.66)$$

relating the coordinate velocity \dot{z}^i to the covariant four-velocity u_i and the shift vector β^i . Conceptually, Eq. (4.66) tells us that the coordinate velocity is comprised of two pieces - one giving velocity of the particle with respect to the coordinates and one giving the ‘velocity’ of the coordinates.

The final variation is with respect to the particle’s worldline. Taking this variation, we arrive at

$$\delta I_{PP}|_{\delta z^i} = m \int dt \left[u_i \delta \dot{z}^i - \Lambda \frac{\partial \mathcal{H}}{\partial z^i} \delta z^i \right] \quad (4.67)$$

Integrating the first term in Eq. (4.67) by parts and discarding the boundary term, we then obtain

$$\delta I_{PP}|_{\delta z^i} = -m \int dt \left[\frac{d}{dt} u_i + \Lambda \frac{\partial \mathcal{H}}{\partial z^i} \right] \delta z^i \quad (4.68)$$

where the partial derivative of the Hamiltonian is given by

$$\frac{\partial \mathcal{H}}{\partial z^i} = \frac{1}{2} \frac{\partial \gamma^{k\ell}}{\partial z^i} u_k u_\ell + \frac{u_0 - \beta^k u_k}{\alpha^2} \frac{\partial \beta^\ell}{\partial z^i} u_\ell + \frac{(u_0 - \beta^k u_k)^2}{\alpha^3} \frac{\partial \alpha}{\partial z^i} \quad (4.69)$$

Setting this variation to zero and using Eqs. (4.63) and (4.64) to simplify Eq. (4.69), we obtain

$$\frac{d}{dt} u_i + \frac{\partial}{\partial z^i} \left(-\beta^k u_k + \alpha \sqrt{1 + ||u||^2} \right) = 0 \quad (4.70)$$

for the equation of motion for the point particle.

Finally, we define $\epsilon^i = \dot{z}^i + \beta^i$ and $||\epsilon||^2 = \epsilon^i \gamma_{ij} \epsilon^j$. From these definitions, we obtain

$$||\epsilon||^2 = \frac{\alpha^2 ||u||^2}{1 + ||u||^2} \quad , \quad (4.71)$$

$$||u||^2 = \frac{||\epsilon||^2}{\alpha^2 - ||\epsilon||^2} \quad , \quad (4.72)$$

and

$$\Lambda = \alpha \sqrt{1 - \frac{||\epsilon||^2}{\alpha^2}} \quad . \quad (4.73)$$

These relations are useful in simplifying some of the intermediate steps. In addition, Eq. (4.73) serves as a guide for expressing the 3+1 density derived below.

4.5 Ideal Fluid - ADM Formalism

We now turn to expressing the ideal fluid action in 3+1 form. As in the covariant case, we must first determine how to describe the fluid worldlines. Modification to the analyses in the previous sections is minimal - requiring an application of the principles we used to transition from a single particle to a fluid in combination with the modifications to the worldline discussed for the 3+1 point particle case. We must next turn to determining the thermodynamic constraints. To carry this out, we must recast the conservation of baryon mass density in its 3+1 form. Once this is obtained, the transformation of Eq. (4.25) and the subsequent variations are straightforward extensions of what we've already covered.

4.5.1 Density Revisited

To recast the conservation of baryon density into 3+1 form, we start with Eq. (4.23)

$$d^3 z \rho \frac{\partial z^0}{\partial a^0} \frac{\sqrt{-g}}{\sqrt{-g_{\mu\nu} \dot{z}^\mu \dot{z}^\nu}} = \tilde{\rho}_0 d^3 a \quad . \quad (4.74)$$

Combining Eq. (4.30) and Eq. (4.73), we express the denominator as

$$\sqrt{-g_{\mu\nu} \dot{z}^\mu \dot{z}^\nu} = \alpha \sqrt{1 - \frac{||\epsilon||^2}{\alpha^2}} \quad , \quad (4.75)$$

where we remind the reader that

$$\epsilon^i = \beta^i + \dot{z}^i \quad (4.76)$$

and

$$||\epsilon||^2 = \epsilon^i \epsilon^j \gamma_{ij} \quad . \quad (4.77)$$

Using this relation, Eq. (3.25), and the gauge choice $a^{\bar{0}} = t = z^0$, we can rewrite Eq. (4.74) as

$$d^3 z \rho \frac{\sqrt{\gamma}}{\sqrt{1 - ||\epsilon||^2/\alpha^2}} = \tilde{\rho}_0 d^3 a \quad . \quad (4.78)$$

Defining the Jacobian determinant as

$$\mathcal{J} = \frac{\partial(z^1, z^2, z^3)}{\partial(a^1, a^2, a^3)} \quad , \quad (4.79)$$

we arrive at the final form

$$\rho \mathcal{J} \frac{\sqrt{\gamma}}{\sqrt{1 - ||\epsilon||^2/\alpha^2}} = \tilde{\rho}_0 \quad . \quad (4.80)$$

Eq. (4.80) will be our fundamental thermodynamic constraint equation.

4.5.2 3+1 Action

Having the desired thermodynamic constraint Eq. (4.80) in hand, we now express our action principle as

$$I_M = \int d^3 a dt \tilde{\rho}_0 (1 + e) [u_0 + u_i \dot{z}^i - \Lambda \mathcal{H}] \quad (4.81)$$

where \mathcal{H} is now given by the expression in Eq. (4.60). The total action for the gravitational and matter fields is

$$I = I_{ADM} + I_M \quad (4.82)$$

with I_{ADM} given by Eq. (3.68).

Since the density, defined implicitly through Eq. (4.80), does not depend on either the Lagrange multiplier Λ or any of the components of the covariant four-velocity u_0

and u_i , the variation of I_M with respect to these functions yields the same relations as in the point particle case. These being:

$$u_0 = \beta^i u_i - \alpha \sqrt{1 + \|u\|^2} \quad , \quad (4.83)$$

$$\begin{aligned} \Lambda &= \frac{\alpha^2}{\beta^i u_i - u_0} \\ &= \frac{\alpha}{\sqrt{1 + \|u\|^2}} \\ &= \alpha \sqrt{1 - \|\epsilon\|^2/\alpha^2} \quad , \end{aligned} \quad (4.84)$$

and

$$\epsilon^i = \dot{z}^i + \beta^i = \Lambda \gamma^{ij} u_j = \frac{\alpha \gamma^{ij} u_j}{\sqrt{1 + \|u\|^2}} \quad (4.85)$$

for the variations of I_M with respect to Λ , u_0 , and u_i , respectively.

We now carry out the variation of I_M with respect to changes in the fluid world-lines. Taking the variation yields

$$\begin{aligned} \delta I_M|_{\delta z^i} &= \int d^3 a dt \tilde{\rho}_0 \left\{ \frac{P}{\rho} \delta \rho|_{\delta z^i} [u_0 + \dot{z}^i u_i] \right. \\ &\quad \left. + (1 + e) u_i \delta \dot{z}^i - (1 + e) \Lambda \delta \mathcal{H}|_{\delta z^i} \right\} \quad . \end{aligned} \quad (4.86)$$

As seen in Eq. (4.80), the density of a given fluid element depends on both its trajectory, z^i , and its time and spatial derivatives, \dot{z}^i and $z^i{}_{,j} \equiv \frac{\partial z^i}{\partial a^j}$. Therefore, the density variation can be written as

$$\delta \rho|_{\delta z^i} = \frac{\partial \rho}{\partial z^i} \delta z^i + \frac{\partial \rho}{\partial \dot{z}^i} \delta \dot{z}^i + \frac{\partial \rho}{\partial z^i{}_{,j}} \delta z^i{}_{,j} \quad . \quad (4.87)$$

Substituting Eq. (4.87) into Eq. (4.86) and using $u_0 + u_i \dot{z}^i = -\Lambda$ and $\delta \mathcal{H}|_{\delta z^i} = \frac{\partial \mathcal{H}}{\partial z^i} \delta z^i$ gives

$$\begin{aligned} \delta I_M|_{\delta z^i} &= \int d^3 a dt \tilde{\rho}_0 \left\{ -\Lambda \frac{P}{\rho} \left(\frac{\partial \rho}{\partial z^i} \delta z^i + \frac{\partial \rho}{\partial \dot{z}^i} \delta \dot{z}^i + \frac{\partial \rho}{\partial z^i{}_{,j}} \delta z^i{}_{,j} \right) \right. \\ &\quad \left. + (1 + e) u_i \delta \dot{z}^i - (1 + e) \Lambda \frac{\partial \mathcal{H}}{\partial z^i} \delta z^i \right\} \quad . \end{aligned} \quad (4.88)$$

Next, we integrate by parts the second, third, and fourth terms of Eq. (4.88) to move the derivatives from the variations to the terms multiplying them. Carrying

out the integration by parts and ignoring the boundary terms, we arrive at

$$\begin{aligned} \delta I_M|_{\delta z^i} &= \int d^3a dt \tilde{\rho}_0 \frac{d}{dt} \left[-(1+e) u_i + \Lambda \frac{P}{\rho^2} \frac{\partial \rho}{\partial z^i} \right] \delta z^i \\ &+ \int d^3a dt \tilde{\rho}_0 \frac{\partial}{\partial a^j} \left[\Lambda \frac{P}{\rho^2} \frac{\partial \rho}{\partial z^i} \right] \delta z^i \\ &- \int d^3a dt \tilde{\rho}_0 \Lambda \left[(1+e) \frac{\partial \mathcal{H}}{\partial z^i} + \frac{P}{\rho^2} \frac{\partial \rho}{\partial z^i} \right] \delta z^i \quad , \end{aligned} \quad (4.89)$$

where $\frac{d}{dt} \equiv \left(\frac{\partial}{\partial t}\right)_{a^i}$ is the time derivative along a given fluid element. We'll take each integral in turn. In the first integral, we use Eqs. (4.80) and (4.84) to get

$$\begin{aligned} &\int d^3a dt \tilde{\rho}_0 \frac{d}{dt} \left[-(1+e) u_i + \Lambda \frac{P}{\rho^2} \frac{\partial \rho}{\partial z^i} \right] \delta z^i \\ &= \int d^3z \frac{\alpha \rho \sqrt{\gamma}}{\Lambda} \frac{d}{dt} \left[-(1+e) u_i + \Lambda \frac{P}{\rho^2} \frac{\partial \rho}{\partial z^i} \right] \delta z^i \quad . \end{aligned} \quad (4.90)$$

Next, we calculate $\frac{\partial \rho}{\partial z^i}$ by taking the derivative of Eq. (4.80) and expanding

$$\frac{\partial \rho}{\partial z^i} \left(\frac{\mathcal{J} \sqrt{\gamma}}{\sqrt{1 - \|\epsilon\|^2/\alpha^2}} \right) + \frac{\rho \mathcal{J} \sqrt{\gamma}}{2 \left(\sqrt{1 - \|\epsilon\|^2/\alpha^2} \right)^3} \frac{\partial}{\partial z^i} \left(1 - \frac{\|\epsilon\|^2}{\alpha^2} \right) = 0 \quad . \quad (4.91)$$

From the definition of ϵ^i ,

$$\begin{aligned} \frac{\partial}{\partial z^i} \frac{\|\epsilon\|^2}{\alpha^2} &= \frac{\gamma^{kl}}{\alpha^2} \{ \delta^k_i \epsilon^k + \epsilon^\ell \delta^\ell_i \} \\ &= \frac{2\epsilon_i}{\alpha^2} \quad . \end{aligned} \quad (4.92)$$

Substituting Eq. (4.92) into Eq. (4.91) and multiplying both sides by $\frac{\sqrt{1 - \|\epsilon\|^2/\alpha^2}}{\mathcal{J} \sqrt{\gamma}}$, we get

$$\frac{\partial \rho}{\partial z^i} = \frac{-\rho \epsilon_i}{\alpha^2 \left(\sqrt{1 - \|\epsilon\|^2/\alpha^2} \right)^2} = -\rho \frac{u_i}{\Lambda} \quad , \quad (4.93)$$

where Eqs. (4.84) and (4.85) were used to simplify the last step. Substituting Eq. (4.93) into Eq. (4.90), we get the final form

$$\begin{aligned} &\int d^3a dt \tilde{\rho}_0 \frac{d}{dt} \left[-(1+e) u_i + \Lambda \frac{P}{\rho^2} \frac{\partial \rho}{\partial z^i} \right] \delta z^i \\ &= \int d^3z \frac{\alpha \rho \sqrt{\gamma}}{\Lambda} \frac{d}{dt} \left[- \left(1 + e + \frac{P}{\rho} \right) u_i \right] \delta z^i \quad . \end{aligned} \quad (4.94)$$

We next examine the second integral in Eq. (4.89) as follows. First, we take a derivative of Eq. (4.80) with respect to $z^i{}_{,j}$ to obtain

$$\frac{\partial \rho}{\partial z^i{}_{,j}} \frac{\mathcal{J} \sqrt{\gamma}}{\sqrt{1 - \|\epsilon\|^2/\alpha^2}} + \frac{\rho \sqrt{\gamma}}{\sqrt{1 - \|\epsilon\|^2/\alpha^2}} \mathcal{J}_i^j = 0 \quad , \quad (4.95)$$

where \mathcal{J}_i^j is the cofactor of the Jacobian \mathcal{J} (see Eqs. (A.13) and (A.14)). Solving this equation gives

$$\frac{\partial \rho}{\partial z^i{}_{,j}} = -\frac{\rho}{\mathcal{J}} \mathcal{J}_i^j \quad . \quad (4.96)$$

Substituting Eq. (4.96) back into the integral yields

$$\begin{aligned} \int d^3 a dt \tilde{\rho}_0 \frac{\partial}{\partial a^j} \left(\Lambda \frac{P}{\rho^2} \frac{\partial \rho}{\partial z^i{}_{,j}} \right) \delta z^i &= \int d^3 a dt \frac{\partial}{\partial a^j} \left(\tilde{\rho}_0 \Lambda \frac{P}{\rho^2} \frac{\partial \rho}{\partial z^i{}_{,j}} \right) \delta z^i \\ &= - \int d^3 a dt \frac{\partial}{\partial a^j} (\alpha \sqrt{\gamma} P \mathcal{J}_i^j) \delta z^i \\ &= - \int d^3 a dt \frac{\partial}{\partial z^k} (\alpha \sqrt{\gamma} P) \frac{\partial z^k}{\partial a^j} \mathcal{J}_i^j \delta z^i \\ &= - \int d^3 a dt \frac{\partial}{\partial z^k} (\alpha \sqrt{\gamma} P) \mathcal{J} \delta_i^k \delta z^i \\ &= - \int d^3 z dt \frac{\partial}{\partial z^i} (\alpha \sqrt{\gamma} P) \delta z^i \quad , \quad (4.97) \end{aligned}$$

where we've used the constancy of $\tilde{\rho}_0$ (Eq. (4.80)), and Eqs. (A.15), and (A.6). At this point, each of the integrals is over $d^3 z$ so we can express $\delta I_m|_{\delta z^i}$ as

$$\begin{aligned} \delta I_m|_{\delta z^i} &= \int d^3 z dt \delta z^i \left\{ \frac{-\alpha \rho \sqrt{\gamma}}{\Lambda} \frac{d}{dt} \left[\left(1 + e + \frac{P}{\rho} \right) u_i \right] - \frac{\partial}{\partial z^i} (\alpha \sqrt{\gamma} P) \right. \\ &\quad \left. - \rho \alpha \sqrt{\gamma} \left[(1 + e) \frac{\partial \mathcal{H}}{\partial z^i} + \frac{P}{\rho^2} \frac{\partial \rho}{\partial z^i} \right] \right\} \quad . \quad (4.98) \end{aligned}$$

Setting Eq. (4.98) equal to zero results in

$$\begin{aligned} \frac{1}{\Lambda} \frac{\partial}{\partial t} \left[\left(1 + e + \frac{P}{\rho} \right) u_i \right] + \frac{1}{\rho \alpha \sqrt{\gamma}} \frac{\partial}{\partial z^i} (\alpha \sqrt{\gamma} P) \\ + \frac{P}{\rho^2} \frac{\partial \rho}{\partial z^i} + (1 + e) \frac{\partial \mathcal{H}}{\partial z^i} = 0 \quad . \quad (4.99) \end{aligned}$$

Now we need to express the remaining derivatives in Eq. (4.99). First, we differentiate Eq. (4.60) with respect to $\frac{\partial}{\partial z^i}$

$$\begin{aligned} \frac{\partial \mathcal{H}}{\partial z^i} &= \frac{1}{2} \left[\frac{\partial \gamma^{k\ell}}{\partial z^i} u_k u_\ell + \frac{2(u_0 - \beta^\ell u_\ell)}{\alpha^2} \frac{\partial \beta^\ell}{\partial z^i} u_\ell + \frac{2(u_0 - \beta^\ell u_\ell)^2}{\alpha^3} \frac{\partial \alpha}{\partial z^i} \right] \\ &= \frac{1}{2} \frac{\partial \gamma^{k\ell}}{\partial z^i} u_k u_\ell - \frac{u_\ell}{\Lambda} \frac{\partial \beta^\ell}{\partial z^i} + \frac{\alpha}{\Lambda^2} \frac{\partial \alpha}{\partial z^i} \quad . \quad (4.100) \end{aligned}$$

Next, we perform the same differentiation on Eq. (4.80) to obtain

$$\begin{aligned} \frac{\partial}{\partial z^i} \left[\frac{\rho \mathcal{J} \alpha \sqrt{\gamma}}{\sqrt{\alpha^2 - \|\epsilon\|^2}} \right] &= \frac{\partial \rho}{\partial z^i} \frac{\mathcal{J} \alpha \sqrt{\gamma}}{\sqrt{\alpha^2 - \|\epsilon\|^2}} + \frac{\rho \mathcal{J}}{\sqrt{\alpha^2 - \|\epsilon\|^2}} \frac{\partial}{\partial z^i} (\alpha \sqrt{\gamma}) \\ &\quad - \frac{1}{2} \frac{\rho \mathcal{J} \alpha \sqrt{\gamma}}{(\sqrt{\alpha^2 - \|\epsilon\|^2})^3} \frac{\partial}{\partial z^i} (\alpha^2 - \|\epsilon\|^2) \quad . \quad (4.101) \end{aligned}$$

Setting Eq. (4.101) equal to zero and isolating $\frac{\partial \rho}{\partial z^i}$ gives

$$\begin{aligned} \frac{\partial \rho}{\partial z^i} &= \frac{-\rho}{\alpha \sqrt{\gamma}} \frac{\partial \rho}{\partial z^i} (\alpha \sqrt{\gamma}) \\ &\quad + \frac{\rho}{(\sqrt{\alpha^2 - \|\epsilon\|^2})^2} \left(2\alpha \frac{\partial \alpha}{\partial z^i} - 2 \frac{\partial \beta^\ell}{\partial z^i} \epsilon_\ell - \epsilon^k \epsilon^\ell \frac{\partial \gamma}{\partial z^i} \right) \\ &= \frac{-\rho}{\alpha \sqrt{\gamma}} \frac{\partial \rho}{\partial z^i} (\alpha \sqrt{\gamma}) + \frac{\rho \alpha}{\Lambda^2} \frac{\partial \alpha}{\partial z^i} - \frac{\rho u_\ell}{\Lambda} \frac{\partial \beta^\ell}{\partial z^i} - \frac{1}{2} \rho u^k u^\ell \frac{\partial \gamma_{k\ell}}{\partial z^i} \quad , \quad (4.102) \end{aligned}$$

where we have used

$$\frac{\partial}{\partial z^i} \|\epsilon\|^2 = 2 \frac{\partial \beta^k}{\partial z^i} \epsilon_k + \epsilon^k \epsilon^\ell \frac{\partial \gamma_{k\ell}}{\partial z^i} \quad . \quad (4.103)$$

Substituting Eqs. (4.102) and (4.100) into Eq. (4.99) and using Eq. (A.8) gives

$$\begin{aligned} &\frac{1}{\Lambda} \frac{\partial}{\partial t} \left[\left(1 + e + \frac{P}{\rho} \right) u_i \right] + \frac{1}{\rho} \frac{\partial P}{\partial z^i} \\ &+ \left(1 + e + \frac{P}{\rho} \right) \left[\frac{\alpha}{\Lambda^2} \frac{\partial \alpha}{\partial z^i} - \frac{u_k}{\Lambda} \frac{\partial \beta^k}{\partial z^i} + \frac{1}{2} \frac{\partial \gamma^{k\ell}}{\partial z^i} u_k u_\ell \right] = 0 \quad . \quad (4.104) \end{aligned}$$

As a check on the quality of the derivation leading up to Eq. (4.104), we consider a similar derivation by Laguna, Miller, and Zurek (LMZ) [69]. In their notation, our quantity ϵ^i is what they refer to as the Hawley, Smarr, and Wilson transport velocity [56] V^i . Using this identification in conjunction with Eqs. (4.64), (4.66), and (4.72), we find that $V_i = \Lambda u_i$. From this point, it is relatively easy to see LMZ's Equation (2.11) is exactly Eq. (4.104) by noting that $S_i = h u_i$, $D = \rho \alpha / \Lambda$, and

$$\frac{1}{2} \frac{\alpha}{h \gamma} S_\mu S_\nu \partial_i g^{\mu\nu} = \Lambda h \frac{\partial}{\partial z^i} \mathcal{H} \quad (4.105)$$

and $h = (1 + e + P/\rho)$.

Now we consider the variation of the matter action Eq. (4.81) with respect to the variations in the lapse. Taking the variation yields

$$\delta I_M|_{\delta\alpha} = - \int d^3a dt \tilde{\rho}_0 \Lambda \left[\frac{P}{\rho^2} \delta \rho|_{\delta\alpha} + (1 + e) \delta \mathcal{H}|_{\delta\alpha} \right] \quad , \quad (4.106)$$

where $u_0 + u_i \dot{z}^i = -\Lambda$ was used to simplify the relationship. Since neither ρ nor \mathcal{H} depend on derivatives of the lapse, these variations can be written as $\delta\rho|_{\delta\alpha} = \frac{\partial\rho}{\partial\alpha}\delta\alpha$ and $\delta\mathcal{H}|_{\delta\alpha} = \frac{\partial\mathcal{H}}{\partial\alpha}\delta\alpha$. Computing these partial derivatives will be done in turn.

To compute $\frac{\partial\rho}{\partial\alpha}$, begin with the constraint equation Eq. (4.80). Taking a derivative with respect to the lapse on both sides results in

$$\frac{\partial}{\partial\alpha} \left[\frac{\rho}{\sqrt{1 - \|\epsilon\|^2/\alpha^2}} \right] = 0 \quad . \quad (4.107)$$

Expanding the left-hand side leads to

$$\frac{\partial\rho}{\partial\alpha} = \frac{\rho\|\epsilon\|^2}{\alpha\Lambda^2} \quad . \quad (4.108)$$

The partial derivative of the Hamiltonian with respect the lapse is easily computed from the 3+1 form given in Eq. (4.60) yielding

$$\frac{\partial\mathcal{H}}{\partial\alpha} = \frac{1}{\alpha^3} (u_0 - u_i\beta^i)^2 \quad . \quad (4.109)$$

For our purposes, it easier to recast Eq. (4.109) using Eq. (4.84) giving

$$\frac{\partial\mathcal{H}}{\partial\alpha} = \frac{\alpha}{\Lambda^2} \quad . \quad (4.110)$$

Substituting Eqs. (4.108) and (4.110) into Eq. (4.106) gives the relation

$$\begin{aligned} \delta I_M|_{\delta\alpha} &= - \int d^3a dt \tilde{\rho}_0 \Lambda \left[\frac{P}{\rho^2} \frac{\rho\|\epsilon\|^2}{\alpha\Lambda^2} + (1+e)\frac{\alpha}{\Lambda^2} \right] \delta\alpha \\ &= - \int d^3z dt \sqrt{\gamma} \left[\frac{P\|\epsilon\|^2 + \rho\alpha^2(1+e)}{\Lambda^2} \right] \delta\alpha \\ &= - \int d^3z dt \sqrt{\gamma} [P\|u\|^2 + \rho(1+e)(1+\|u\|^2)] \delta\alpha \quad , \quad (4.111) \end{aligned}$$

where Eqs. (4.73) and (4.80) were used in the second line and Eqs. (4.73) and (4.64) were used in the third. Combining this result with Eqs. (3.69) and (3.70) (and relabeling the dummy variable of integration from z to x) yields

$$R + \frac{Tr(\pi)^2}{2\gamma} - \frac{Tr(\pi^2)}{\gamma} = 16\pi [P\|u\|^2 + \rho(1+e)(1+\|u\|^2)] \quad , \quad (4.112)$$

the Hamiltonian constraint in the presence of matter.

Next, we derive the ADM-hydrodynamic momentum constraint equations resulting from taking a variation of the combined action with respect to variations in the shift. To begin, we take the variation of the matter action Eq. (4.81) yielding

$$\delta I_M|_{\delta\beta_i} = - \int d^3a dt \tilde{\rho}_0 \Lambda \left[\frac{P}{\rho^2} \delta\rho|_{\delta\beta_i} + (1+e) \delta\mathcal{H}|_{\delta\beta_i} \right] , \quad (4.113)$$

where $u_0 + u_i \dot{z}^i = -\Lambda$ was used to simplify the relationship. Again, since neither ρ nor \mathcal{H} depend on derivatives of the shift, these variations can be written as $\delta\rho|_{\delta\beta_i} = \frac{\partial\rho}{\partial\beta_i} \delta\beta_i$ and $\delta\mathcal{H}|_{\delta\beta_i} = \frac{\partial\mathcal{H}}{\partial\beta_i} \delta\beta_i$. Computing these partial derivatives will be done in turn.

To compute $\frac{\partial\rho}{\partial\beta_i}$, begin with the constraint equation Eq. (4.80). Taking a derivative with respect to the shift on both sides results in

$$\frac{\partial}{\partial\beta_i} \left[\frac{\rho}{\sqrt{1 - \|\epsilon\|^2/\alpha^2}} \right] = 0 . \quad (4.114)$$

Expanding the left-hand side leads to

$$\frac{\partial\rho}{\partial\beta_i} = -\frac{\rho\epsilon^i}{\Lambda^2} . \quad (4.115)$$

The partial derivative of the Hamiltonian with respect the shift is easily computed from the 3+1 form given in Eq. (4.60) yielding

$$\frac{\partial\mathcal{H}}{\partial\beta_i} = -\frac{\gamma^{ij}u_i}{\Lambda} . \quad (4.116)$$

Substituting Eq. (4.115) and Eq. (4.116) into Eq. (4.113) gives

$$\begin{aligned} \delta I_M|_{\delta\beta_i} &= - \int d^3a dt \tilde{\rho}_0 \Lambda \left[\frac{P}{\rho^2} \left(\frac{-\rho\epsilon^i}{\alpha\Lambda^2} \right) - (1+e) \frac{\gamma^{ij}u_j}{\Lambda} \right] \\ &= - \int d^3x dt \alpha \rho \sqrt{\gamma} \left(\frac{P}{\rho} + 1 + e \right) \frac{\gamma^{ij}u_j}{\Lambda} , \end{aligned} \quad (4.117)$$

where Eq. (4.66) relating ϵ^i to u_j was used in the last line.

The final step is to combine these results with Eqs. (4.64), (3.71), and (3.72) (again relabeling a dummy variable of integration) to get

$$D_j \pi^{ij} = -8\pi\rho \left(1 + e + \frac{P}{\rho} \right) \sqrt{\gamma} \sqrt{1 + \|u\|^2} \gamma^{ij} u_j , \quad (4.118)$$

the momentum constraints in the presence of matter.

We now derive the ADM-hydrodynamic evolution equations for the conjugate momentum. Since I_M has no dependence on the conjugate momentum π^{ij} , Eq. (3.79) remains the same as in the vacuum case.

Finally, we take the variation of the matter action Eq. (4.81) with respect to variations in the 3-metric

$$\begin{aligned}\delta I_M|_{\delta\gamma_{ij}} &= \int d^3a dt \tilde{\rho}_0 \left\{ \frac{P}{\rho^2} \delta\rho|_{\delta\gamma_{ij}} [u_0 + z^i u_i - \Lambda \mathcal{H}] \right. \\ &\quad \left. - (1+e)\Lambda \delta\mathcal{H}|_{\delta\gamma_{ij}} \right\} \\ &= - \int d^3a dt \rho \alpha \sqrt{\gamma} \left\{ \frac{P}{\rho^2} \delta\rho|_{\delta\gamma_{ij}} + (1+e)\delta\mathcal{H}|_{\delta\gamma_{ij}} \right\} \quad , \quad (4.119)\end{aligned}$$

where Eq. (4.80) and the relations $u_0 + z^i u_i = -\Lambda$ and $\mathcal{H} = 0$ were used. Since neither the density nor the Hamiltonian depends on derivatives of the 3-metric, the variations can be written as $\delta\rho|_{\delta\gamma_{ij}} = \frac{\partial\rho}{\partial\gamma_{ij}}\delta\gamma_{ij}$ and $\delta\mathcal{H}|_{\delta\gamma_{ij}} = \frac{\partial\mathcal{H}}{\partial\gamma_{ij}}$, respectively. Each of these are taken in turn below.

To compute $\frac{\partial\rho}{\partial\gamma_{ij}}$, we take the derivative of Eq. (4.80)

$$\frac{\partial}{\partial\gamma_{ij}} \left[\frac{\rho\sqrt{\gamma} J}{\sqrt{1 - \|\epsilon\|^2/\alpha^2}} \right] = 0 \quad . \quad (4.120)$$

Note that through Eq. (4.80) the density ρ has a dependence on γ_{ij} through two terms. The first is through $\sqrt{\gamma}$ and the second is through $\|\epsilon\|^2$.

The variation of $\sqrt{\gamma}$ easily obtained from the formulae Eq. (A.9). Focus on the terms involved in $\|\epsilon\|^2$

$$\begin{aligned}\frac{\partial}{\partial\gamma_{ij}} \|\epsilon\|^2 &= \frac{\partial}{\partial\gamma_{ij}} \epsilon^k \epsilon^l \gamma_{kl} \\ &= \frac{\partial\epsilon^k}{\partial\gamma_i} \epsilon^l \gamma_{kl} + \epsilon^k \frac{\partial\epsilon^l}{\partial\gamma_{ij}} \gamma_{kl} + \epsilon^i \epsilon^j \\ &= 2 \frac{\partial\epsilon^k}{\partial\gamma_{ij}} \epsilon^l \gamma_{kl} + \epsilon^i \epsilon^j \quad . \quad (4.121)\end{aligned}$$

Expand the term $\frac{\partial \epsilon^k}{\partial \gamma_{ij}}$

$$\begin{aligned}
\frac{\partial \epsilon^k}{\partial \gamma_{ij}} &= \frac{\partial}{\partial \gamma_{ij}} (z^k + \beta^k) \\
&= \frac{\partial}{\partial \gamma_{ij}} \beta^k \\
&= \frac{\partial}{\partial \gamma_{ij}} \gamma^{km} \beta_m \\
&= -\beta^{(i} \gamma^{j)k} \quad .
\end{aligned} \tag{4.122}$$

Substituting back into Eq. (4.121) yields

$$\frac{\partial}{\partial \gamma_{ij}} \|\epsilon\|^2 = \epsilon^i \epsilon^j - 2\epsilon^{(i} \beta^{j)} \quad . \tag{4.123}$$

Combining Eq. (4.122) with the variation of $\sqrt{\gamma}$, we arrive at

$$\frac{\partial \rho}{\partial \gamma_{ij}} = -\frac{\rho}{2} \left[\gamma^{ij} + u^i u^j - \frac{2u^{(i} \beta^{j)}}{\Lambda} \right] \quad . \tag{4.124}$$

Next, we compute the partial derivative of the Hamiltonian with respect to the three-metric

$$\begin{aligned}
\frac{\partial}{\partial \gamma_{ij}} \mathcal{H} &= \frac{\partial}{\partial \gamma_{ij}} \frac{1}{2} \left[\gamma^{kl} u_k u_l - \frac{(\beta^k u_k - u_0)^2}{\alpha^2} + 1 \right] \\
&= -\frac{1}{2} u^i u^j - \frac{(\beta^k u_k - u_0)}{\alpha^2} \frac{\partial}{\partial \gamma_{ij}} \gamma^{kl} \beta_l u_k \\
&= -\frac{1}{2} u^i u^j + \frac{(\beta^k u_k - u_0)}{\alpha^2} \beta^{(i} u^{j)} \quad .
\end{aligned} \tag{4.125}$$

Using $(\beta^k u_k - u_0) = \frac{\alpha^2}{\Lambda}$, the above relation becomes

$$\frac{\partial}{\partial \gamma_{ij}} \mathcal{H} = \frac{u^{(i} \beta^{j)}}{\Lambda} - \frac{1}{2} u^i u^j \quad . \tag{4.126}$$

Substituting Eq. (4.124) and Eq. (4.126) into Eq. (4.119) yields

$$\begin{aligned}
\delta I_M |_{\delta \gamma_{ij}} &= \int d^3z dt \left[\frac{P}{2} \alpha \sqrt{\gamma} \gamma^{ij} \right. \\
&\quad \left. + \frac{1}{2} \rho h \alpha \sqrt{\gamma} u^i u^j - \rho h \alpha \sqrt{\gamma} \frac{u^{(i} \beta^{j)}}{\Lambda} \right]
\end{aligned} \tag{4.127}$$

with $h = (1 + e + P/\rho)$. Using Eq. (4.84) and combining the results with Eq. (3.100) leads us to

$$\begin{aligned} \partial_t \pi^{ij} &= -\sqrt{\gamma} A^{ij} - \sqrt{\gamma} B \gamma^{ij} + \mathcal{L}_{\vec{\beta}} \pi^{ij} \\ &\quad - 2\beta^{(i} \pi^{j)k}{}_{|k} + 8\pi P \alpha \sqrt{\gamma} \gamma^{ij} \\ &\quad + 8\pi \rho h \alpha \sqrt{\gamma} u^i u^j - 16\pi \rho h \alpha \sqrt{\gamma} u^{(i} \beta^{j)} \sqrt{1 + ||u||^2} \quad , \end{aligned} \quad (4.128)$$

where A^{ij} and B are given by Eqs. (3.92) and (3.93), respectively.

4.6 Solving the ADM Matter Equations

Like the vacuum case, the ADM matter equations cannot be solved analytically in most cases. However, there is one particularly simple solution which can be obtained – the Oppenheimer-Volkov equation governing the behavior of a static, ideal fluid. To begin, consider the static, spherically symmetric metric given by

$$ds^2 = -e^{2\Phi(r)} dt^2 + e^{2\Lambda(r)} dr^2 + r^2 d\Omega^2 \quad .^3 \quad (4.129)$$

Since the metric is time-independent and the shift is zero, $K_{ij} = 0$, and as a consequence $\pi^{ij} = 0$. From the momentum equation Eq. (4.118), we conclude

$$D_j \pi^{ij} = 0 \implies u_j = 0 \quad . \quad (4.130)$$

The Hamiltonian equation Eq. (4.112) now becomes

$$R = 16\pi \rho (1 + e) \quad . \quad (4.131)$$

Likewise, the evolution equations for the conjugate momentum, Eq. (4.128), and the fluid flow, Eq. (4.105), become

$$\alpha R^{ij} - D^i D^j \alpha + \gamma^{ij} \left(D^\ell D_\ell \alpha - \frac{\alpha}{2} R \right) = 8\pi \alpha P \gamma^{ij} \quad (4.132)$$

and

$$-\frac{1}{\rho} \frac{\partial P}{\partial z^i} = \left(1 + e + \frac{P}{\rho} \right) \frac{\partial}{\partial z^i} \ln \alpha \quad , \quad (4.133)$$

³The function $\Lambda(r)$ should not be confused with the Lagrange multiplier Λ used elsewhere in the text.

respectively. From the definition of the metric in Eq. (4.129), we identify $\alpha = \exp \Phi(r)$. Substituting this result into Eq. (4.133) and simplifying yields

$$-\frac{dP}{dr} = \rho \left(1 + e + \frac{P}{\rho} \right) \frac{d\Phi}{dr} . \quad (4.134)$$

Using GRTensorII [98], the three-dimensional Ricci scalar

$$\begin{aligned} R &= 2 \frac{2r\partial_r\Lambda + e^{2\Lambda} - 1}{r^2 e^{2\Lambda}} \\ &= \frac{2}{r^2} \frac{d}{dr} [r(1 - e^{-2\Lambda})] \end{aligned} \quad (4.135)$$

and Ricci tensor (only non-zero components are displayed)

$$\begin{aligned} R^{rr} &= 2 \frac{\partial_r\Lambda}{r e^{4\Lambda}} \\ R^{\theta\theta} &= \frac{r\partial_r\Lambda + e^{2\Lambda} - 1}{r^4 e^{2\Lambda}} \\ R^{\phi\phi} &= \frac{r\partial_r\Lambda + e^{2\Lambda} - 1}{r^4 \sin^2(\theta) e^{2\Lambda}} \end{aligned} \quad (4.136)$$

are readily calculated. If we define the mass function

$$m(r) = \frac{r}{2} (1 - e^{-2\Lambda}) , \quad (4.137)$$

then we can re-write the Ricci scalar as

$$R = \frac{4}{r^2} \frac{d}{dr} m(r) . \quad (4.138)$$

Substituting Eq. (4.138) into Eq. (4.131), we arrive at

$$\frac{d}{dr} m(r) = 4\pi r^2 \rho (1 + e) . \quad (4.139)$$

In the same fashion, substituting Eq. (4.136) into Eq. (4.132), simplifying, and keeping only the rr component leads us to

$$e^\Phi e^{-2\Lambda} \frac{2r\partial_r\Phi - e^{2\Lambda} + 1}{r^2} = 8\pi e^\Phi P \quad (4.140)$$

or

$$2r \frac{d}{dr} \Phi - e^{2\Lambda} + 1 = 8\pi r^2 e^{2\Lambda} P . \quad (4.141)$$

Using Eq. (4.137) to isolate $\exp(-2\Lambda) = 1 - 2m(r)/r$, we can simplify Eq. (4.141) to

$$\frac{d\Phi}{dr} = \frac{4\pi r^3 P + m(r)}{r[r - 2m(r)]} . \quad (4.142)$$

Combining Eq. (4.139) and Eq. (4.142), we arrive at the well-known Oppenheimer-Volkov (OV) equation

$$\frac{dP}{dr} = -\frac{p(1 + e + P/\rho)(m + 4\pi r^3 P)}{r(r - 2m)} . \quad (4.143)$$

The OV equation, combined with the equation for dm/dr and equation of state, constitutes three equations for the three unknown functions $\rho(r)$, $m(r)$ and $P(r)$. This set provides a complete description of an static ideal fluid. In the absence of matter, $\rho = P = 0$, and Eq. (4.139) and Eq. (4.142) reduce to

$$\frac{d}{dr}m(r) = 0 \quad (4.144)$$

and

$$\frac{d}{dr}\Phi = \frac{m(r)}{r[r - 2m(r)]} . \quad (4.145)$$

Eq. (4.144) requires $m(r) = M$, where M is some constant. Using this result in Eq. (4.145), we arrive at

$$e^{2\Phi} = 1 - \frac{2M}{r} = \alpha^2 \quad (4.146)$$

which is the well-known Schwarzschild exterior solution. Exact interior solutions with $\rho \neq 0$ and $P \neq 0$ are much harder to come by. Section 23.7 of MTW [89] discusses the constant-density solution in detail. Chapter 10 of Schutz [110] presents Buchdahl's solution [29] as well as strategies for solving Eqs. (4.139) and (4.143) numerically.

This ADM approach to deriving a model of stellar-structure will serve as our reference point when we derive the Fat Particle *Publish and Subscribe* model in Chapter 5.

Chapter 5

Relativistic Fat Particles

5.1 Introduction

In the previous two chapters we developed variational principles to describe both the gravitational and hydrodynamic degrees of freedom. Building on this work, we are now in a position to investigate how we can model Fat Particles as extended fluid objects in general relativity. We will pursue this investigation in the same fashion we employed in the classical case, discussed in Chapter 2.

Recall that in the classical case, we used two simple rules to derive our Fat Particle equations. First, we needed a discretization rule to transform the continuum action to a discrete analog. The rule, based on the conservation of mass formula

$$\rho(\vec{z}, t) d^3z = \rho_0(\vec{a}, 0) d^3a \quad ,$$

amounted to replacing the initial density $\rho_0(\vec{a}, 0)$ as a discrete sum of delta functions

$$\rho_0(\vec{a}, 0) = \sum_A m_A \delta(\vec{a} - \vec{r}_A) \quad .$$

Second, we needed a smoothing rule giving the effective gravitational force at the Fat Particle's center. Following the lead from the SPH community, we proposed the rule

$$\Phi_A = \frac{\int d^3x W(\vec{z}_A - \vec{x}) \Phi(\vec{x})}{\int d^3x W(\vec{z}_A - \vec{x})} \quad .$$

From these two rules, we were able to justify the standard SPH definition of density, to derive a consistent set of SPH equations modeling a self-gravitating fluid, and to show that a model of classical Fat Particles was well-posed and well-behaved.

These results were relatively easy to derive because of the large body of classical work. The situation is dramatically different in general relativity. It is not obvious what modifications we must make to either the discretization rule or the smoothing rule to get a consistent set of SPH or Fat Particle equations. Judging by the sparseness of the existing literature, we are not alone in this case. Of the few works we found [97, 66, 80, 69, 36, 96], all the results were performed against a fixed background spacetime. In addition most of the computational results were performed for one-dimensional specialized problems like the relativistic Riemann shock-tube [66, 80, 69, 36]. However, just like the classical results, implementations differed in many ways, most notably in the smoothing rule employed. In the papers by Mann [80], Chow and Monaghan [36], and Monaghan and Price [96], smoothing between the fluid elements was performed in the same fashion as in the classical case. In the paper by Laguna, Miller, and Zurek [69], the smoothing was done in ‘covariant’ fashion by weighting the smoothing kernel with the three-metric associated with the spacetime slicing employed. Also, in most cases, the SPH equations were derived from the continuum differential equations not from a variational principle, giving us no insight on how to discretize our action. Monaghan and Price [96] start from a variational principle, where they employ the same discretization rule used in the classical case. However, since they provided only the formalism with no numerical tests, we were again left with no rigorous justification of the smoothing rule one should adopt.

To handle these open issues, we choose to divide the problem into manageable pieces, moving onto the next study only when the first was reasonably justified. The remainder of this chapter is devoted to our analysis in this regard. We start first by introducing, in Section 5.2, a simple model of a single Fat Particle in orbit around a static black hole. Employing a rigorous physical test, we were able to determine a ‘covariant’ smoothing rule. Application of this rule allowed us to estimate how finite-sized effects may play a role in modeling gravitational wave emission and a range of orbital radii over which the particulars of the internal hydrodynamic composition can be safely ignored. Despite our success, there were still a few open questions that

remained. We discuss these issues and suggest ways to address them. In Section 5.3, we return to our variational principle. Combining our covariant smoothing procedure with a discretization rule, we derive our form of the single Fat Particle equation with full back-reaction. While solving these equations in full generality is beyond the scope of numerical relativity at this time, we do explore some of the content of these equations.

5.2 Development of the Single Fat Particle - *Subscribe Only* Picture

In this section we develop a single Fat Particle model in the limit where its mass is small enough that it is an ignorable perturbation on a background spacetime. In this picture, our Fat Particle receives its ‘marching orders’ from the background metric using kernel interpolation (*i.e.*, smoothing) without giving anything back in return. We term this one-way communication from the spacetime to the Fat Particle as the *Subscribe Only* picture. Physically, we envision this system as being comprised of a main-sequence star or compact object (a white dwarf or neutron star) in orbit around a much more massive black hole.

As stated above, our focus in this section is on the implementation and the determination of a ‘covariant’ smoothing rule. By focusing on a single particle, we can delay dealing with the discretization rule until later. Even with this simplification, we are still faced with a choice in implementing a numerical scheme.

Our presentation of the model below is as follows. After deriving the equations of motion, we discuss how we developed a numerical implementation of the model. Stability in this model is easy to define and we demonstrate it with circular orbit initial conditions. Accuracy of the method, which depends on the convergence of the smoothing procedure, is much harder to define. Our convergence criteria is based on examining the right-hand side of the Fat Particle equations of motion for a fixed set of initial conditions. We find that the accuracy afforded within the original formulation of the equations of motion is not high enough to allow us to select out

the best smoothing rule. To resolve this difficulty, we introduce an approximation, which allows us to select the best smoothing method by imposing a simple physical requirement on the phase shift between a test and Fat Particle moving on the same orbit. We then present the results for a selection of trajectories using different spacetime descriptions, smoothing kernels, and smoothing lengths. We find that the results obey a simple set of scaling relationships.

5.2.1 Equations of Motion

The Fat Particle equations of motion in the Subscribe Only picture are easy to derive from the action in Eq. (4.59). With no extra effort, we can treat the metric functions (covariant components) defined at the particle center as smoothed functions. Taking the same set of variations as in Section 4.4, we arrive at

$$\frac{d}{dt} \begin{pmatrix} z^i \\ u_i \end{pmatrix} = \begin{pmatrix} -\langle \beta^i \rangle + \frac{\langle \alpha \rangle \langle \gamma^{ij} \rangle u_j}{\sqrt{1 + \|\langle u \rangle\|^2}} \\ \frac{\partial}{\partial z^i} \left[\langle \beta^i \rangle u_i + \langle \alpha \rangle \sqrt{1 + \|\langle u \rangle\|^2} \right] \end{pmatrix}, \quad (5.1)$$

where

$$\|\langle u \rangle\|^2 = \langle \gamma^{ij} \rangle u_i u_j \quad (5.2)$$

and

$$\langle \beta^i \rangle = \langle \gamma^{ij} \rangle \langle \beta_j \rangle \quad (5.3)$$

The inverse smoothed three metric is defined as usual as

$$\langle \gamma^{ij} \rangle \langle \gamma_{jk} \rangle = \delta^i_k \quad (5.4)$$

We define the

$$\frac{\partial \langle \gamma^{ij} \rangle}{\partial \vec{z}} = -\langle \gamma^{im} \rangle \frac{\partial \langle \gamma_{m\ell} \rangle}{\partial \vec{z}} \langle \gamma^{\ell j} \rangle \quad (5.5)$$

$$\frac{\partial \langle \beta^i \rangle}{\partial \vec{z}} = \frac{\partial \langle \gamma^{ij} \rangle}{\partial \vec{z}} \langle \beta_j \rangle + \langle \gamma^{ij} \rangle \frac{\partial \langle \beta_j \rangle}{\partial \vec{z}} \quad (5.6)$$

The remaining component of the four velocity is given by

$$u_0 = \langle \beta^i \rangle u_i - \langle \alpha \rangle \sqrt{1 + \|\langle u \rangle\|^2} \quad (5.7)$$

5.2.2 Numerical Implementation

Up to this point, we've been able to derive the Fat Particle equations of motions without having to define the specific method by which smoothed metric functions are obtained from the actual metric functions. Before we introduce the candidate smoothing methods below, we should say something about how we implemented the model computationally.

Because we anticipated the need to explore a variety of different algorithms, we developed our code in C++ using the *tensor++* library available from Nascatech Inc. [99]. In *tensor++*, the user defines and works with multidimensional array objects that represent given tensors. Built-in rules for addition, contraction, outer products, etc., allow these objects to mimic the usual algebraic rules for tensors (see *e.g.*, Section 3.5 of [89]) without burdening the user with the need to always deal directly with components. For example, consider three tensors $A_{ijk} = i + j + k$, $B_i^j = j - i$ and $C_{ijklm} = A_{ilj} B_k^l$, where $i, j, k, \ell, m = 1 \dots 3$. A C programming implementation would look essentially like:¹

```
double A[3][3][3], B[3][3][3], C[3][3][3][3];
int    i, j, k, l, m;

//initialize variables
for(i = 0; i < 3; i++)
  for(j = 0; j < 3; j++)
    for(k = 0; k < 3; k++)
      {
        A[i][j][k] = i + j + k;
        B[i][j][k] = j - i;
        for(m = 0; m < 3; m++)
          C[i][j][k][m] = 0.0;
```

¹We would like to emphasize that while this code snippet is a good representative it is not at the level of professional code development.

```

    }

for(i = 0; i < 3; i++)
    for(j = 0; j < 3; j++)
        for(k = 0; k < 3; k++)
            for(m = 0; m < 3; m++)
                for(l = 0; l < 3; l++)
                    C[i][j][k][m] = C[i][j][k][m] + A[i][l][j] * B[k][l][m];

```

A possible corresponding *tensor++* implementation would look like:

```

tensor A(3,3,3,3), B(3,3,3,3), C;
int i,j,k;

//initialize variables
for(i = 0; i < 3; i++)
    for(j = 0; j < 3; j++)
        for(k = 0; k < 3; k++)
            {
                A.Set(i+j+k,i,j,k);
                B.Set(j-i,i,j,k);
            }

C <= A.Contract(B,2,2);

```

In addition to the code being more compact, there is a much smaller chance of introducing a coding error since the contraction is handled automatically.

A tensor field is then modeled by constructing an array of pointers to *tensor++* objects. Figure 5.1 schematically shows a representation of a three-dimensional hypersurface, where values of the lapse, shift, and three-metric at each grid point are

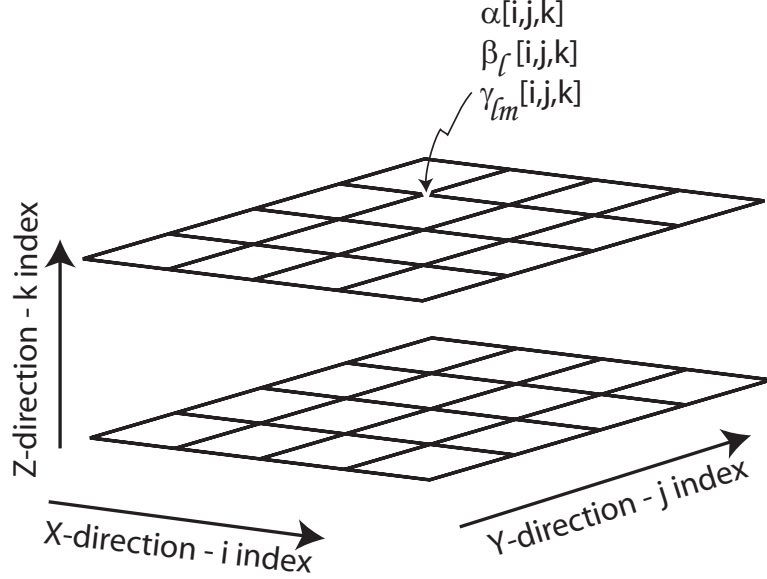


Figure 5.1: Schematic representation of the data structures used in the Subscribe Only Fat Particle study. A three-dimensional array of pointers to *tensor++* objects serves as a discrete model of a three-dimensional hypersurface.

specified by $\alpha[i][j][k]$, $\beta_\ell[i][j][k]$, and $\gamma_{\ell m}[i][j][k]$, respectively. Memory space for this grid is allocated at the beginning of the run and populated once. The Fat Particle is then free to move within the confines of the numerical grid. Discrete kernel smoothing is used to approximate the corresponding integrals. We chose this approach over dynamically constructing the lapse, shift, and three-metric only in the vicinity of the Fat Particle for two reasons. We expect to couple the Fat Particle formalism to traditional numerical relativity simulations, where by definition one does not know the values of the metric functions except at a set of discrete points. Thus we get a better indication of what will happen when this coupling is implemented by pursuing this approach. Also, computing the metric functions once at start up and using them as a lookup table improves performance over repetitively recalculating them.

We implemented four separate methods for constructing the metric functions at the Fat Particle center from the numeric grid. These are:

Bare Smoothing

$$\langle f \rangle_{Bare}(\vec{z}) = \frac{\int d^3x f(\vec{x}) W(\vec{z} - \vec{x})}{\int d^3x W(\vec{z} - \vec{x})}, \quad (5.8)$$

*R3G Smoothing*²

$$\langle f \rangle_{R3G}(\vec{z}) = \frac{\int d^3x f(\vec{x}) \sqrt{\gamma}(\vec{x}) W(\vec{z} - \vec{x})}{\int d^3x \sqrt{\gamma}(\vec{x}) W(\vec{z} - \vec{x})} , \quad (5.9)$$

Spherical Smoothing

$$\langle f \rangle_{Spherical}(\vec{z}) = \frac{\int d^3x f(\vec{x}) W(|\vec{z} - \vec{x}|^2)}{\int d^3x W(|\vec{z} - \vec{x}|^2)} , \quad (5.10)$$

and

Scalar Smoothing

$$\langle f \rangle_{Scalar}(\vec{z}) = \frac{\int d^3x f(\vec{x}) \sqrt{\gamma}(\vec{x}) W(|\vec{z} - \vec{x}|^2)}{\int d^3x \sqrt{\gamma}(\vec{x}) W(|\vec{z} - \vec{x}|^2)} . \quad (5.11)$$

The first two smoothing prescriptions have been used in the literature [80, 36, 96] and [69]. The last two involve a modification of the smoothing kernel in an attempt to make the difference between two spatial position vectors more covariant. The argument of the kernel in these latter two cases is now written as

$$|\vec{z} - \vec{x}|^2 = [z^i - x^i] \gamma_{ij}(\vec{x}) [z^j - x^j] . \quad (5.12)$$

Note that the denominator in each of the smoothing rules (Eqs. (5.8)-(5.11)) is included to ensure that the smoothed value of a constant is equal to the constant itself. We define the *support* of the Fat Particle to be that coordinate region of the hypersurface in which the smoothing kernel is non-zero. For the explicit forms of the kernels, we used the Misner n -family of kernels, with $n = 2, 3$, or 4 and the Gaussian kernel W_G defined in Eq. (2.45) and Eq. (2.46), respectively.

Numerical integration of the equations of motion was done with an RK2 (see *e.g* [68]). We chose this method over higher order methods, such as embedded Runge-Kutta algorithms or Bulirsch-Stoer [108], since a second-order method would be employed in the full particle-field implementation. The step size was selected by working initially with the test particle geodesics defined by Eq. (4.66) and Eq. (4.70) and the accuracy of the method was monitored by tracking the behavior of the

²The term R3G stands for weighting the smoothing with the root of the three-metric.

conserved energy $H = -u_0$ and the conserved angular momentum $L_k = [ijk]z^i u_j$.³ The conservation of these parameters is discussed in detail in Section 5.2.3 below.

As a matter of coding methodology, each function (*i.e.*, subroutine) was unit tested using some combination of mathcad [84], Matlab [85], or Maple [81] before being admitted into the code. In addition, a Matlab implementation of the test particle geodesics served as both a code integration test bed and as a source of ‘ideal’ ephemerides that were used to select out a candidate smoothing prescription. Figure 5.2 shows typical numerical output from the test particle code for a $16M$ radius circular orbit in the standard Schwarzschild spacetime.

5.2.3 Black Hole Metrics

We consider three different descriptions of a Schwarzschild black hole - the standard Schwarzschild metric, the same metric expressed in isotropic coordinates, and the metric with a different spacetime slicing expressed in terms of the Painlevé-Gullstrand coordinate system. In each case, we will first express the metric as it is usually written in spherical coordinates and then convert from spherical coordinates to Cartesian coordinates via the usual transformation

$$\begin{aligned} x &= r \sin(\theta) \cos(\phi) \\ y &= r \sin(\theta) \sin(\phi) \\ z &= r \cos(\theta) \quad , \end{aligned} \tag{5.13}$$

with the corresponding conjugate components of the four-velocity being referred to as u , v , and w . The spacetime described by each metric possesses a time-like Killing vector and spherical symmetry. As a result, there is a conserved energy, H , and angular momentum \vec{L} for the motion of a test particle. For convenience, we will use the abbreviations STD, ISO, and PG when referring to these metrics and any corresponding results obtained from them.

³Here $[ijk]$ is the antisymmetric symbol with values $0, \pm 1$. See Eq. (A.3) for a complete definition.

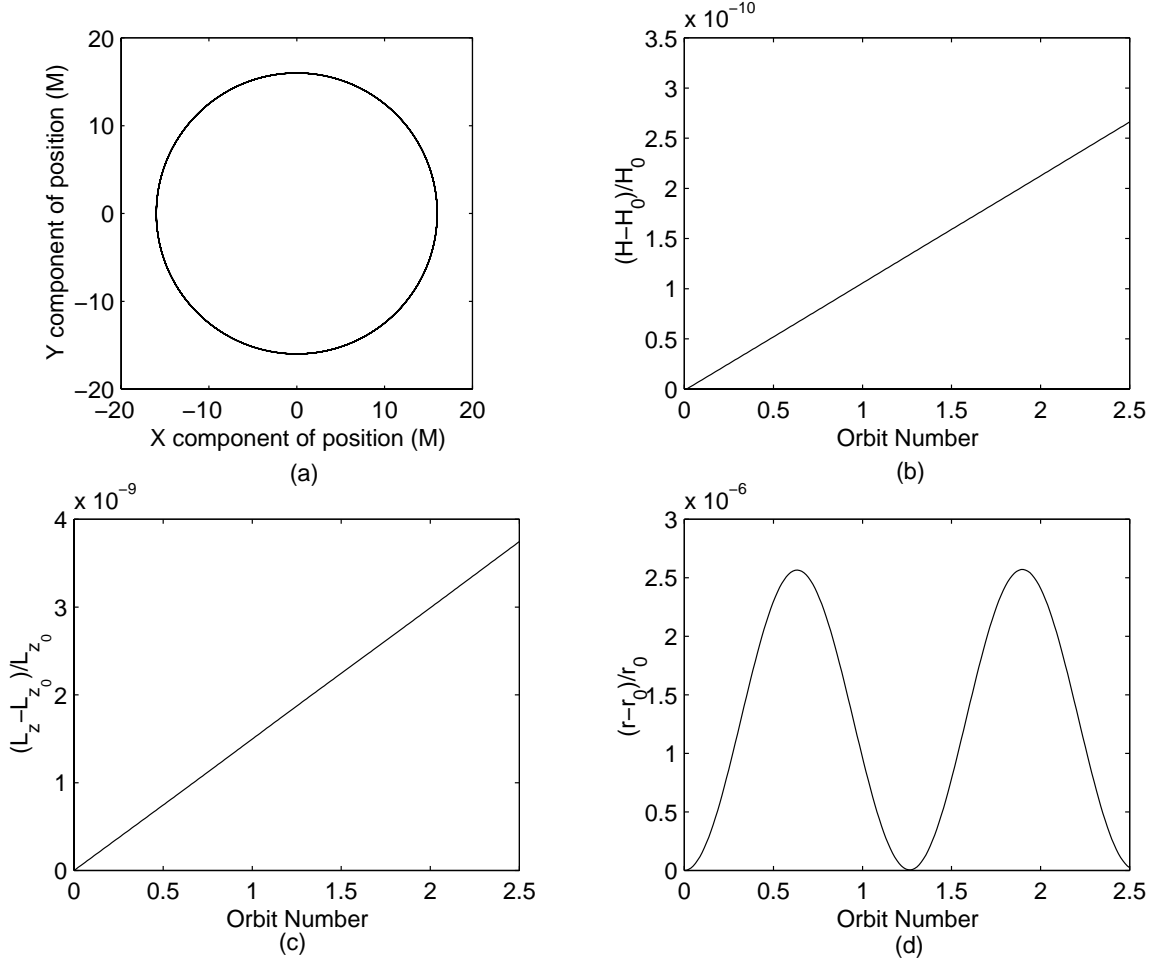


Figure 5.2: Numerical representation of a test particle geodesic in the standard Schwarzschild spacetime for a $r = 16M$ circular orbit; (a) Orbit trace in the $X - Y$ plane, (b) fractional deviation of the energy H from its initial value, (c) fractional deviation of the z -component of the angular momentum L_z from its initial value, (d) fractional deviation of the orbital radius R from its initial value.

Schwarzschild Standard Metric (STD)

Our first description is given by the classic Schwarzschild metric [111] (see MTW Chapter 23 [89] for a detailed analysis) in the usual spherical spatial coordinates

$$ds^2 = - \left(1 - \frac{2M}{r} \right) dt^2 + \frac{dr^2}{\left(1 - \frac{2M}{r} \right)} + r^2 d\Omega^2 \quad . \quad (5.14)$$

Converting to Cartesian coordinates the metric takes the form ⁴

$$ds^2 = - \left(1 - \frac{2M}{r}\right) dt^2 + \left(\delta_{ij} + \frac{x^i x^j}{r^2} \frac{2M/r}{1 - 2M/r}\right) dx^i dx^j \quad . \quad (5.15)$$

From Eq. (5.15) it is easy to read off the lapse, shift, and three-metric given by

$$\alpha = \sqrt{1 - 2M/r} \quad , \quad (5.16)$$

$$\beta_k = 0 \quad , \quad (5.17)$$

and

$$\gamma_{ij} = \delta_{ij} + \frac{x^i x^j}{r^2} \frac{2M/r}{1 - 2M/r} \quad . \quad (5.18)$$

The corresponding spatial derivatives are given by

$$\alpha_{,k} = \frac{x^k M}{r^3} \left(1 - \frac{2M}{r}\right)^{-1/2} \quad , \quad (5.19)$$

$$\beta_{i,k} = 0 \quad , \quad (5.20)$$

and

$$\gamma_{ij,k} = Q \left[\delta_{ik} x^j + \delta_{jk} x^i + \left(\frac{3}{r^2} + Q\right) x^i x^j x^k \right] \quad , \quad (5.21)$$

with $Q = \frac{2M}{r^2(r-2M)}$.

Schwarzschild Isotropic Metric (ISO)

The second metric we will be employing is the Schwarzschild spacetime described in isotropic coordinates [110]. Making the coordinate transformation

$$r = R \left(1 + \frac{M}{2R}\right)^2 \quad (5.22)$$

the metric in Eq. (5.10) is written as

$$ds^2 = - \left[\frac{1 - M/2R}{1 + M/2R}\right]^2 dt^2 + \left[1 + \frac{M}{2R}\right]^4 (dR^2 + R^2 d\Omega^2) \quad . \quad (5.23)$$

⁴This is easily done by first working the metric into the form $ds^2 = \frac{1-f}{f} dr^2 + dx^2 + dy^2 + dz^2$ with $f = 1 - 2M/r$.

In this metric, the event horizon is now at $R = \frac{M}{2}$. Converting to Cartesian coordinates we arrive at

$$ds^2 = - \left[\frac{1 - M/2R}{1 + M/2R} \right]^2 dt^2 + \left[1 + \frac{M}{2R} \right]^4 (dx^2 + dy^2 + dz^2) \quad (5.24)$$

with $R^2 = x^k x^k$. From Eq. (5.24) we read off the lapse, shift, and three-metric as

$$\alpha = \left[\frac{1 - M/2R}{1 + M/2R} \right] \quad , \quad (5.25)$$

$$\beta_i = 0 \quad , \quad (5.26)$$

and

$$\gamma_{ij} = \left[1 + \frac{M}{2R} \right]^4 \delta_{ij} \quad . \quad (5.27)$$

The corresponding spatial derivatives are

$$\alpha_{,k} = \frac{x^k M}{R^3} \frac{1}{(1 + M/2R)^2} \quad , \quad (5.28)$$

$$\beta_{i,k} = 0 \quad , \quad (5.29)$$

and

$$\gamma_{ij,k} = -2 \left(1 + \frac{M}{2R} \right)^3 \frac{M}{R^3} x^k \delta_{ij} \quad . \quad (5.30)$$

Schwarzschild Painlevé-Gullstrand Metric (PG)

The third metric we considered is the Schwarzschild spacetime with a new time coordinate, defined by

$$T = t - 4M \left(\sqrt{r/2M} + \frac{1}{2} \ln \left| \frac{\sqrt{r/2M} - 1}{\sqrt{r/2M} + 1} \right| \right) \quad , \quad (5.31)$$

to label the spatial hypersurfaces. Radial geodesics in this spacetime correspond to observers moving that arrive at infinity with zero energy.⁵ This metric is regular at all values of $r \neq 0$, reflecting that the outgoing observers never pass through

⁵Reversing the sign to the term involving the radius converts outgoing radial geodesics into infalling ones. In this case, the observers start at infinity at rest and proceed to fall into the hole. See the discussion by Martel and Poisson [83] for more details.

an event horizon. Carrying out the coordinate transformation in Eq. (5.31), the standard Schwarzschild metric becomes

$$ds^2 = -dT^2 + \left(dr - \sqrt{2M/r}dT\right)^2 + r^2 d\Omega^2 \quad . \quad (5.32)$$

Converting to Cartesian coordinates yields

$$ds^2 = -dT^2 + \delta_{ij} \left(dx^i - x^i \sqrt{2M/r^3} dt\right) \left(dx^j - x^j \sqrt{2M/r^3} dt\right) \quad (5.33)$$

with $r^2 = x^i x^i$. From Eq. (5.33) we read off the lapse, shift, and three-metric as

$$\alpha = 1 \quad (5.34)$$

$$\beta_i = -x^k \sqrt{2M/r^3} \quad , \quad (5.35)$$

and

$$\gamma_{ij} = \delta_{ij} \quad . \quad (5.36)$$

The corresponding spatial derivatives are

$$\alpha_{,k} = 0 \quad , \quad (5.37)$$

$$\beta_{i,k} = \sqrt{\frac{2M}{r^3}} \left(\frac{3}{2} \frac{x^i x^k}{r^2} - \delta^{ik} \right) \quad , \quad (5.38)$$

and

$$\gamma_{ij,k} = 0 \quad . \quad (5.39)$$

5.2.4 Circular Orbit Initial Conditions

The next step in our investigation is to determine the initial conditions that we should use. Based on the work of Peters *et. al.* [105, 104], we expect that a system of two isolated masses in bound motion about each other will radiate most at the periapsis of their orbit. This preferential emission of gravitational radiation will tend to circularize the orbits. Thus we select as initial conditions, those that lead to circular orbits.

We will exploit the constant direction of the angular momentum vector by aligning our Cartesian coordinate system so that the z -axis is parallel to \vec{L} . This is equivalent

to selecting the polar angle to be $\theta = \frac{\pi}{2}$. The resulting orbital motion will take place in the $x - y$ plane. In addition, we will align the x -axis with the starting position of the body in question (test particle or Fat Particle). Thus our initial conditions will be of the form

$$\bar{S} = (x, 0, 0, u, v, 0)^T \quad , \quad (5.40)$$

where T stands for the matrix transpose. Our remaining task will be to find expressions for u and v .

We develop here a formalism for determining the relevant formulas for the STD, ISO, and PG Schwarzschild spacetimes. All three metrics can be described in matrix form as

$$g_{\mu\nu} = \begin{pmatrix} -g_{tt} & g_{tr} & 0 & 0 \\ g_{tr} & g_{rr} & 0 & 0 \\ 0 & 0 & g_{\Omega}r^2 & 0 \\ 0 & 0 & 0 & g_{\Omega}r^2 \sin^2 \theta \end{pmatrix} \quad (5.41)$$

with the corresponding matrix inverse

$$g^{\mu\nu} = \begin{pmatrix} -g_{rr}/N & g_{tr}/N & 0 & 0 \\ g_{tr}/N & g_{tt}/N & 0 & 0 \\ 0 & 0 & 1/g_{\Omega}r^2 & 0 \\ 0 & 0 & 0 & 1/g_{\Omega}r^2 \sin^2 \theta \end{pmatrix} \quad , \quad (5.42)$$

and where $N \equiv g_{rr}g_{tt} + g_{tr}^2$. The covariant four-velocity can be written in terms of the conserved quantities H and L_z and an unknown function u_r as

$$u_{\nu} = (-H, u_r, 0, L_z) \quad . \quad (5.43)$$

Using Eq. (5.42) to raise an index

$$u^{\mu} = \left(\frac{u_r g_{tr} + H g_{rr}}{N}, \frac{u_r g_{tt} - H g_{tr}}{N}, 0, \frac{L_z}{g_{\Omega}r^2 \sin^2 \theta} \right) \quad (5.44)$$

allows us to express u^t as a function of u^r and H

$$u^t = \frac{g_{tr}}{g_{tt}} u^r + \frac{H}{g_{tt}} \quad . \quad (5.45)$$

The normalization of the four-velocity, taken in terms of the four-velocity with index up $u^\mu u^\nu g_{\mu\nu} = -1$, yields the radial equation

$$\left(\frac{dr}{d\tau}\right)^2 = \frac{g_{tt}}{g_{rr}g_{tt} + g_{tr}^2} \left[\frac{H^2}{g_{tt}} - \frac{L_z^2}{g_\Omega r^2} - 1 \right] . \quad (5.46)$$

The conditions for a circular orbit are that the initial radial velocity and radial acceleration are zero, ensuring that the radius remains constant through the orbital evolution. The first condition for a circular orbit, $\frac{dr}{d\tau} = 0$, gives

$$H^2/g_{tt} = \left(1 + \frac{L_z^2}{g_\Omega r^2}\right) . \quad (5.47)$$

Likewise, the second circular orbit condition, $\frac{d^2r}{d\tau^2} = 0$

$$H^2/g_{tt} = \left(\frac{g_{tt}}{g_{tt,r}}\right) \frac{\partial}{\partial r} \left(\frac{L_z^2}{g_\Omega r^2}\right) . \quad (5.48)$$

Substituting the right-hand side of Eq. (5.47) into the left-hand side of Eq. (5.48) and solving for L_z^2 yields

$$L_z^2 = \frac{g_{tt,r} g_\Omega^2 r^4}{W} , \quad (5.49)$$

where $W = g_{tt}(g_\Omega r^2)_{,r} - g_{tt,r} g_\Omega r^2$. Substituting Eq. (5.49) back into Eq. (5.47) gives

$$H^2 = g_{tt} \left(1 + \frac{g_{tt,r} g_\Omega r^2}{W}\right) . \quad (5.50)$$

The orbital frequency is defined

$$\frac{d\phi}{dt} = \frac{d\phi}{d\tau} \frac{dt}{d\tau} = \frac{u^\phi}{u^t} = \frac{g_{tt}}{g_\Omega r^2} \frac{L_z}{H} = \omega . \quad (5.51)$$

The kinematics of the initial orbit demand

$$v = \frac{u_\phi}{r} \Big|_{r=x} = \frac{L_z}{r} \Big|_{r=x} \quad (5.52)$$

and

$$u = u_r \Big|_{r=x} , \quad (5.53)$$

with

$$u_r = \frac{g_{tr}}{g_{tt}} H \quad (5.54)$$

Metric	H	L_z	ω	u	v
STD	$\frac{r-2M}{\sqrt{r(r-3M)}}$	$r\sqrt{\frac{M}{r-3M}}$	$\sqrt{M/r^3}$	0	$\sqrt{\frac{M}{x-3M}}$
ISO	$\frac{(2R-M)^2}{(2R+M)C}$	$\frac{\sqrt{M(2R+M)^4}}{2\sqrt{RC}}$	$8\frac{\sqrt{MR^3}}{(2R+M)^3}$	0	$\frac{\sqrt{M(2x+M)^4}}{2\sqrt{x^3C}}$
PG	$\frac{r-2M}{\sqrt{r(r-3M)}}$	$r\sqrt{\frac{M}{r-3M}}$	$\sqrt{M/r^3}$	$\sqrt{\frac{2M}{x-3M}}$	$\sqrt{\frac{M}{x-3M}}$

Table 5.1: Conserved quantities, orbital frequency, and initial values of the four-velocity for a test particle circular orbit with initial position described by $y = z = 0$ and $x = r$ for STD or PG spacetimes and $x = R$ for the ISO spacetime. The parameter $C = \sqrt{4R^2 - 8MR + M^2}$.

determined from setting u^r to zero. Table 5.1 lists the various formulae evaluated for the three spacetimes considered.

The formulae are used in the remaining analysis as a first guess for the initial conditions that allow a Fat Particle to move in a circular orbit and to construct reference ephemerides once the Fat Particle orbit has been generated.

5.2.5 Stability

We've found the coupled set of nonlinear ordinary differential equations defined by Eq. (5.1) to be extremely stable. Of the thousands of runs we've performed, we never had a code crash. Monitoring of the energy and angular momentum shows them to be noisy but otherwise well conserved. Figure 5.3 shows a typical 'heads-up' display from each run. Occasionally, a set of initial conditions takes the Fat Particle out of the defined hypersurface grid. When this occurs, we detect it and terminate the run. Even in these cases we found that energy and angular momentum to be noisy but again well conserved.

5.2.6 Convergence

Having established the stability of the Fat Particle Subscribe Only model, we now turn to a definition of the convergence of model. Chiefly, we wish to establish how many discrete hyperspace grid points are required in the support of the Fat Particle

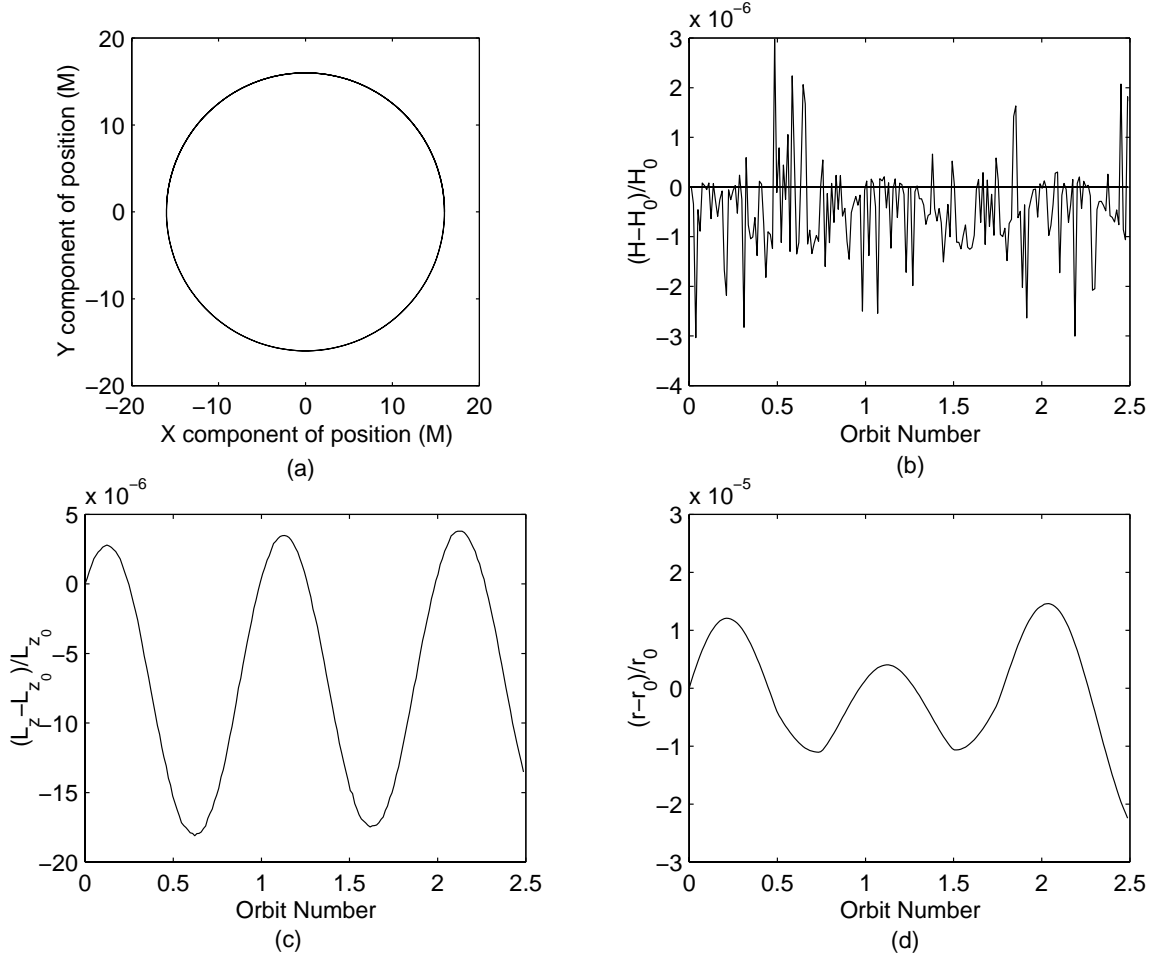


Figure 5.3: A typical example of a Fat Particle orbital evolution. This case corresponds to a nearly circular orbit at an STD radius of $r = 16M$ (here $M = 1$) integrated for 2.5 orbits: (a) Orbit trace in the $X - Y$ -plane, (b) fractional deviation of the energy H from its initial value, (c) fractional deviation of the z -component of the angular momentum L_z from its initial value, (d) fractional deviation of the orbital radius R from its initial value. Compare with Figure 5.2

to converge to a given orbital behavior. Defining a convergence criterion turns out to be much more difficult than it may first appear. A state comparison between Fat Particle ephemerides generated with different numbers of grid points is unfeasible. To see why this is, consider the Fat Particle initial state \bar{S}_0^* which gives a circular orbit. This state will not be given by the formulae in Table 5.1, that is to say that we expect that the numerical value of \bar{S}_0^* will depend on the number of grid points used in estimating the continuum integrals. In addition, evaluation of the right-hand side of the Fat Particle differential equations will depend on the number of grid points, implicitly through the state and explicitly through the estimates made of the metric functions at the particle center. Separating these two contributions to any set of state differences is generally impossible.

To solve this dilemma, we vary the number of grid points for a fixed set of initial conditions and we measure the resulting right-hand side. With the initial configuration described in Section 5.2.4, this amounts to calculating dy/dt and du/dt from Eq. (5.1). Figures 5.4 and 5.5 show the values for these components as a function of the number of points included in the support of the Fat Particle, for the bare smoothing prescription given in Eq. (5.8).

As can be seen from Figure 5.4, the evaluation of dy/dt is generally converging but is still subjected to variations that we attribute to the mismatching between the spherical kernel that defines the Fat Particle and the Cartesian grid, on which the metric functions are defined. The situation is different for the computation of du/dt . From Figure 5.5, we see that the evaluation of this component does not settle down as the number of points is increased. This difference is directly related to the fact that derivatives of the metric functions are required to carry out this computation. As we saw in Chapter 2, computation of metric derivatives using the kernel derivative (KD) method (written here for the bare smoothing prescription)

$$\partial_{\vec{z}} \langle f \rangle_{bare} = \frac{\int d^3x f(\vec{x}) \partial_{\vec{z}} W(\vec{z} - \vec{x})}{\int d^3x W(\vec{z} - \vec{x})} - \langle f \rangle_{bare} \frac{\int d^3x \partial_{\vec{z}} W(\vec{z} - \vec{x})}{\int d^3x W(\vec{z} - \vec{x})} \quad (5.55)$$

is subjected to a greater numerical noise than the corresponding smoothed derivative (SD) method. Figures 5.6 and 5.7 show the values for the same components as a

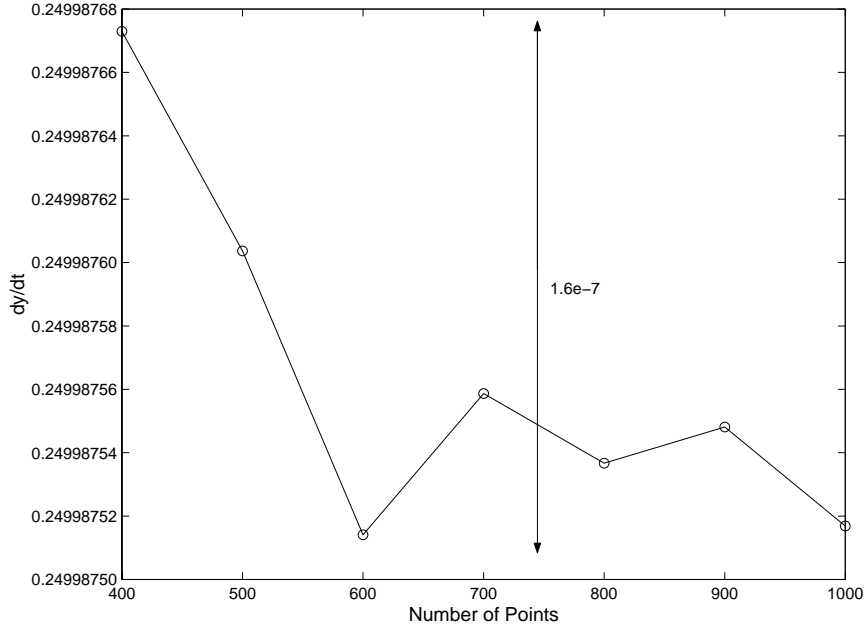


Figure 5.4: The convergence of the right-hand side component for dy/dt for $r = 16$ using kernel derivatives (KD) for the bare smoothing prescription. The vertical line represents the difference between the maximum and minimum points on the curve.

function of the number of points, again computed for the bare smoothing prescription but in this case using the smoothed derivative (SD) equivalent.

Figure 5.6 shows the same behavior as is evident in Figure 5.4. This is expected because dy/dt has no dependence on metric derivatives. However, the differences between Figures 5.7 and 5.5 is pronounced. If we define, as a measure of goodness, the difference, ϵ_{abs} , between the maximum and minimum point on each curve, then we can get a quantitative measure of how much improvement results from switching from kernel derivatives to smoothed derivatives. These values, for dy/dt , du/dt , and the energy H and the corresponding relative differences, ϵ_{rel} are shown in Table 5.2.

Switching from kernel derivatives to smoothed derivatives decreases the amount of numerical noise by two orders of magnitude. However, this improvement is not without a cost. First of all, smoothed derivatives requires knowledge of the derivative of the metric functions at the hypersurface grid points which means that the amount of memory increases dramatically. Second, one can only say with confidence that

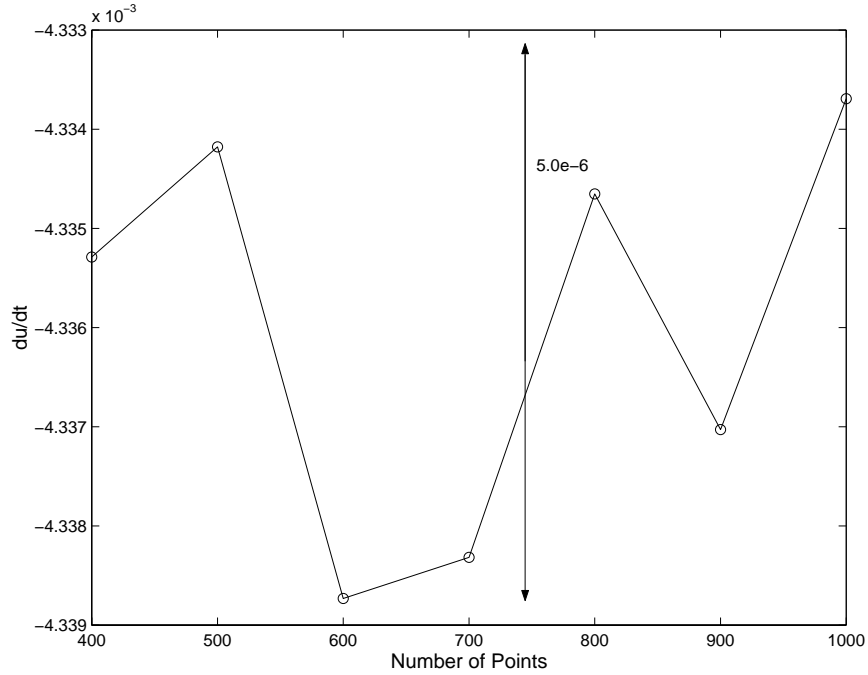


Figure 5.5: The convergence of the right-hand side component for du/dt for $r = 16$ using kernel derivatives (KD) for the bare smoothing prescription. The vertical line represents the difference between the maximum and minimum points on the curve.

	$KD\epsilon_{abs}$	$KD\epsilon_{rel}$	$SD\epsilon_{abs}$	$SD\epsilon_{rel}$
dx/dt	$1.60e - 7$	$6.40e - 7$	$1.60e - 7$	$6.40e - 7$
du/dt	$5.00e - 6$	$1.15e - 3$	$8.00e - 8$	$1.85e - 5$
H	$6.00e - 7$	$6.18e - 7$	$6.10e - 7$	$6.28e - 7$

Table 5.2: Estimates of absolute and relative uncertainties in the evaluation of the non-zero components of the right-hand side of the Fat Particle Subscribe Only equations and the energy, evaluated for both kernel and smoothed derivatives. The smoothed derivative (SD) computations introduce noise two orders of magnitude less than those introduced by the kernel derivative (KD) computations.

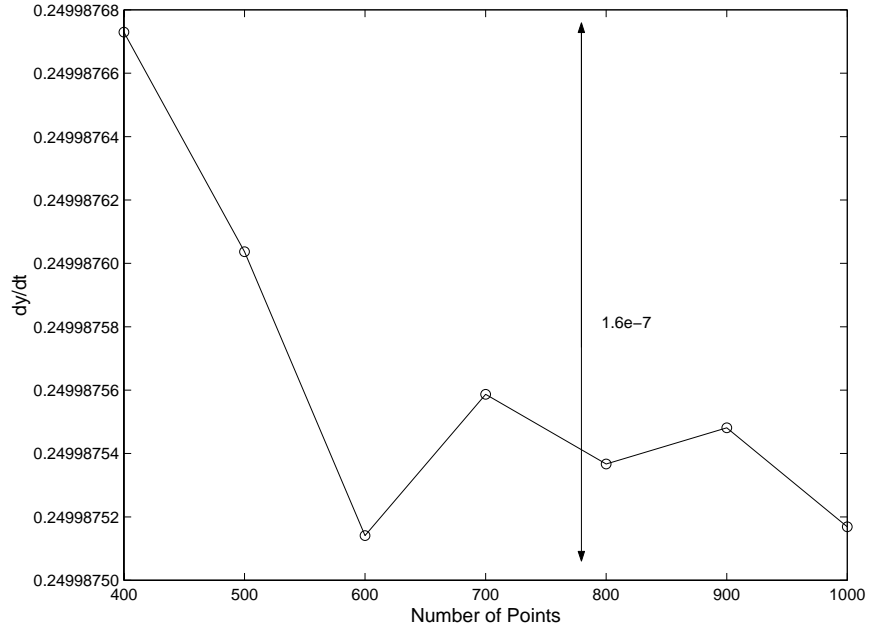


Figure 5.6: The convergence of the right-hand side component for dy/dt for $r = 16$ using smoothed derivatives (SD). The vertical line represents the difference between the maximum and minimum points on the curve.

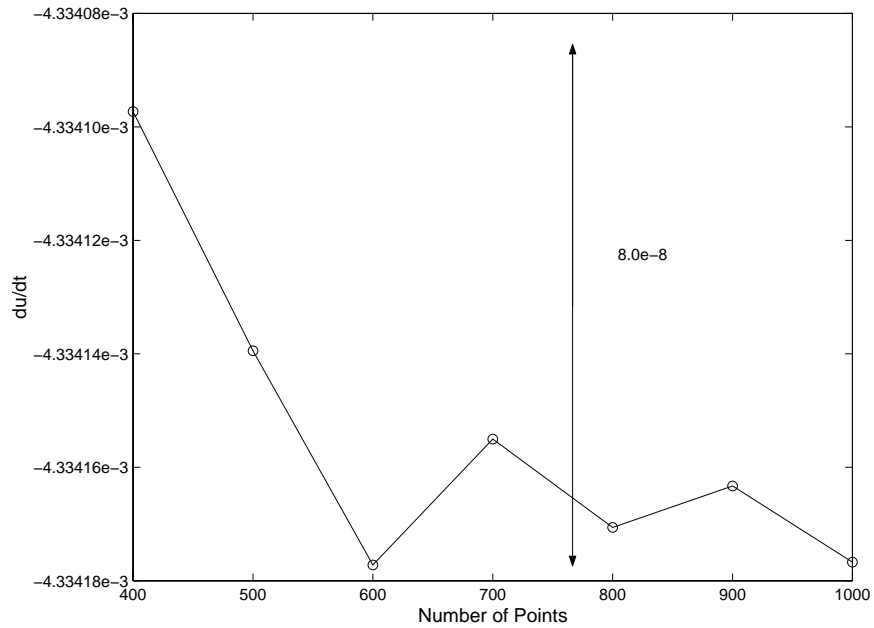


Figure 5.7: The convergence of the right-hand side component for du/dt for $r = 16$ using smoothed derivatives (SD). The vertical line represents the difference between the maximum and minimum points on the curve.

Radius	$\partial_{\vec{z}} \langle \alpha \rangle$	$\delta_{KD/SD}$	rel. error
20	$2.64e - 3$	$1.35e - 4$	$5.14e - 2$
18	$3.27e - 3$	$1.88e - 4$	$5.73e - 2$
16	$4.18e - 3$	$2.70e - 4$	$6.47e - 2$
14	$5.51e - 3$	$4.10e - 4$	$7.44e - 2$
12	$7.61e - 3$	$6.65e - 4$	$8.74e - 2$

Table 5.3: Estimation of the error between evaluating derivatives of the metric functions for kernel and smoothed derivatives using the R3G smoothing prescription.

the kernel and smoothed derivatives are equivalent when using the base smoothing prescription. Correction terms, due to the conversion from $\partial_{\vec{z}}$ to $\partial_{\vec{x}}$ and the corresponding integration by parts, are present in all the other smoothing prescriptions. For example, the difference between kernel and smoothed derivatives for the R3G smoothing prescription is given by

$$\frac{\partial}{\partial \vec{z}} \langle f \rangle - \left\langle \frac{\partial}{\partial \vec{x}} f \right\rangle = \underbrace{\langle f \rangle \frac{\partial}{\partial \vec{z}} \log \langle \sqrt{\gamma} \rangle - \left\langle f \frac{\partial}{\partial \vec{x}} \log \sqrt{\gamma} \right\rangle}_{\delta_{KD/SD}} . \quad (5.56)$$

The right-hand side of Eq. (5.56) possesses two properties worth noting. First, if $f = \text{constant}$, then the correction is identically zero. Second, the correction terms are $O(h^2)$ and thus become negligible for most SPH applications. For Fat Particle applications, the correction term is not ignorable. In addition, the presence of the kernel derivative makes estimating the correction term difficult. To get some sense of the error involved, we considered the evaluation of the derivative of the lapse function for the STD metric using both kernel and smoothed derivative methods with the R3G smoothing prescription.⁶ Table 5.3 presents the estimates of the kernel derivative of the smoothed lapse and the correction term from Eq. (5.55) as well as the relative error. The approximation varies as a function of radius and is good within 5 – 9 percent.

Propagating these errors through the numerous operations and matrix inverses

⁶The choice of the lapse as the test function is not arbitrary. For the STD metric, $\alpha = \sqrt{\gamma}^{-1}$.

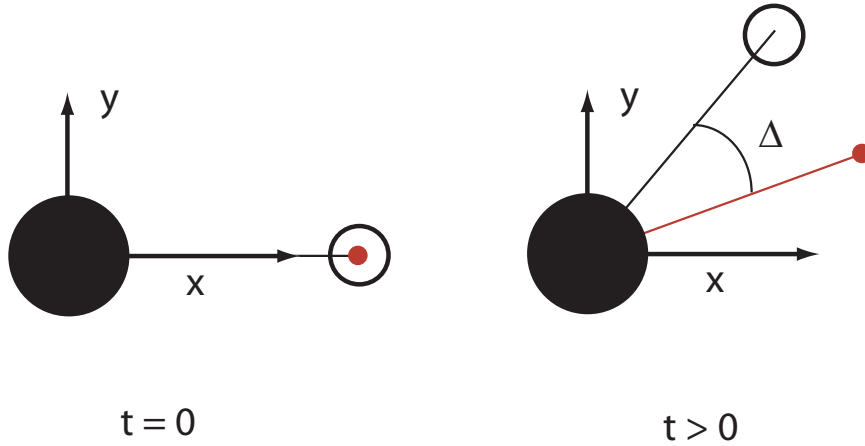


Figure 5.8: A schematic representation of the expected phase shift between a Fat Particle and a test particle, starting together, each on a circular orbit of the same radius. A secular growth in the phase shift, denoted by Δ , is expected.

that comprise the computation of du/dt (see Eqs. (5.1)-(5.6)) is extremely difficult, so we can only take the results in Table 5.3 as a qualitative guide.

5.2.7 Smoothing Choice - Phase Angle Tests

In order to select from the four smoothing prescriptions, we decided to impose a simple physical requirement. Because of its finite-size, a Fat Particle in circular orbit at a given radius should have a different energy and period than the corresponding test particle. Consider a Fat Particle and test particle that start together at $t = 0$. As each orbit evolves, a phase shift will develop between the position of the Fat Particle and the test particle. This is schematically shown in Figure 5.8. We require that the phase difference, denoted by Δ be consistent as we change coordinates in the hypersurface. Physically, this means that if the Fat Particle is ahead of the test particle in one coordinate system, it must stay ahead in another coordinate system. The sign of Δ is chosen to be positive when the Fat Particle leads to the test particle and negative when it lags.

The STD and ISO metrics, as defined in Eq. (5.14) and Eq. (5.23), form our test bed spacetime. For convenience, each orbit generated is labeled by its STD orbital

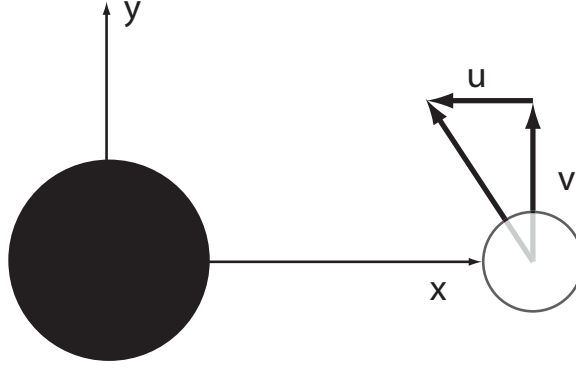


Figure 5.9: Targeting geometry in selecting the Fat Particle initial conditions that yield circular orbits.

radius, regardless of which metric was used. The conversion

$$R = \frac{1}{2} \left(r - M + \sqrt{r(r - 2M)} \right) \quad (5.57)$$

was used to actually calculate the orbit radius in the ISO case. For example, an orbit with $r = 12M$ in the STD case, corresponds to an orbit at $R = 10.9772255\dots$ in the ISO case. However, both orbits will be labeled as $r = 12M$ orbits with a note as to which metric was used. Our Fat Particle distribution was given in terms of the W_3 kernel (see Eq. (2.45) for definition) and metric functions evaluated at the particle center were approximated using the four smoothing prescriptions discussed in Section 5.2.2. Small numerical errors associated with the smoothing will tend to move the Fat Particle relativistic force away from the radial direction. Like the motion of a low-altitude spacecraft in near circular orbit (LEO) about the Earth, these small in-track forces will tend to make the orbit osculate (see the book by Bate, Mueller, and White [7] for an introduction or the book by Vinti [123] for a complete exposition). In analogy with the Delta- V targeting used to control a LEO spacecraft, circular orbit initial conditions for given radius were determined by varying the values of the in-plane components u and v of the covariant four-velocity using a Newton-Raphson differential correction scheme, until the radius over several orbits was constant and the standard deviation was below a prescribed tolerance. Figure 5.9 shows the relevant geometry.

To avoid any additional phase shifts due to mismatches in the orbital radii, the

	Bare	R3G	Scalar	Spherical
$\bar{r}(M)$	18.00000	18.00000	18.00000	18.00000
$\sigma_r(M)$	$7.487e-5$	$6.502e-5$	$9.511e-5$	$9.183e-5$
$\bar{R}(M)$	16.98528	16.98524	16.98528	16.98528
$\sigma_R(M)$	0.000551	$8.385e-5$	$8.968e-6$	$1.041e-5$

Table 5.4: A summary of the phase shift computations for ‘targeted’ Fat Particle orbits with smoothed derivatives. The targeting involved varying the in-plane components of the covariant velocity to achieve the exact value for the radius ($r = 18M$ for standard Schwarzschild coordinates and $R = 16.98528M$ for isotropic coordinates) and zero standard deviation.

test particle reference orbit was constructed after the Fat Particle targeting was completed. The average radius of the Fat Particle orbit was used in conjunction with the velocity initial conditions listed in Table 5.1. Finally, the phase shift Δ was measured at each time by fitting the evolution of Δ to a straight line.

Initial testing showed that the phase shift from the finite-size effects was relatively small and that numerical noise due to kernel derivatives was swamping the determination of Δ . As a result, we switched to using smoothed derivatives for the phase shift computations here and for the remainder of this analysis.

For our next test case, we targeted circular orbits at $r = 18M$ for a Fat Particle of size $h = 1M$ with a distribution defined by the W_3 kernel. The average and the standard deviation of the orbital radius (\bar{r} and σ_r for the STD metric and \bar{R} and σ_R for the ISO metric) are shown in Table 5.4 for the four smoothing prescriptions.

These results showed the resulting orbital motion to be circular to a high degree of accuracy. Table 5.5 shows the corresponding phase shift per orbit. As is seen in Table 5.5, only the R3G and Spherical smoothing prescriptions resulted in a consistent phase shift between the STD and ISO circular orbits. In each of the other smoothing prescriptions, the phase shift was opposite in sign. However, we considered it unlikely that the phase shifts predicted by the Spherical smoothing prescription to be reasonable since the magnitudes differed by over 30 times. More

	Δ_{STD}	Δ_{ISO}
Bare	0.0105	-0.0061
R3G	0.0167	0.0132
Spherical	-0.0011	-0.0320
Scalar	0.0045	-0.0156

Table 5.5: The phase shift Δ measured as degrees per orbit for the test orbits listed in Table 5.4.

	Bare	R3G	Scalar	Spherical
$\bar{r}(M)$	7.000017	6.998622	7.000028	6.998230
$\sigma_r(M)$	0.000344	0.000980	0.000296	0.001941
$\bar{R}(M)$	5.957958	5.958163	5.958040	5.958040
$\sigma_R(M)$	0.000139	0.000521	0.000215	0.000041

Table 5.6: A summary of the phase shift computations for ‘targeted’ Fat Particle orbits with smoothed derivatives. The targeting involved varying the in-plane components of the covariant velocity to achieve the exact value for the radius ($r = 7M$ for standard Schwarzschild coordinates and $R = 5.958040M$ for isotropic coordinates) and zero standard deviation.

likely, the small value of the Spherical phase shift in the STD orbit was at the limit of the numeric noise in the problem.

We then moved the Fat Particle to a radius of $r = 7M$ and repeated the targeting and phase shift computations. Note that with a smoothing length $h = 1M$, the inner edge of the Fat Particle grazes the innermost stable circular orbit (ISCO). Tables 5.6 and 5.7 show the relevant orbital statistics and corresponding phase shifts.

As expected, the phase shifts for the $r = 7M$ orbits were much larger than those at $r = 18M$ and once again the R3G smoothing prescription gave a consistent phase shift between the STD and ISO cases. The Spherical smoothing prescription showed an order of magnitude difference and in addition the phase shifts were now opposite in sign.

These results strongly suggest that the R3G smoothing prescription gives a phys-

	Δ_{STD}	Δ_{ISO}
Bare	0.2706	-0.0784
R3G	0.4071	0.2937
Spherical	0.0370	-0.4933
Scalar	0.1322	-0.2269

Table 5.7: The phase shift, Δ , measured as degrees per orbit for the test orbits listed in Table 5.6.

STD Radius (M)	Δ_{STD}	Δ_{ISO}	$\Delta_{STD}/\Delta_{ISO}$	$\frac{\gamma_{ISO}}{\gamma_{STD}}$	percent error
18	0.0167	0.0132	1.267	1.259	0.609
15	0.0299	0.0227	1.318	1.321	0.266
12	0.0622	0.0463	1.343	1.422	5.526
7	0.4071	0.2937	1.386	1.879	26.231

Table 5.8: Phase shifts Δ for a W_3 Fat Particle with $h = 1$ using the R3G smoothing prescription in both the STD and ISO metrics. Also shown are the ratios of these phase shifts compared to the ratios of the determinants of the three-metric γ .

ically consistent model of the Fat Particle. To further strengthen this conclusion, we examined orbits at two additional radii $r = 15M$ and $r = 12M$. The phase shift data are shown in the second and third columns of Table 5.8.

Also shown in Table 5.8 are the ratio of the phase shift in the STD metric to the corresponding shift in the ISO metric. These ratios are in good correspondence to the ratios of the determinants of the three-metrics evaluated at the appropriate radius (using Eq. (5.57) to convert from STD radius to ISO radius). The ratio of the determinants of the three-metrics physically represents the ratio of the squares of the infinitesimal volumes at a given radius. Thus the close agreement between this ratio and the ratio of phase shifts suggests that we can ascribe a given phase shift to a given amount of volume. This idea is explored in depth in the next section.

5.3 Finite-Size Corrections to the Motion of a Fat Particle

In this section, we explore the affect of a Fat Particle’s finite size on its orbital motion and corresponding energy spectrum. We adopt the R3G smoothing prescription and the smoothed derivative method used in the previous section. We want to determine if it is possible to estimate these finite size effects in a way that is independent of the size, internal distribution or shape of the Fat Particle. To this end, we targeted 120 different circular Fat Particle orbits - each with a different size ($h = 1, 2, \text{ or } 3M$), internal distribution ($W_2, W_3, W_4, \text{ or } W_G$), or shape (STD or ISO metric) over five different radii ($r = 12, 14, 16, 18, \text{ and } 20M$). For each case, a test particle orbit was constructed at the average orbital radius and the phase shift, energy, and period were measured. Although all runs were performed with $M = 1$ as the input value for the mass of the black-hole, the code was written and initially tested with arbitrary M .

Based on the general features of kernel smoothing and the results of presented in Table 5.8, we hypothesize that the observed phase shift Δ is related to the phase shift Δ_{unit} by

$$\Delta = \Delta_{unit} \left(\frac{h_{eff}}{M\sqrt{\gamma}} \right)^2 = \Delta_{unit} \left(\frac{h\xi}{M\sqrt{\gamma}} \right)^2, \quad (5.58)$$

where the parameter h_{eff} is the effective radius of the Fat Particle and ξ is a dimensionless parameter that has been introduced to account for differences in the internal distributions (*i.e.*, profiles) of the kernels. Figure 2.4 shows the internal distributions for the one-dimensional kernels used in the smoothing studies in Chapter 2. If the scaling relationship holds, then Eq. (5.58) can be used to find a universal value for the phase shift that depends neither on the size, internal distribution, or shape.

First, consider the comparison between phase shift data with different scaling lengths using the same smoothing kernel. Figure 5.10 shows the corresponding raw phase shift data and the same data scaled by $1/h^2$ for a W_3 Fat Particle in both the STD and ISO metrics. The scaling relationship is very accurately followed.

To account for the differences in the internal distributions of the kernels, we

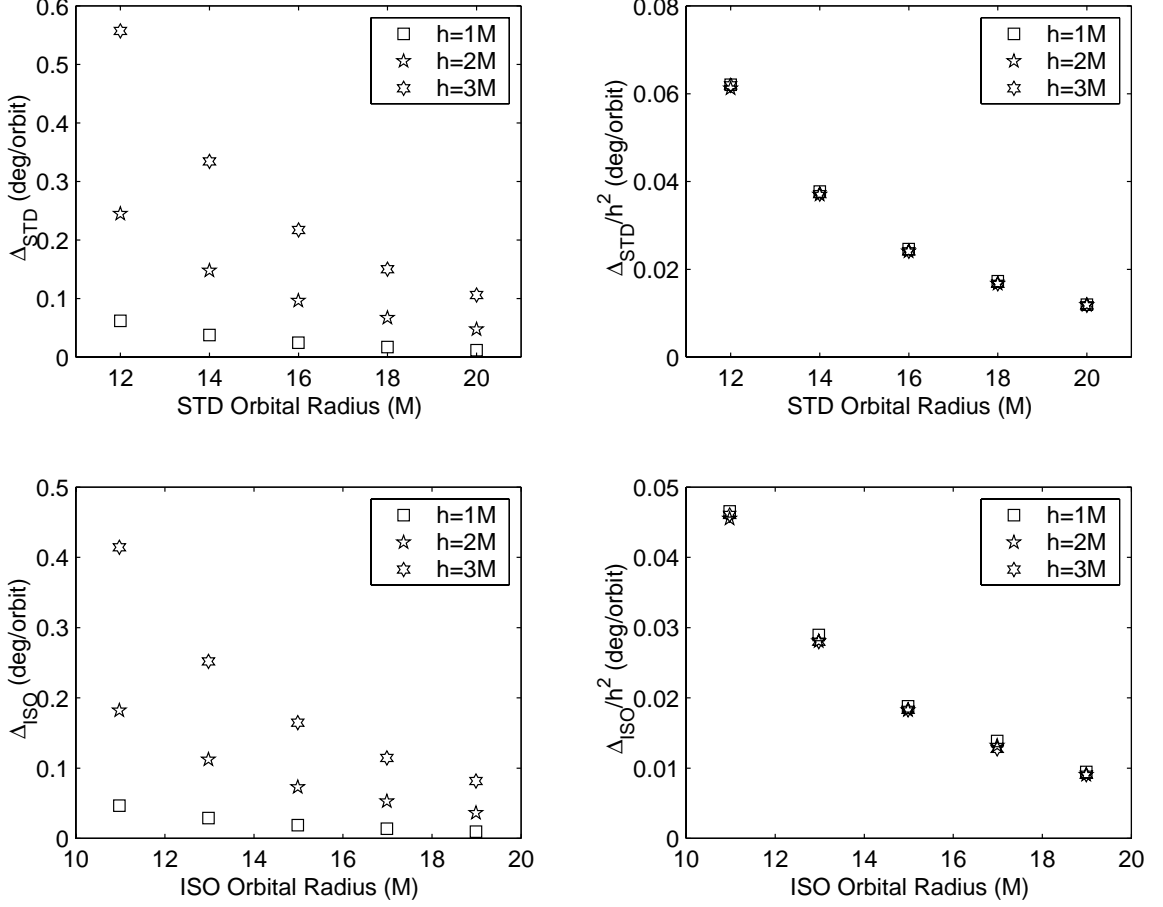


Figure 5.10: Scaling plots for (a) Δ_{STD} (b) Δ_{STD}/h^2 (c) Δ_{ISO} and (d) Δ_{ISO}/h^2 .

	W_2	W_3	W_4	W_G
ξ	0.55403	0.49938	0.44972	0.36246

Table 5.9: Value of the dimensionless parameter ξ which satisfies Eq. (5.59).

determined the value of ξ such that

$$\int_0^{\xi h} \int_0^\pi \int_0^{2\pi} dr d\theta d\phi r^2 \sin(\theta) W(r) = \frac{1}{2} . \quad (5.59)$$

The values for ξ are listed in Table 5.9 for the three Misner n -family kernels W_2 , W_3 , and W_4 and the Gaussian kernel W_G defined in Eq. (2.45) and Eq. (2.46), respectively.

We can now scale the phase shift in a fixed metric description with ξ . Figure 5.11 shows the phase shift curves for all four kernels with radius $h = 1M$ before and after the scaling for both the STD and ISO spacetimes. The agreement is good, with

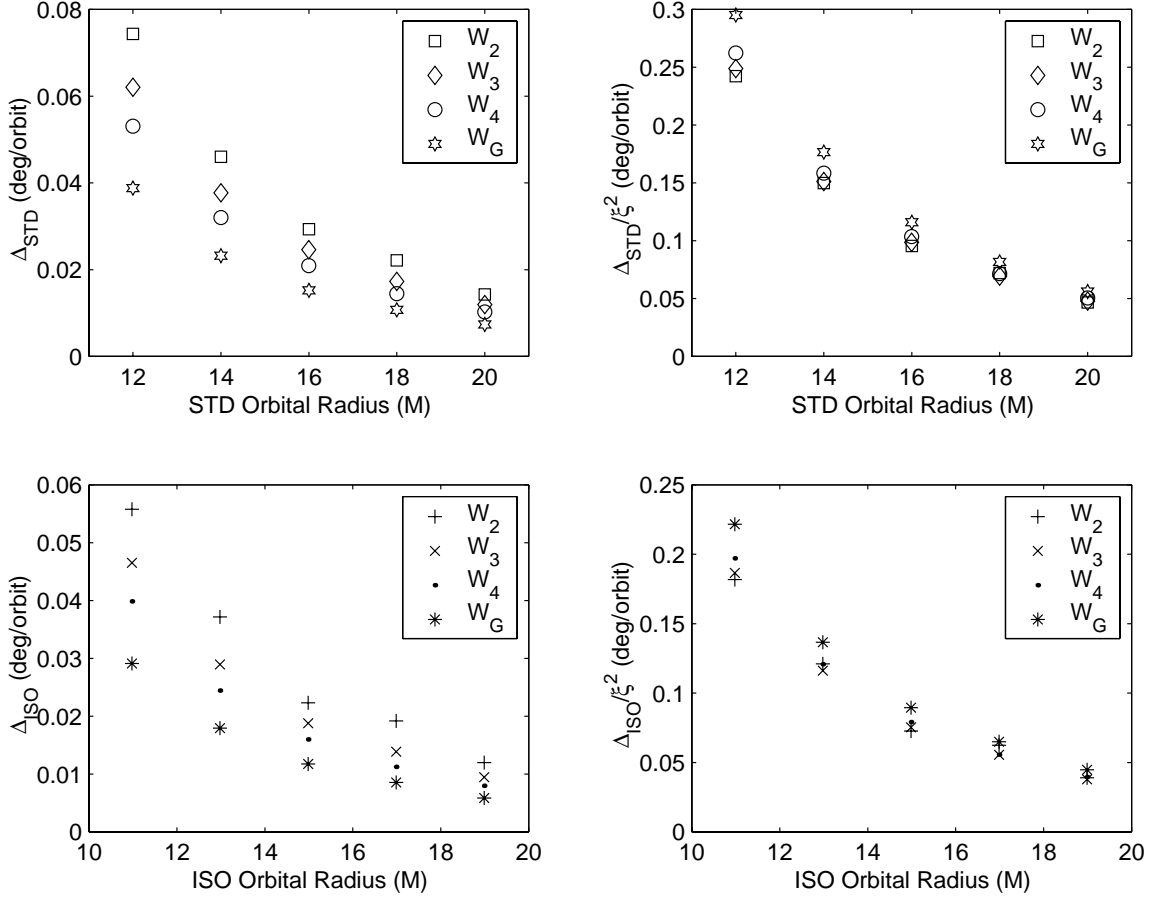


Figure 5.11: Scaling plots for (a) Δ_{STD} (b) Δ_{STD}/ξ^2 (c) Δ_{ISO} and (d) Δ_{ISO}/ξ^2 .

the phase shift data associated with W_G clearly not matching as well as the Misner kernels. This is expected considering that the integral over W_G must be evaluated numerically and is thus prone to more error than the others.

Next, we examine the scaling from one spacetime to another. Figure 5.12 shows the phase shift data before and after the scaling for a Fat Particle of radius $h = 1M$ for both the W_3 kernel (top) and the W_G kernel (bottom). The ISO radii in Figure 5.12 were converted to their STD equivalents using Eq. (5.22). Once again the scaling works well.

Finally, we produce the fully scaled values for the unit phase shift Δ_{unit} , which is shown in Figure 5.13. While the agreement is good, especially if the data from the Gaussian kernel W_G is discounted, it seems clear that the assumption that the internal hydrodynamics of the Fat Particle can be ignored is beginning to break down

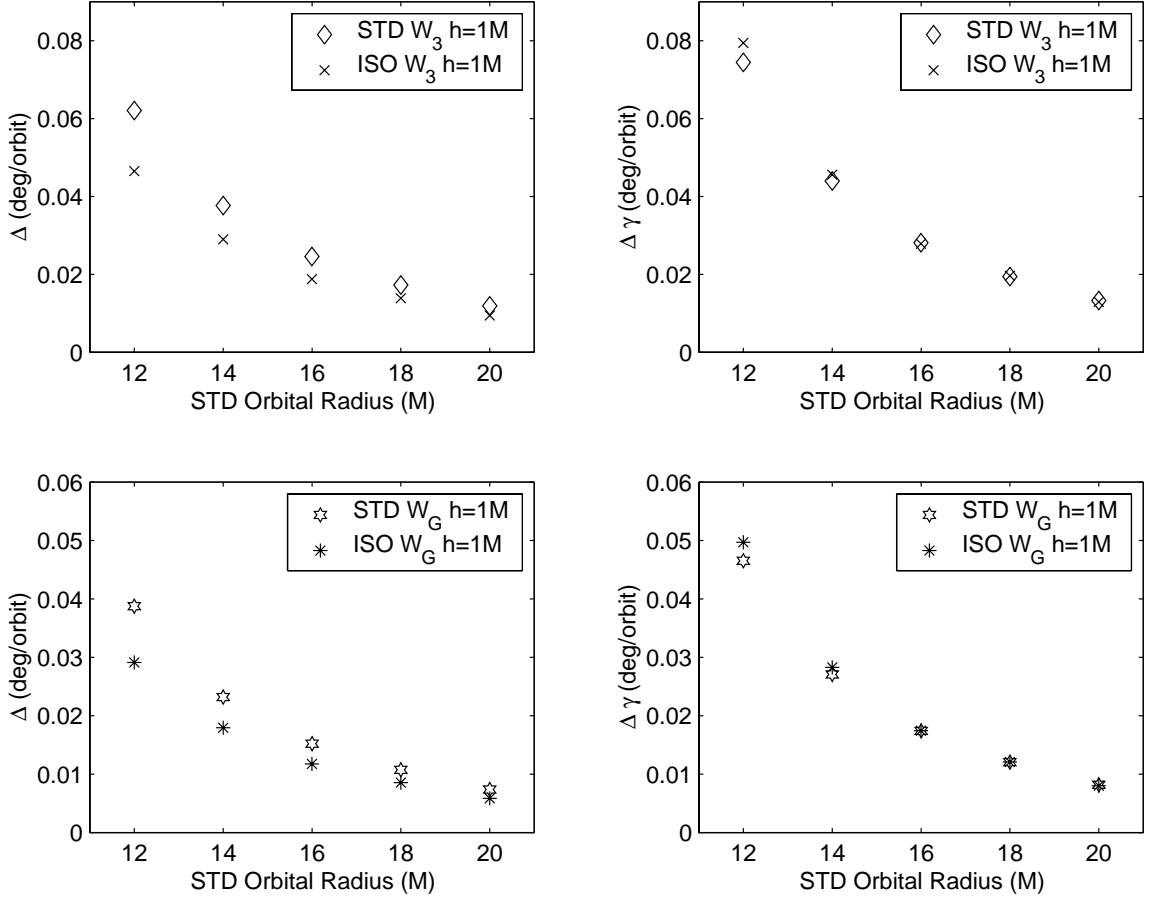


Figure 5.12: Scaling plots for (a) Δ_{STD} (b) $\Delta_{STD}\gamma_{STD}$ (c) Δ_{ISO} and (d) $\Delta_{ISO}\gamma_{ISO}$.

at $r = 12M$. Included in Figure 5.13 is a fit of Δ_{unit} versus standard Schwarzschild orbital radius. The numerical fit is

$$\Delta_{unit} = 1843.542 \left(\frac{M}{r} \right)^{3.502} \quad (5.60)$$

which we refer to as the $A/r^{7/2}$ fit in the figure. The inverse $7/2$ power for the finite-size correction to the phase shift can be understood purely from dimensional grounds as follows. The frequency of Fat Particle motion will differ from the corresponding test particle frequency by corrections due to its finite size. The lowest order of these corrections must be proportional to the second moment of the Fat Particle's distribution, which will have dimensions of a length squared. A dimensionless correction is obtained by dividing by the only characteristic length in the problem, the orbital

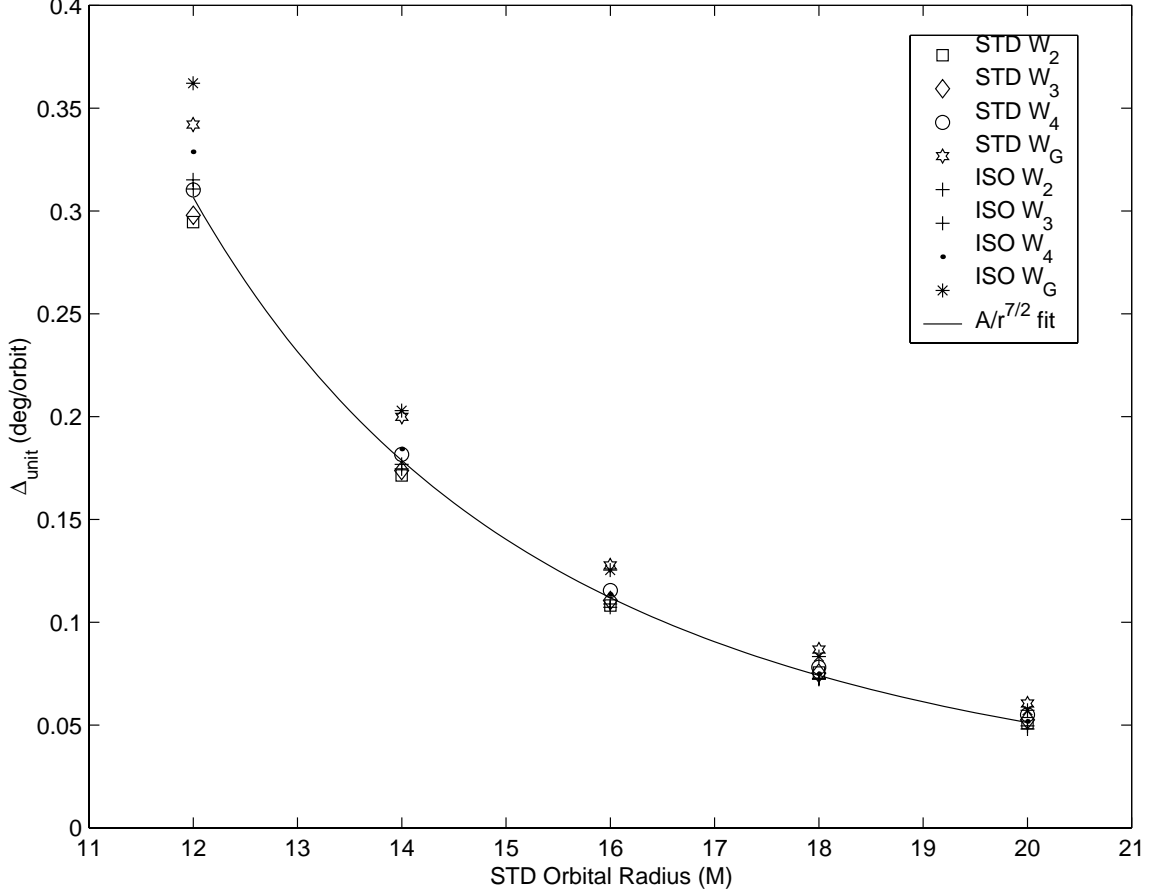


Figure 5.13: Scaling plot for Δ_{unit} .

radius r , leading to, in lowest order, the expression for the Fat Particle frequency

$$\omega_{FP} = 2\pi \frac{\sqrt{M}}{r^{3/2}} \left[1 + \frac{\mathbf{I}}{r^2} + \dots \right] , \quad (5.61)$$

where \mathbf{I} should be regarded as a moment-of-inertia per unit mass (units of length squared). Since the phase shift Δ that results between the Fat and test particles is sensitive to this correction, it should also have a $1/r^{7/2}$ dependence. Note that we know of no way to estimate the size of the correction term from dimensional grounds.

The data for Δ_{unit} can be used to estimate the actual phase shift for a compact object as follows: Consider a white dwarf of 1 solar mass ($1M_{\odot}$) in orbit around a black hole. The radius of such an object in MKS units is approximately $h = 6000$ km [109]. In geometric units, $1M_{\odot}$ is approximately 1.5km. Thus, if the kernel radius of the white dwarf is taken to be $h = 1M$, then the mass of the black hole is

approximately $4318M_\odot$. Thus the assumption that the white dwarf is moving on a fixed metric background is a good one. Now assume that the density of the white dwarf to be given by the profile of W_3 . The phase shift per orbit that the white dwarf would experience at $r = 14M$ compared to the corresponding geodesic motion of a test particle would be approximately 0.044 deg/orbit.

It is instructive to compare the phase shift from Eq. (5.58) to the phase shift expected due solely to gravitational radiation damping. To estimate this latter effect, we rely on the formula derived by Peters [104] for the orbit-averaged rate of change of the period, P , of a binary system comprised of masses M and m . The formula is given by

$$\left\langle \frac{dP}{dt} \right\rangle = \frac{-192\pi}{5} \frac{\mu (m+M)^{3/2}}{a^{5/2} (1-e^2)^{7/2}} \left(1 + \frac{73}{24}e^2 + \frac{37}{96}e^4 \right) , \quad (5.62)$$

where a is the semi-major axis of the orbit, e is the eccentricity, and $\mu = mM/(m+M)$ is the reduced mass. For our white dwarf/black hole (WD/BH) scenario, we require that the eccentricity is zero. In addition, since the mass of the black hole, M , is much greater than the mass of the white dwarf, m , we can approximate the reduced mass as $\mu = m$. The semi-major axis is then identified with the orbital radius of the test particle and Eq. (5.62) becomes

$$\frac{dP}{dt} = \frac{-192\pi}{5} m \sqrt{\frac{M^3}{r^5}} . \quad (5.63)$$

The rate with which the orbital frequency changes is

$$\frac{d\omega}{dt} = \frac{-\omega}{P} \frac{dP}{dt} = \frac{-\omega^2}{2\pi} \frac{dP}{dt} . \quad (5.64)$$

Taking the right-hand side of Eq. (5.64) to be constant, we can immediately integrate to obtain

$$\phi = \phi_0 + \omega t - \frac{\omega^2}{4\pi} \frac{dP}{dt} t^2 . \quad (5.65)$$

The phase shift of the test particle at the same radius is $\phi = \phi_0 + \omega t$ and the relative phase shift is

$$\Delta(t) = \frac{-\omega^2}{4\pi} \frac{dP}{dt} t^2 . \quad (5.66)$$

Evaluating Eq. (5.66) over one orbit, we arrive at our estimate of the phase shift in radians per orbit

$$\begin{aligned}\Delta &= -\pi \frac{dP}{dt} \\ &= \frac{192\pi^2 m}{5} \sqrt{\frac{M^3}{r^5}} \quad .\end{aligned}\tag{5.67}$$

We can go beyond the quadrupole formula to account for higher order corrections. Wagoner and Will [125] have derived the 1.0PN corrections⁷ to the quadrupole radiation formula, resulting in the formula

$$\Delta = \frac{192\pi^2 m}{5} \sqrt{\frac{M^3}{r^5}} \left\{ 1 - \left(\frac{1247}{336} + \frac{35}{12} \frac{m}{M} \right) v^2 \right\}\tag{5.68}$$

where $v = r\omega$. Likewise, Poisson computes the correction to 1.5PN [106] as

$$\Delta = \frac{192\pi^2 m}{5} \sqrt{\frac{M^3}{r^5}} \left\{ 1 - \frac{1247}{336} v^2 + 4\pi v^3 \right\} \quad .\tag{5.69}$$

Will and Wiseman [131] have derived the correction up to 2.0PN

$$\begin{aligned}\Delta &= \frac{192\pi^2 m}{5} \sqrt{\frac{M^3}{r^5}} \left\{ 1 - \frac{M}{r} \left(\frac{2927}{336} + \frac{5}{4} \frac{m}{M} \right) + 4\pi \left(\frac{M}{r} \right)^{3/2} \right. \\ &\quad \left. + \left(\frac{M}{r} \right)^2 \left(\frac{293383}{9072} + \frac{380}{9} \frac{m}{M} \right) \right\} \quad .\end{aligned}\tag{5.70}$$

Figure 5.14 shows a comparison of the phase shifts due to behavior for the WD/BH we've been analyzing. Comparing Eqs. (5.60) and (5.67), we see that the phase shift due to gravitational radiation damping completely overwhelms the phase shift due to finite size effects at large orbital radii. However, as the radius gets smaller the finite size effect becomes dominant. The switch over in magnitude happens around $93.68M$ and the velocity of the white dwarf is approximately $0.1c$.

Finally, we examine the case of the inspiral of two equal mass neutron stars, each of approximately $1.5M_\odot$ and compare the phase shift due to finite size effects to

⁷As pointed out by Will and Wiseman [131], this notation is confusing but adopted out of convention. The quadrupole formula corresponds to a 2.5PN correction to the equations of motion. Thus a 1.0PN correction to the gravitational radiation corresponds to a 3.5PN correction to the equations of motion, and so on.

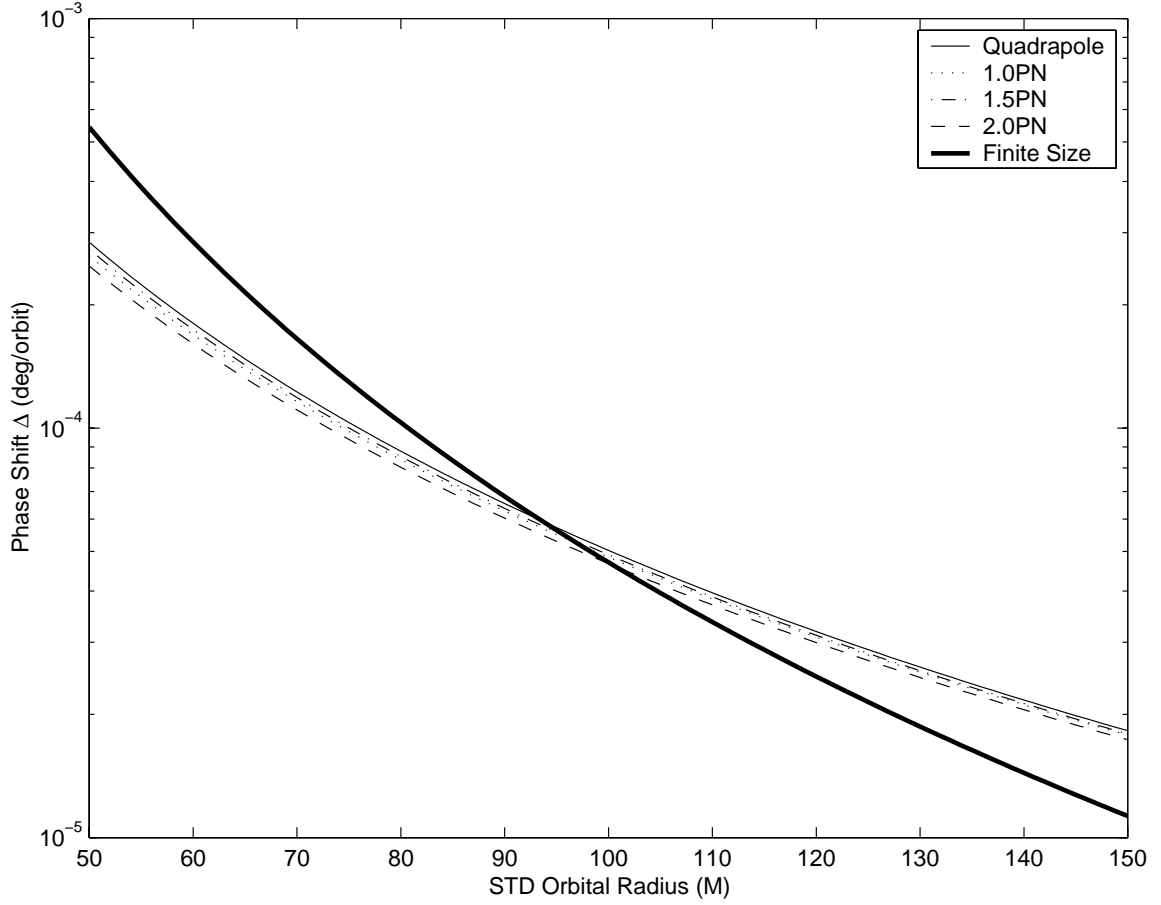


Figure 5.14: A comparison of the phase shift due to gravitational radiation to those due to finite size affects for the white dwarf/black hole system discussed in the text.

those due to radiation damping. This is a stretch of the Fat Particle formalism as this configuration violates the assumption that the Fat Particle moves in a fixed metric spacetime. Nonetheless, we take the finite-size phase shift as a order-of-magnitude estimate. Plugging in the relevant values, one finds that the finite-size phase shift is at least two orders of magnitude less than the shift caused by the emission of gravitational radiation. This is in agreement with the post-Newtonian claim that finite size effects in the NS/NS inspiral are negligible (see *e.g.* [19]).

5.4 Fat Particles - Publish and Subscribe

We draw this chapter to a close with a brief analysis of the Fat Particle equations in the Publish and Subscribe picture, which is the model that accommodates full coupling between the matter and gravitational fields. A complete solution to these equations requires the full machinery of numerical relativity and is thus beyond the our scope. For simplicity, we restrict the number of Fat Particles to one. Following the analysis in Chapter 2, we could derive the corresponding SPH equations and then reduce to one particle. However, we choose to derive the equations from a one-particle discretization of the continuum action Eq. (4.81). Before we proceed with this discretization, we remind the reader of the covariant smoothing rule we obtained earlier. Defining the R3G-weighted normalization⁸

$$\mathcal{N}_{\sqrt{\gamma}}(\vec{z}) = \int d^3x \sqrt{\gamma(\vec{x})} W(\vec{z} - \vec{x}) \quad (5.71)$$

and the R3G ratio

$$R_\gamma = \frac{\sqrt{\gamma}}{\mathcal{N}_{\sqrt{\gamma}}} \quad (5.72)$$

we can define the values of the metric functions at the particle's center. The values for the lapse, shift, and three metric are given by

$$\langle \alpha \rangle(\vec{z}) = \int d^3x R_\gamma \alpha(\vec{x}) W(\vec{z} - \vec{x}) \quad , \quad (5.73)$$

$$\langle \beta_i \rangle(\vec{z}) = \int d^3x R_\gamma \beta_i(\vec{x}) W(\vec{z} - \vec{x}) \quad , \quad (5.74)$$

and

$$\langle \gamma_{ij} \rangle(\vec{z}) = \int d^3x R_\gamma \gamma_{ij}(\vec{x}) W(\vec{z} - \vec{x}) \quad , \quad (5.75)$$

respectively. Since we'll need the variations of these functions as we vary the metric functions in spacetime, we collect the formulae here. The variations of the smoothed form of the lapse and the shift with respect to the underlying variations of the lapse and shift are given by

$$\delta \langle \alpha \rangle|_{\delta\alpha(\vec{x})} = \int d^3x R_\gamma W(\vec{z} - \vec{x}) \delta\alpha(\vec{x}) \quad (5.76)$$

⁸Since the same coordinate time is used to define all of the functions in this section, we will suppress explicit reference to the time when no confusion would result.

and

$$\delta \langle \beta_i \rangle |_{\delta \beta_i(\vec{x})} = \int d^3x R_\gamma W(\vec{z} - \vec{x}) \delta \beta_i(\vec{x}) \quad . \quad (5.77)$$

The situation changes a little when variations of the three-metric are considered. To start, the R3G-weighted normalization has the form

$$\delta \mathcal{N}_{\sqrt{\gamma}} |_{\delta \gamma_{ij}(\vec{x})} = \int d^3x \frac{\sqrt{\gamma}}{2} \gamma^{ij} W(\vec{z} - \vec{x}) \delta \gamma_{ij}(\vec{x}) \quad . \quad (5.78)$$

The corresponding variations in the smoothed lapse and shift are

$$\delta \langle \alpha \rangle |_{\delta \gamma_{ij}(\vec{x})} = \int d^3x \frac{R_\gamma}{2} \gamma^{ij} W(\vec{z} - \vec{x}) [\alpha(\vec{x}) - \langle \alpha \rangle] \delta \gamma_{ij}(\vec{x}) \quad (5.79)$$

and

$$\delta \langle \beta_k \rangle |_{\delta \gamma_{ij}(\vec{x})} = \int d^3x \frac{R_\gamma}{2} \gamma^{ij} W(\vec{z} - \vec{x}) [\beta_k(\vec{x}) - \langle \beta_k \rangle] \delta \gamma_{ij}(\vec{x}) \quad . \quad (5.80)$$

Note that the contribution to the variations of the smoothed lapse and shift from variations of the three-metric vanish as the size of the Fat Particle shrinks to zero, $h \rightarrow 0$, as would be the case in an SPH computation. The variation of the smoothed three-metric is

$$\delta \langle \gamma_{k\ell} \rangle |_{\delta \gamma_{ij}(\vec{x})} = \int d^3x R_\gamma W(\vec{z} - \vec{x}) \left[1 + \frac{\gamma^{ij}}{2} (\gamma^{k\ell} - \langle \gamma^{k\ell} \rangle) \right] \delta \gamma_{ij}(\vec{x}) \quad , \quad (5.81)$$

where the smoothed inverse metric is the matrix inverse of the smoothed metric and its variation is defined by

$$\delta \langle \gamma^{k\ell} \rangle |_{\delta \gamma_{ij}(\vec{x})} = - \langle \gamma^{km} \rangle \delta \langle \gamma_{mn} \rangle |_{\delta \gamma_{ij}} \langle \gamma^{n\ell} \rangle \quad . \quad (5.82)$$

Now we are in the position to define the discretization rule. Using the discussion in Section 2.6 as a guide, we make the ansatz that the discretization rule should be given by

$$\tilde{\rho}_0 = m \delta(\vec{a} - \vec{z}) \quad . \quad (5.83)$$

Substituting Eq. (5.83) into Eq. (4.81) gives the combined action

$$\begin{aligned} I = & \frac{1}{16\pi} \int d^3x dt [\pi^{ij} \partial_t \gamma_{ij} - \alpha R^0 - \beta_i R^i] \\ & + \int dt m (1 + e[\langle \rho \rangle]) [u_0 + \dot{z}^i u_i - \Lambda \langle \mathcal{H} \rangle] \quad . \end{aligned} \quad (5.84)$$

The smoothed Hamiltonian is given by

$$\langle \mathcal{H} \rangle = \frac{1}{2} \left[\langle \gamma^{ij} \rangle u_i u_j - \frac{(u_0 - \langle \beta^i \rangle u_i)^2}{\langle \alpha \rangle} + 1 \right] . \quad (5.85)$$

Taking the variation $\delta I|_{\delta\Lambda}$ of Eq. (5.85) and setting this result to zero implies $\langle \mathcal{H} \rangle = 0$, from which we derive

$$u_0 = \langle \beta^i \rangle u_i - \langle \alpha \rangle \sqrt{1 + \|\langle u \rangle\|^2} \quad (5.86)$$

with

$$\|\langle u \rangle\|^2 = \langle \gamma^{ij} \rangle u_i u_j . \quad (5.87)$$

Eq. (5.86) is the smoothed analog of Eq. (4.83). Likewise, setting the variation of Eq. (5.84) with respect to u_0 to zero, $\delta I|_{\delta u_0} = 0$, implies

$$\Lambda = \frac{\langle \alpha \rangle^2}{\langle \beta^i \rangle u_i - u_0} = \frac{\langle \alpha \rangle}{\sqrt{1 + \|\langle u \rangle\|^2}} \quad (5.88)$$

compared to Eq. (4.84). We define a smoothed form of ϵ^i

$$\langle \epsilon^i \rangle = z^i + \langle \beta^i \rangle = \Lambda \langle \gamma^{ij} \rangle u_j \quad (5.89)$$

in the same way as in Eq. (4.85) and we immediately find the equivalent identification

$$\Lambda = \langle \alpha \rangle \sqrt{1 - \frac{\|\langle \epsilon \rangle\|^2}{\langle \alpha \rangle}} . \quad (5.90)$$

We next turn to the variation of Eq. (5.84) with respect to the lapse. The resulting constraint equation, which is the analog of Poisson's equation in general relativity, allows us to read off the form of the density. Taking the variation (and assuming that the smoothed density, like its continuum counterpart, is independent of the metric derivatives) yields

$$\delta I|_{\delta\alpha} = \int d^3x dt \frac{-R^0}{16\pi} \delta\alpha - \int dt m\Lambda \left[\frac{P[\langle \rho \rangle]}{\langle \rho \rangle^2} \frac{\partial \langle \rho \rangle}{\partial \langle \alpha \rangle} + (1 + e[\langle \rho \rangle]) \frac{\partial \langle \mathcal{H} \rangle}{\partial \langle \alpha \rangle} \right] \delta \langle \alpha \rangle . \quad (5.91)$$

Using Eq. (5.85), we can compute the partial of the Hamiltonian

$$\frac{\partial \langle \mathcal{H} \rangle}{\partial \langle \alpha \rangle} = \frac{\langle \alpha \rangle}{\Lambda^2} = \frac{1 + \|\langle u \rangle\|^2}{\langle \alpha \rangle} , \quad (5.92)$$

where we've used the last relation in Eq. (5.88) to eliminate Λ . Substituting Eq. (5.92) into Eq. (5.91), we get

$$\begin{aligned}
R + \frac{Tr(\pi^2)}{2\gamma} - \frac{Tr(\pi)^2}{\gamma} &= 16\pi \frac{mW(\vec{x} - \vec{z})}{\mathcal{N}_{\sqrt{\gamma}}} \langle \alpha \rangle \sqrt{1 - \frac{\|\langle \epsilon \rangle\|^2}{\langle \alpha \rangle}} \frac{P[\langle \rho \rangle]}{\langle \rho \rangle^2} \frac{\partial \langle \rho \rangle}{\partial \langle \alpha \rangle} \\
&+ 16\pi \frac{mW(\vec{x} - \vec{z})}{\mathcal{N}_{\sqrt{\gamma}}} \sqrt{1 - \frac{\|\langle \epsilon \rangle\|^2}{\langle \alpha \rangle}} \\
&(1 + e[\langle \rho \rangle]) (1 + \|\langle u \rangle\|^2) \quad . \quad (5.93)
\end{aligned}$$

Comparison of the last term in Eq. (5.93) to Eq. (4.112) suggests that we *define* the Fat Particle density as

$$\rho(\vec{x}) = \begin{cases} \frac{mW(\vec{x} - \vec{z})}{\mathcal{N}_{\sqrt{\gamma}}} \sqrt{1 - \frac{\|\langle \epsilon \rangle\|^2}{\langle \alpha \rangle}} & |\vec{z} - \vec{x}| < h \\ 0 & |\vec{z} - \vec{x}| \geq h \end{cases} , \quad (5.94)$$

where we remind the reader that the term $|\vec{z} - \vec{x}|$ denotes the coordinate distance between the Fat Particle's center at \vec{z} and the point in question \vec{x} . To see if this definition fits, we use it to compute the remaining partial derivative in Eq. (5.93)

$$\frac{\partial \langle \rho \rangle}{\partial \langle \alpha \rangle} = \frac{\langle \rho \rangle \|\langle \epsilon \rangle\|^2}{\langle \alpha \rangle \Lambda^2} , \quad (5.95)$$

where the density at the Fat Particle center is given by

$$\langle \rho \rangle = \rho(\vec{z}) = \frac{mW(0)}{\mathcal{N}_{\sqrt{\gamma}}} \sqrt{1 - \frac{\|\langle \epsilon \rangle\|^2}{\langle \alpha \rangle}} \quad . \quad (5.96)$$

Substituting Eq. (5.95) back into Eq. (5.93) and simplifying, we arrive at

$$\begin{aligned}
R + \frac{Tr(\pi^2)}{2\gamma} - \frac{Tr(\pi)^2}{\gamma} &= 16\pi \left(\rho \frac{P[\langle \rho \rangle]}{\langle \rho \rangle} \|\langle u \rangle\|^2 \right. \\
&\left. + \rho (1 + e[\langle \rho \rangle]) (1 + \|\langle u \rangle\|^2) \right) \quad , \quad (5.97)
\end{aligned}$$

which is formally the same as the expression in Eq. (4.112). In particular, the source on the right-hand side of Eq. (5.97) is non-zero only within the compact support of the Fat Particle.

As a further check on the consistency of the density definition, consider substituting Eq. (5.94) into the integral form of the baryon conservation law in Eq. (4.21).

Doing so gives

$$\begin{aligned}
\int d^3x \rho(\vec{x}) \sqrt{-g} u^0 &= \int d^3x \frac{mW(\vec{x} - \vec{z})}{\mathcal{N}_{\sqrt{\gamma}}} \sqrt{\gamma} \\
&= \frac{m}{\mathcal{N}_{\sqrt{\gamma}}} \int d^3x \sqrt{\gamma} W(\vec{x} - \vec{z}) \\
&= m \quad ,
\end{aligned} \tag{5.98}$$

provided we define

$$u^0 = \frac{1}{\alpha \sqrt{1 - \|\langle \epsilon \rangle\|^2 / \langle \alpha \rangle^2}} \quad , \tag{5.99}$$

which we are free to do since the four velocity at a point away from the Fat Particle is not specified from any prior relation. We next take the variation of Eq. (5.84) with respect to the shift to obtain the smoothed equivalent of the continuum momentum constraint Eq. (4.118)

$$-R^i = 16\pi m \Lambda \left[\frac{P[\langle \rho \rangle]}{\langle \rho \rangle^2} \frac{\partial \langle \rho \rangle}{\partial \langle \beta_i \rangle} + (1 + e[\langle \rho \rangle]) \frac{\partial \langle \mathcal{H} \rangle}{\partial \langle \beta_i \rangle} \right] R_\gamma W(\vec{z} - \vec{x}) \quad . \tag{5.100}$$

Taking the derivatives with respect to $\langle \beta_i \rangle$ of the smoothed density

$$\frac{\partial \langle \rho \rangle}{\partial \langle \beta_\ell \rangle} = \frac{-\langle \rho \rangle \langle \epsilon^\ell \rangle}{\Lambda^2} = \frac{-\langle \rho \rangle \langle \gamma^{\ell m} \rangle u_m}{\Lambda} \tag{5.101}$$

and the smoothed Hamiltonian

$$\frac{\partial \langle \mathcal{H} \rangle}{\partial \langle \beta_i \rangle} = \frac{-\langle \gamma^{ij} \rangle u_j}{\Lambda} \tag{5.102}$$

and substituting these relations into Eq. (5.100) and simplifying yields

$$D_j \pi^{ij} = -8\pi \rho \sqrt{\gamma} \sqrt{1 + \|\langle u \rangle\|^2} \left(1 + e[\langle \rho \rangle] + \frac{P[\langle \rho \rangle]}{\langle \rho \rangle} \right) \langle \gamma^{ij} \rangle u_j \quad . \tag{5.103}$$

We next take the variation of Eq. (5.84) with respect to changes in the three-metric.

Carrying out this variation gives

$$\begin{aligned}
\delta I|_{\delta\gamma_{ij}(\vec{x})} &= \delta I_{ADM}|_{\delta\gamma_{ij}} - \int dt m \Lambda \left[\frac{P[\langle \rho \rangle]}{\langle \rho \rangle^2} \delta \langle \rho \rangle|_{\delta\gamma_{ij}(\vec{x})} \right. \\
&\quad \left. + (1 + e[\langle \rho \rangle]) \delta \langle \mathcal{H} \rangle|_{\delta\gamma_{ij}(\vec{x})} \right] \quad ,
\end{aligned} \tag{5.104}$$

where the variation of the ADM action is given by (see Eqs. (3.99) and (3.100))

$$\begin{aligned}
\delta I_{ADM}|_{\delta\gamma_{ij}} &= \int d^3x \left\{ -\partial_t \pi^{ij} - A^{ij} \sqrt{\gamma} - B \sqrt{\gamma} \gamma^{ij} \right. \\
&\quad \left. - 2\beta^{(i} \pi^{j)k}{}_{|k} + \mathcal{L}_{\vec{\beta}} \pi^{ij} \right\} \delta \gamma_{ij} \quad .
\end{aligned} \tag{5.105}$$

The individual variations of the smoothed density and smoothed Hamiltonian in Eq. (5.104) are given by

$$\begin{aligned} \delta \langle \rho \rangle |_{\delta \gamma_{ij}(\vec{x})} &= \frac{\partial \langle \rho \rangle}{\partial \mathcal{N}_{\sqrt{\gamma}}} \delta \mathcal{N}_{\sqrt{\gamma}} |_{\delta \gamma_{ij}} + \frac{\partial \langle \rho \rangle}{\partial \langle \alpha \rangle} \langle \alpha \rangle |_{\delta \gamma_{ij}} \\ &+ \frac{\partial \langle \rho \rangle}{\partial \langle \beta_\ell \rangle} \langle \beta_\ell \rangle |_{\delta \gamma_{ij}} + \frac{\partial \langle \rho \rangle}{\partial \langle \gamma_{k\ell} \rangle} \langle \gamma_{k\ell} \rangle |_{\delta \gamma_{ij}} \end{aligned} \quad (5.106)$$

and

$$\delta \langle \mathcal{H} \rangle |_{\delta \gamma_{ij}(\vec{x})} = \frac{\partial \langle \mathcal{H} \rangle}{\partial \langle \alpha \rangle} \langle \alpha \rangle |_{\delta \gamma_{ij}} \frac{\partial \langle \mathcal{H} \rangle}{\partial \langle \beta_\ell \rangle} \langle \beta_\ell \rangle |_{\delta \gamma_{ij}} \frac{\partial \langle \mathcal{H} \rangle}{\partial \langle \gamma_{k\ell} \rangle} \langle \gamma_{k\ell} \rangle |_{\delta \gamma_{ij}} \quad , \quad (5.107)$$

respectively. We will not attempt to substitute these expressions back into Eq. (5.105) due to the complexity but we catalog the various partial derivatives that we have yet to quote below. These being:

$$\frac{\partial \langle \rho \rangle}{\partial \langle \gamma_{mn} \rangle} = \frac{\langle \rho \rangle \langle \beta^{(n)} \rangle \langle \epsilon^m \rangle}{\Lambda^2} - \frac{\langle \rho \rangle \langle \epsilon^m \rangle \langle \epsilon^n \rangle}{2 \Lambda \Lambda} \quad , \quad (5.108)$$

$$\frac{\partial \langle \rho \rangle}{\partial \mathcal{N}_{\sqrt{\gamma}}} = \frac{-\langle \rho \rangle}{\mathcal{N}_{\sqrt{\gamma}}} \quad , \quad (5.109)$$

and

$$\frac{\partial \langle \mathcal{H} \rangle}{\partial \langle \gamma_{k\ell} \rangle} = \frac{u_s \langle \gamma^{s(k)} \rangle \langle \beta^\ell \rangle}{\Lambda} - \frac{1}{2} \langle \gamma^{ks} \rangle u_s \langle \gamma^{\ell t} \rangle u_t \quad . \quad (5.110)$$

The final variation to take is with respect to changes in the fluid worldlines z^i . Taking this variation yields

$$\begin{aligned} \delta I_{PS} |_{\delta z^i} &= \delta I_{FP} |_{\delta z^i} \\ &= \int dt m \left[\frac{P[\langle \rho \rangle]}{\langle \rho \rangle^2} \delta \langle \rho \rangle |_{\delta z^i} (-\Lambda) \right. \\ &\quad \left. + (1 + e[\langle \rho \rangle]) u_i \delta z^i - \Lambda \delta \langle \mathcal{H} \rangle |_{\delta z^i} \right] \delta z^i \quad , \end{aligned} \quad (5.111)$$

with the smoothed density variation as

$$\delta \langle \rho \rangle |_{\delta z^i} = \frac{\partial \langle \rho \rangle}{\partial z^i} \delta z^i + \frac{\partial \langle \rho \rangle}{\partial \dot{z}^i} \delta \dot{z}^i \quad (5.112)$$

and the smoothed Hamiltonian variation as

$$\delta \langle \mathcal{H} \rangle |_{\delta z^i} = \frac{\partial \langle \mathcal{H} \rangle}{\partial z^i} \delta z^i \quad . \quad (5.113)$$

Substituting Eqs. (5.112) and (5.113) back into Eq. (5.111)

$$\begin{aligned} \delta I_{FP}|_{\delta z^i} &= \int dt m [(1 + e[\langle \rho \rangle]) u_i \delta z^i \\ &\quad - \Lambda \frac{P[\langle \rho \rangle]}{\langle \rho \rangle^2} \left(\frac{\partial \langle \rho \rangle}{\partial z^i} \delta z^i + \frac{\partial \langle \rho \rangle}{\partial \dot{z}^i} \delta \dot{z}^i \right) - \Lambda \frac{\partial \langle \mathcal{H} \rangle}{\partial z^i} \delta z^i] \quad . \end{aligned} \quad (5.114)$$

Integrating Eq. (5.114) by parts to move the derivatives from the variations to their coefficients, we arrive at

$$\begin{aligned} \delta I_{FP}|_{\delta z^i} &= - \int dt m \left\{ \frac{d}{dt} \left[(1 + e[\langle \rho \rangle]) u_i - \Lambda \frac{P[\langle \rho \rangle]}{\langle \rho \rangle^2} \frac{\partial \langle \rho \rangle}{\partial z^i} \right] \right. \\ &\quad \left. + \Lambda \left[\frac{P[\langle \rho \rangle]}{\langle \rho \rangle^2} \frac{\partial \langle \rho \rangle}{\partial z^i} + \frac{\partial \langle \mathcal{H} \rangle}{\partial z^i} \right] \right\} \delta z^i \quad . \end{aligned} \quad (5.115)$$

Setting the variation to zero gives

$$\begin{aligned} &\frac{d}{dt} \left[(1 + e[\langle \rho \rangle]) u_i - \Lambda \frac{P[\langle \rho \rangle]}{\langle \rho \rangle^2} \frac{\partial \langle \rho \rangle}{\partial z^i} \right] \\ &+ \Lambda \left[\frac{P[\langle \rho \rangle]}{\langle \rho \rangle^2} \frac{\partial \langle \rho \rangle}{\partial z^i} + (1 + e[\langle \rho \rangle]) \frac{\partial \langle \mathcal{H} \rangle}{\partial z^i} \right] = 0 \end{aligned} \quad (5.116)$$

as the smoothed form of the relativistic Euler equation. We can simplify the first term in Eq. (5.116) by first calculating

$$\frac{\partial \langle \rho \rangle}{\partial \dot{z}^i} = \frac{-\langle \rho \rangle \langle \gamma_{ij} \rangle \langle \epsilon^\ell \rangle}{\Lambda^2} = \frac{-\langle \rho \rangle u_i}{\Lambda} \quad (5.117)$$

and then substituting this into Eq. (5.116) to obtain

$$\frac{d}{dt} \left[\left(1 + e[\langle \rho \rangle] + \frac{P[\langle \rho \rangle]}{\langle \rho \rangle} \right) u_i \right] + \left[\frac{P[\langle \rho \rangle]}{\langle \rho \rangle^2} \frac{\partial \langle \rho \rangle}{\partial z^i} + \frac{\partial \langle \mathcal{H} \rangle}{\partial z^i} \right] = 0 \quad . \quad (5.118)$$

The partial derivatives of the smoothed density and smoothed Hamiltonian with respect to z^i are given by

$$\frac{\partial \langle \rho \rangle}{\partial z^i} = \frac{\partial \langle \rho \rangle}{\partial \mathcal{N}_{\sqrt{\gamma}}} \partial_{z^i} \mathcal{N}_{\sqrt{\gamma}} + \frac{\partial \langle \rho \rangle}{\partial \langle \alpha \rangle} \partial_{z^i} \langle \alpha \rangle + \frac{\partial \langle \rho \rangle}{\partial \langle \beta_\ell \rangle} \partial_{z^i} \langle \beta_\ell \rangle + \frac{\partial \langle \rho \rangle}{\partial \langle \gamma_{ij} \rangle} \partial_{z^i} \langle \gamma_{ij} \rangle \quad (5.119)$$

and

$$\frac{\partial \langle \mathcal{H} \rangle}{\partial z^i} = + \frac{\partial \langle \mathcal{H} \rangle}{\partial \langle \alpha \rangle} \partial_{z^i} \langle \alpha \rangle + \frac{\partial \langle \mathcal{H} \rangle}{\partial \langle \beta_\ell \rangle} \partial_{z^i} \langle \beta_\ell \rangle + \frac{\partial \langle \mathcal{H} \rangle}{\partial \langle \gamma_{ij} \rangle} \partial_{z^i} \langle \gamma_{ij} \rangle \quad (5.120)$$

with the individual derivatives already cited. To analyze the Fat Particle equations, we follow our approach in Section 4.6 and look for solutions of these equations that are consistent with the static, spherically symmetric metric

$$ds^2 = -e^{2\Phi(r)} dt^2 + e^{2\Lambda(r)} dr^2 + r^2 d\Omega^2 \quad .$$

As discussed before, since the metric is time-independent and the shift is zero, we get $K^{ij} = 0$, which in turn implies

$$D_j \pi^{ij} = 0 \implies u_j = 0 \quad , \quad (5.121)$$

$$\rho(\vec{x}) = \frac{mW(\vec{x} - \vec{z})}{\mathcal{N}_{\sqrt{\gamma}}} \quad , \quad (5.122)$$

and

$$\langle \rho \rangle = \frac{mW(0)}{\mathcal{N}_{\sqrt{\gamma}}} \quad . \quad (5.123)$$

The Hamiltonian constraint, given in Eq. (5.97), becomes

$$R = 16\pi\rho(1 + e[\langle \rho \rangle]) \quad , \quad (5.124)$$

from which we get

$$\frac{d}{dr}m(r) = 4\pi r^2 \rho(1 + e[\langle \rho \rangle]) \quad , \quad (5.125)$$

which is the smoothed analog of Eq. (4.139).

Next, we turn to the π^{ij} evolution equation. The only non-zero component of $\delta \langle \rho \rangle|_{\delta\gamma_{ij}(\vec{x})}$ is

$$\frac{\partial \langle \rho \rangle}{\partial \mathcal{N}_{\sqrt{\gamma}}} \delta \mathcal{N}_{\sqrt{\gamma}}|_{\delta\gamma_{ij}(\vec{x})} = \int d^3x \left(\frac{-\langle \rho \rangle}{2\mathcal{N}_{\sqrt{\gamma}}} \right) \sqrt{\gamma} \gamma^{ij} W(\vec{z} - \vec{x}) \delta\gamma_{ij} \quad . \quad (5.126)$$

Likewise, the only non-zero component of $\delta \langle \mathcal{H} \rangle|_{\delta\gamma_{ij}(\vec{x})}$ is

$$\frac{\partial \langle \mathcal{H} \rangle}{\partial \langle \alpha \rangle} \delta \langle \alpha \rangle|_{\delta\gamma_{ij}(\vec{x})} = \int d^3x \frac{\mathcal{R}_\gamma}{2} \gamma^{ij} W(\vec{x} - \vec{z}) \left[\frac{\alpha}{\langle \alpha \rangle} - 1 \right] \delta\gamma_{ij} \quad . \quad (5.127)$$

Substituting Eqs. (5.126) and (5.127) into Eq. (5.97) gives the smoothed equivalent of Eq. (4.132)

$$\begin{aligned} & \alpha R^{ij} - D^i D^j \alpha + \gamma^{ij} \left(D^\ell D_\ell \alpha - \frac{\alpha}{2} R \right) = \\ & 8\pi \langle \alpha \rangle \left[P[\langle \rho \rangle] \frac{\rho}{\langle \rho \rangle} - \rho(\alpha - \langle \alpha \rangle) \right] \gamma^{ij} \quad . \end{aligned} \quad (5.128)$$

Finally, we examine the smoothed version of the fluid flow equation. To do so, we first note that since the velocity is zero Eq. (5.118) can be written as

$$\left[\frac{P[\langle \rho \rangle]}{\langle \rho \rangle^2} \frac{\partial \langle \rho \rangle}{\partial z^i} + \frac{\partial \langle \mathcal{H} \rangle}{\partial z^i} \right] = 0 \quad . \quad (5.129)$$

Under the requirement that $u_i = 0$, the partial derivatives in Eq. (5.129) are

$$\frac{\partial \langle \rho \rangle}{\partial z^i} = \frac{\langle \rho \rangle}{\mathcal{N}_{\sqrt{\gamma}}} \partial_{z^i} \quad (5.130)$$

and

$$\frac{\partial \langle \mathcal{H} \rangle}{\partial \langle \alpha \rangle} = \frac{1}{\langle \alpha \rangle} \partial_{z^i} \langle \alpha \rangle \quad . \quad (5.131)$$

Using Eqs. (5.130) and (5.131), Eq. (5.129) becomes

$$\partial_{z^i} \langle \alpha \rangle = \frac{\langle \alpha \rangle P[\langle \rho \rangle]}{\mathcal{N}_{\sqrt{\gamma}} \langle \rho \rangle} \partial_{z^i} \mathcal{N}_{\sqrt{\gamma}} \quad . \quad (5.132)$$

The left-hand side of Eq. (5.132) can be recast as

$$\partial_{z^i} \langle \alpha \rangle = \frac{\partial_{z^i} \tilde{\alpha}}{\mathcal{N}_{\sqrt{\gamma}}} - \frac{\langle \alpha \rangle}{\mathcal{N}_{\sqrt{\gamma}}} \partial_{z^i} \mathcal{N}_{\sqrt{\gamma}} \quad , \quad (5.133)$$

where $\tilde{\alpha} = \int d^3x \alpha \sqrt{\gamma} W(\vec{z} - \vec{x})$.

Equating the right-hand sides of Eqs. (5.131) and (5.132) gives

$$\partial_{z^i} \tilde{\alpha} = \langle \alpha \rangle \left(1 + \frac{P[\langle \rho \rangle]}{\langle \rho \rangle} \right) \partial_{z^i} \mathcal{N}_{\sqrt{\gamma}} \quad . \quad (5.134)$$

Eq. (5.134) can be simplified to yield

$$\int d^3x \alpha \sqrt{\gamma} \partial_{z^i} W(\vec{x} - \vec{z}) = \int d^3x \langle \alpha \rangle \left(1 + \frac{P[\langle \rho \rangle]}{\langle \rho \rangle} \right) \sqrt{\gamma} \partial_{z^i} W(\vec{x} - \vec{z}) \quad . \quad (5.135)$$

Taken together, Eqs. (5.125), (5.128), (5.135) give a set of integro-differential equations for the functions $\Phi(r)$ and $\Lambda(r)$. Whether this set has a consistent solution is still an open question and will be the subject of future work.

Chapter 6

Conclusion

In this dissertation, we examined the notion of Fat Particles (FPs), which we used as proxies for compact objects, such as white dwarfs or neutron stars. We make the assumption that the hydrodynamic particulars of these compact objects are not nearly as important as their overall size and gross motion of their center-of-mass. Doing so allows us to model the Fat Particle's finite extent by means of a even, symmetric, smoothing kernel W of radius h attached to the particle's center-of-mass \vec{z} . Contributions of various fields over the volume of the Fat Particle are obtained by weighting the field values at points \vec{x} within the compact support of the kernel by the value $W(\vec{x} - \vec{z}; h)$ and then summing. This smoothing rule is a modified form of the kernel estimation technique used in Smoothed Particle Hydrodynamics (SPH). The Fat Particle equations governing the evolution of the gravitational and fluid degrees of freedom are obtained in by i) starting from a continuum action principle describing an ideal fluid, ii) introducing a discretization rule that expresses the initial fluid as a sum over delta-functions, and iii) by taking the appropriate variations. We feel that this algorithm is the best guarantee for obtaining a set of equations that respects the continuum conservation laws. Variations of only the fluid trajectories leads to the *Subscribe Only* model, in which the Fat Particle moves under the influence of an external gravitational field but contributes nothing in return. In contrast, variations of the fluid trajectories and the gravitational fields leads to the *Publish and Subscribe* model which is a full back-reacting system.

By following this algorithm in Newtonian gravity and general relativity, we ob-

tained several important results. First, we demonstrated that Newtonian Fat Particles in the Publish and Subscribe model were well-defined and gave sensible results. They comfortably serve as sources for Poisson’s equation and are capable of sustaining a self-generated gravitational field without moving under its influence. In the process of obtaining this result, we were able to rigorously arrive at the accepted SPH density definition from first principles, which, to our knowledge, has never been done before. Using a single particle Subscribe Only model in Einstein’s theory, we were able to obtain finite-size corrections to the circular motion of a negligible-mass, compact object orbiting in a fixed background metric. From these corrections, we numerically estimated the finite-size phase shift, by comparing the Fat Particle to a test particle on the same circular orbit. We found a universal scaling law (going as $r^{-7/2}$ where r is the orbital radius) that describes the phase shift in a way that is independent of the Fat Particle’s size, shape, and distribution. We showed that these finite-size effects eventually dominate radiation damping effects in describing the motion of a white dwarf around a more massive black hole but that they are several orders of magnitude less important than the gravitational radiation damping in the case of the inspiral of a binary neutron star system. These results are the first strong field estimates of the finite-size corrections to the motion of compact objects that we know of and are relevant to the production of theoretical wave templates used by LIGO or LISA. Finally, we derived the *Publish and Subscribe* Fat Particle equations in general relativity for a single Fat Particle. Comparison of these equations for a static, symmetric spacetime with their continuum analogs shows that the system supports a consistent density definition that limits the contribution of the matter source in the ADM equations (see, *e.g.*, Hamiltonian and momentum constraints Eqs. (5.97) and (4.118)) to the compact support of the kernel and which seems to hold promise for future development. We draw this dissertation to a close with suggestions for future work. This work can be classified into three broad categories; numerical explorations, extensions to the Subscribe Only model, and further development of the Publish and Subscribe model.

On the topic of numerical explorations, three specific items come immediately to

mind. First of all, our Subscribe Only runs were performed with a limited number of points contained in the smoothing kernel. A second generation set of runs can be performed with an arbitrary number of points used in the kernel estimation by computing the metric functions and their derivatives at each time step only within the support of the kernel rather than by using the grid method employed here. This modification would allow us a better understanding of the convergence properties of the smoothing estimation technique and would form a valuable check on the phase shift results presented. However, direct computation of the metric functions, while requiring modest amounts of computer memory, will necessarily cause a drop in run performance. For this reason, only a subset of the runs presented here should be considered. Next, it should be determined how errors in the smoothed covariant metric functions propagate into the computations of the smoothed contravariant metric functions and related parameters like the smoothed right-hand side of the Fat Particle's equations of motion. This analysis falls within the discipline of numerical linear algebra and should be achievable. Finally, the scalar smoothing prescription (see Eq. (5.11)) should be re-visited – this time with the argument of the smoothing kernel (Eq. (5.12)) written in terms of the three-metric γ_{ij} evaluated at the particle center \vec{z} or as some weighted average of its values at \vec{z} and \vec{x} . Doing so may improve the results for smaller orbital radii, although the cost of making this modification is a large increase in the complexity of the equations in the Publish and Subscribe model.

On extending the single particle Subscribe Only picture, there are also several potential branches for exploration. First of all, this model has been tested in one spacetime slicing. The hypersurfaces of the standard Schwarzschild (STD) metric are equivalent to those of the Schwarzschild isotropic (ISO) metric – differing only in the labels attached to the radial distances from the black hole. It would be valuable to examine Fat Particle motion in the different slicing afforded by the Painlevé-Gullstrand (PG) coordinates. Comparisons of the PG results with those already obtained would indicate if modifications to the R3G smoothing prescription are required to capture spacetime features that do not lie within a given spatial hypersurface. It would also

serve as a bridge to modeling motion in more complex spacetimes, such as a Kerr black hole. Second, it is straightforward to produce a simulation of a white dwarf inspiral into a black hole that takes into account both the gravitational damping and finite-size corrections to the equations of motion. This simulation, which would be a combination of our work and the work by Bishop *et. al.* [16], would be a valuable source of templates for LISA. Finally, a multi-particle SPH version of the Subscribe Only picture is readily obtained, given the groundwork presented in this dissertation, and would serve as a natural testing ground for modeling accretion disks around black holes (see, *e.g.*, [14]).

On further development of the Publish and Subscribe model, there are numerous avenues to explore. Most prominent of these is the solution of the single Fat Particle equations (Eqs. (5.125), (5.128), and (5.135)) for a static, spherical symmetric spacetime. These equations, defining what we call an FP star, must be solved by self-consistent iterative means. Early experimentation with a simplified form of these equations indicated that the solutions did seem to converge. However, no definitive conclusion as to the physical validity of these solutions was achieved. It may be likely that valid solutions will require a modification of the discretization rule (Eq. (5.83)) or the definition of the density (Eq. 5.94). What is clear is that the road to a full back-reacting simulation involving Fat Particles starts with a better understanding of the FP star equations and their solutions.

Appendix A

Derivatives of Determinants

In several places in the main body of this text, derivatives of the determinant of the metric or the Jacobian of a map are needed. The algebra of the computations is involved enough that its inclusion would be a distraction and yet is not common enough that a few sprinkled references would suffice. Thus the various results have been gathered here.

A.1 Variations of a Determinant

Let \mathbf{A} be an $N \times N$ matrix

$$\mathbf{A} = \begin{pmatrix} a_{11} & a_{12} & \cdots & a_{1N} \\ a_{21} & a_{22} & \vdots & a_{2n} \\ \vdots & \vdots & \ddots & \vdots \\ a_{N1} & a_{N2} & \cdots & a_{NN} \end{pmatrix} \quad (\text{A.1})$$

with entries $[\mathbf{A}]_{ij} = a_{ij}$ and with $i = 1, 2, \dots, N$, and $j = 1, 2, \dots, N$. Define a signed elementary product from \mathbf{A} [3] to mean any product $\pm a_{i_1 j_1} a_{i_2 j_2} \cdots a_{i_N j_N}$ of N entries from \mathbf{A} , no two of which come from the same row or column. The plus sign is chosen if both i_1, i_2, \dots, i_N and j_1, j_2, \dots, j_N are either even or odd permutations of $1, 2, \dots, N$. The determinant of \mathbf{A} , denoted by a , can be expressed as

$$\det(\mathbf{A}) \equiv a = \frac{1}{N!} [i_1, i_2, \dots, i_N] [j_1, j_2, \dots, j_N] a_{i_1 j_1} a_{i_2 j_2} \cdots a_{i_N j_N}, \quad (\text{A.2})$$

where the permutation symbol $[i_1, i_2, \dots, i_N]$ is defined as

$$[i_1, i_2, \dots, i_N] = \begin{cases} +1 & i_1, i_2, \dots, i_N \text{ an even permutation of } 1, 2, \dots, N \\ -1 & i_1, i_2, \dots, i_N \text{ an odd permutation of } 1, 2, \dots, N \\ 0 & \text{otherwise} \end{cases} \quad (\text{A.3})$$

The first permutation symbol assures that each term $a_{i_1 j_1} a_{i_2 j_2} \cdots a_{i_N j_N}$ comes from a different row while the second permutation symbol assures each term comes from a different column. The determinant is defined to be the sum of the $N!$ different signed elementary products in \mathbf{A} [3]. The product of the two permutation symbols in Eq. (A.2) produces a sum of $N!$ terms, each term being comprised of the $N!$ different signed elementary products. The normalization $1/N!$ is included to account for this overcounting. Differentiating Eq. (A.2) with respect to a_{rs} yields an expression for the cofactors of the determinant

$$C_{rs} = \frac{\partial a}{\partial a_{rs}} = \frac{1}{(N-1)!} [r, i_2, \dots, i_N] [s, j_2, \dots, j_N] a_{i_2 j_2} \cdots a_{i_N j_N} \quad . \quad (\text{A.4})$$

Comparing Eq. (A.2) to Eq. (A.4) leads to

$$C_{rs} a_{ts} = C_{sr} a_{st} = a \delta_{rt} \quad (\text{A.5})$$

of which the familiar Laplace expression [74]

$$a = C_{rs} a_{rs} \quad , \quad (\text{A.6})$$

is a special case. These results can be combined to yield the well-known result

$$[\mathbf{A}^{-1}]_{rs} = \frac{1}{a} C_{sr} \quad (\text{A.7})$$

for the inverse of an $N \times N$ matrix in terms of the transpose of the matrix of cofactors [3]. Using Eq. (A.6) and Eq. (A.7), the formula for the variation of the determinant is

$$\delta a = C_{rs} \delta a_{rs} = a [\mathbf{A}^{-1}]_{sr} \delta a_{rs} \quad . \quad (\text{A.8})$$

A.2 Variations of the Metric

It is common, when performing variational principles in general relativity, to have to compute the variation of the determinant of the metric, denoted by g . To obtain the desired result, the substitutions $a_{rs} \rightarrow g_{\mu\nu}$ and $[\mathbf{A}^{-1}]_{sr} \rightarrow g^{\nu\mu}$ are used in Eq. (A.8) to yield

$$\delta g = g g^{\nu\mu} \delta g_{\mu\nu} = g g^{\mu\nu} \delta g_{\mu\nu} \quad , \quad (\text{A.9})$$

where, in the last equality, we used the fact that the metric and its inverse are symmetric matrices.

A.3 Variations of a Jacobian and Other Associated Derivatives

Consider a general mapping from the ‘old’ coordinates x^ν to the ‘new’ coordinates $q^{\tilde{\mu}}$ where the transformation is given by

$$q^{\tilde{\mu}} = q^{\tilde{\mu}}(x^\nu) \quad . \quad (\text{A.10})$$

The Jacobian of the map is defined to be the matrix of partial derivatives

$$\Lambda^{\tilde{\mu}}{}_{\nu} = \frac{\partial q^{\tilde{\mu}}}{\partial x^\nu} \quad . \quad (\text{A.11})$$

The determinant of this matrix

$$J \equiv \det \Lambda^{\tilde{\mu}}{}_{\nu} = \det \left[\frac{\partial q^{\tilde{\mu}}}{\partial x^\nu} \right] \equiv \det [q^{\tilde{\mu}}{}_{,\nu}] \quad (\text{A.12})$$

plays a fundamental role in the fluid dynamics variational principles discussed in the text. The variation of the Jacobian determinant can be expressed in terms of Eq. (A.8) as

$$\delta J = \frac{\partial J}{\partial \Lambda^{\tilde{\mu}}{}_{\nu}} = J_{\tilde{\mu}}{}^{\nu} \delta \Lambda^{\tilde{\mu}}{}_{\nu} \quad , \quad (\text{A.13})$$

where the cofactors $J_{\tilde{\mu}}{}^{\nu}$ are defined by

$$J_{\tilde{\mu}}{}^{\nu} \equiv \frac{1}{(N-1)!} [\tilde{\mu}, \tilde{\alpha}_2, \dots, \tilde{\alpha}_N] [\nu, \beta_2, \dots, \beta_N] q^{\tilde{\alpha}_2}{}_{,\beta_2} \dots q^{\tilde{\alpha}_N}{}_{,\beta_N} \quad . \quad (\text{A.14})$$

An important property of the cofactors of the Jacobian is

$$\frac{\partial}{\partial x^\nu} J_{\tilde{\mu}}{}^\nu = 0 \quad . \quad (\text{A.15})$$

This property can be seen since each term of the form

$$\frac{1}{(N-1)!} [\tilde{\mu}, \tilde{\alpha}_2, \dots, \tilde{\alpha}_N] [\nu, \beta_2, \dots, \beta_N] q^{\tilde{\alpha}_2}{}_{,\beta_2} \cdots q^{\tilde{\alpha}_m}{}_{,\beta_m \nu} \cdots q^{\tilde{\alpha}_N}{}_{,\beta_N} \quad (\text{A.16})$$

in Eq. (A.15) is a product between symmetric and antisymmetric arrays.

Other relations involving the determinant of the Jacobian arise when defining the concept of a tensor density. The presentation here of both the covariant and Lie derivatives of a tensor density follow closely the respective presentations in section 4.1 and 4.4 of [77]. To define a tensor density, consider the transformation of the metric between the ‘new’ and ‘old’ coordinates given by

$$g_{\tilde{\mu}\tilde{\nu}} = \Lambda_{\tilde{\mu}}{}^\alpha \Lambda_{\tilde{\nu}}{}^\beta g_{\alpha\beta} \quad . \quad (\text{A.17})$$

Taking the determinant of both sides yields

$$\tilde{g} = \bar{J}^2 g \quad , \quad (\text{A.18})$$

where the determinant of the inverse Jacobian of the mapping \bar{J} is defined as

$$\bar{J} \equiv \det \left(\frac{\partial x^\nu}{\partial q^{\tilde{\mu}}} \right) \quad . \quad (\text{A.19})$$

Equation Eq. (A.18) is the simplest example of a tensor density, in this case a scalar density, and the power of \bar{J} in Eq. (A.18) is called the weight. The determinant of the metric is said to be a scalar density of weight 2 and the more usual quantity $\sqrt{-g}$ is a scalar density of weight 1. Generalizing Eq. (A.18) to the determinant of an arbitrary tensor $t_{\alpha\beta}$ of weight w and taking the partial derivative with respect to $q^{\tilde{\alpha}}$ yields

$$\tilde{t}_{,\tilde{\alpha}} = w \bar{J}^{w-1} \frac{\partial \bar{J}}{\partial \Lambda_{\tilde{\mu}}{}^\nu} \frac{\partial \Lambda_{\tilde{\mu}}{}^\nu}{\partial q^{\tilde{\alpha}}} + \bar{J}^w \frac{\partial t}{\partial x^\beta} \frac{\partial x^\beta}{\partial q^{\tilde{\alpha}}} \quad . \quad (\text{A.20})$$

Again Eq. (A.8) can be used to rewrite the first term yielding the expression

$$\tilde{t}_{,\tilde{\alpha}} = w \bar{J}^w \Lambda_{\nu}{}^{\tilde{\mu}} \Lambda^{\tilde{\mu}}{}_{\nu,\tilde{\alpha}} + \bar{J}^w \frac{\partial t}{\partial x^\beta} \frac{\partial x^\beta}{\partial q^{\tilde{\alpha}}} \quad . \quad (\text{A.21})$$

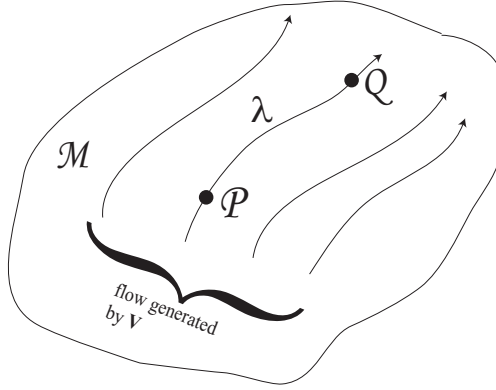


Figure A.1: Schematic representation of the flow on the manifold \mathcal{M} due to the vector field \vec{V} . The point \mathcal{P} is mapped downstream an amount λ to the point \mathcal{Q} .

Using the transformation equation for the connection coefficients (see *e.g.* equation 10.26 of [89])

$$\Gamma^{\tilde{\rho}}_{\tilde{\alpha}\tilde{\beta}} = \Lambda^{\mu}_{\tilde{\alpha}}\Lambda^{\nu}_{\tilde{\beta}}\Lambda^{\tilde{\rho}}_{\sigma}\Gamma^{\sigma}_{\mu\nu} + \frac{\partial\Lambda^{\nu}_{\tilde{\alpha}}}{\partial x^{\tilde{\tau}}}\Lambda^{\tilde{\rho}}_{\nu} \quad , \quad (\text{A.22})$$

the term involving the partial derivative of the Jacobian in Eq. (A.21) can be written as

$$\Lambda_{\nu}^{\tilde{\mu}}\Lambda_{\tilde{\mu},\tilde{\alpha}}^{\nu} = \Gamma^{\tilde{\rho}}_{\tilde{\rho}\tilde{\alpha}} - \Lambda^{\nu}_{\tilde{\alpha}}\Gamma^{\sigma}_{\sigma\nu} \quad . \quad (\text{A.23})$$

Combining leads to

$$(\tilde{t}_{,\tilde{\alpha}} - w\Gamma^{\tilde{\rho}}_{\tilde{\rho}\tilde{\alpha}}\tilde{t}) = \Lambda_{\tilde{\alpha}}^{\beta}\tilde{J}^w(t_{,\beta} - w\Gamma^{\sigma}_{\sigma\beta}t) \quad . \quad (\text{A.24})$$

Equation Eq. (A.24) is the transformation law for a rank $(0,1)$ tensor density of weight w and thus defines the covariant derivative of the scalar density of weight w to be

$$t_{;\beta} = t_{,\beta} - w\Gamma^{\sigma}_{\sigma\beta}t \quad . \quad (\text{A.25})$$

Arbitrary tensor densities are built by multiplying the desired absolute tensors by scalar densities of the appropriate weight.

Finally, the Lie derivative of a tensor density may be defined. Recall that if a manifold is equipped with a vector field then the action of this field can be interpreted as a mapping between those points in the manifold that lie on the same integral curve of \vec{V} (see *e.g.* [77]). Figure A.1 schematically shows this relationship.

Assuming that points \mathcal{P} and \mathcal{Q} are separated along a particular integral curve, then the Lie derivative of a tensor (or tensor density) can be defined symbolically as

$$\mathcal{L}_{\vec{V}}\mathbf{T} = \lim_{\lambda \rightarrow 0} \frac{(\mathbf{T}(\mathcal{Q}) - [\mathbf{T}(\mathcal{P})]_{\mathcal{Q}})}{\lambda} \quad , \quad (\text{A.26})$$

where $\mathbf{T}(\mathcal{Q})$ is the tensor evaluated at point \mathcal{Q} and $[\mathbf{T}(\mathcal{P})]_{\mathcal{Q}}$ is the same tensor, first evaluated at point \mathcal{P} , and then mapped downstream. Since the flow generated by \vec{V} is a diffeomorphism, the mapping downstream can be done for tensors of mixed ranks (see appendix C of [127] for more details). All that is now needed is to express Eq. (A.26) in terms of coordinates to derive the formulae in question. Consider, first the However, the general case of Eq. (A.26) is unwieldy, and following [77] only a (1, 1) tensor density will be examined, from which the general pattern can be inferred. In the equations that follow, all terms will be kept to first order in λ . To begin, assume that the mapping mediated by \vec{V} has the form

$$\tilde{x}^\mu = x^\mu + \lambda V^\mu(x) \quad . \quad (\text{A.27})$$

The Jacobian of this mapping is given by

$$\Lambda^{\tilde{\mu}}{}_{\nu} \equiv \frac{\partial \tilde{x}^\mu}{\partial x^\nu} = \delta_\mu{}^\nu + \lambda V^\mu{}_{,\nu} \quad . \quad (\text{A.28})$$

The inverse Jacobian of this mapping is given by

$$\Lambda_{\tilde{\nu}}{}^{\beta} = \delta_{\nu}{}^{\beta} - \lambda V^{\beta}{}_{,\nu} \quad , \quad (\text{A.29})$$

and the corresponding determinant is

$$\bar{J} \simeq 1 - \lambda V^{\sigma}{}_{,\sigma} \quad . \quad (\text{A.30})$$

Now consider the (1, 1) tensor density $\mathcal{T}^\mu{}_{\nu}$ which transforms as

$$\mathcal{T}^{\tilde{\mu}}{}_{\tilde{\nu}} = \bar{J}^w \Lambda^{\tilde{\mu}}{}_{\alpha} \Lambda_{\tilde{\nu}}{}^{\beta} \mathcal{T}^{\alpha}{}_{\beta} \quad . \quad (\text{A.31})$$

The value of the tensor at downstream point \mathcal{Q} is given by

$$\begin{aligned} \mathbf{T}(\mathcal{Q}) &= \mathcal{T}^{\tilde{\mu}}{}_{\tilde{\nu}}(x^\sigma + \lambda V^\sigma) \\ &= \mathcal{T}^{\tilde{\mu}}{}_{\tilde{\nu}}(x^\sigma) + \lambda \mathcal{T}^{\tilde{\mu}}{}_{\tilde{\nu},\sigma} V^\sigma \quad . \end{aligned} \quad (\text{A.32})$$

Likewise, the value of the tensor at the upstream point which is mapped downstream is

$$\begin{aligned}
[\mathbf{T}(\mathcal{P})]_{\mathcal{Q}} &= (1 - w\lambda V^{\sigma}_{,\sigma}) (\delta^{\mu}_{\alpha} + \lambda V^{\mu}_{,\alpha}) (\delta^{\beta}_{\nu} - \lambda V^{\beta}_{,\nu}) \mathcal{T}^{\alpha}_{\beta} \\
&= \mathcal{T}^{\mu}_{\nu} - \lambda \mathcal{T}^{\mu}_{\beta} V^{\beta}_{,\nu} + \lambda \mathcal{T}^{\alpha}_{\nu} V^{\nu}_{,\alpha} - w\lambda \mathcal{T}^{\mu}_{\nu} V^{\sigma}_{,\sigma} \quad , \quad (\text{A.33})
\end{aligned}$$

where every term on the right-hand side takes the argument x^{σ} . Combining these expressions in Eq. (A.26) and noting, in the limit as $\lambda \rightarrow 0$, that $\tilde{x}^{\sigma} \rightarrow x^{\sigma}$, leads to the desired relation

$$\mathcal{L}_{\vec{V}} \mathcal{T}^{\mu}_{\nu} = \mathcal{T}^{\mu}_{\nu,\sigma} V^{\sigma} + \mathcal{T}^{\mu}_{\beta} V^{\beta}_{,\nu} - \mathcal{T}^{\alpha}_{\nu} V^{\mu}_{,\alpha} + w \mathcal{T}^{\mu}_{\nu} V^{\sigma}_{,\sigma} \quad , \quad (\text{A.34})$$

and the obvious generalizations to higher rank tensors.

Bibliography

- [1] Peter Anninos, Joan Masso, Edward Seidel, Wai-Mo Suen, and Malcolm Tobias, *The near-linear regime of gravitational waves in numerical relativity*, Physical Review D **54** (1996), 6544–6547.
- [2] ———, *Dynamics of gravitational waves in 3d: Formulations, methods, and tests*, Physical Review D **56** (1997), 842–858.
- [3] Howard Anton, *Elementary linear algebra*, John Wiley & Sons, New York, 1984.
- [4] George Arfken, *Mathematical methods for physicists, third edition*, Academic Press, Inc., Orlando, 1985.
- [5] R. Arnowitt, S. Deser, and C Misner, *The dynamics of general relativity*, Gravitation: An Introduction to Current Research (L. Witten, ed.), John Wiley, 1962, pp. p 227–265.
- [6] Barry C. Barish, *First generation interferometers*, Astrophysical Sources for Ground-Base Gravitational Wave Detectors, Philadelphia, Pennsylvania 30 October - 1 November, 2000 (Joan M. Centrella, ed.), American Institute of Physics, 2001, p. 38060.
- [7] Roger R. Bate, Donald D. Mueller, and Jerry E. White, *Fundamentals of astrodynamics*, Dover Publications, Inc., New York, 1971.
- [8] Thomas W. Baumgarte and Stuart L. Shapiro, *Numerical integration of einstein's field equations*, Physical Review D **59** (1998), 024007.

- [9] T. Belytschko, Y. Krongauz, D. Organ, M. Fleming, and P. Krysl, *Meshless methods: An overview and recent developments*, Comput. Methods Appl. Mech. Engrg. **139** (1996), 3–47.
- [10] W. Benz, *Smooth particle hydrodynamics: A review*, Numerical Modeling in Stellar Pulsation: Problems and Prospects (J. Buchler, ed.), Dordrecht:Kluwer, 1990.
- [11] W. Benz and J. G. Hills, *Three-dimensional hydrodynamical simulations of stellar collisions. i. equal-mass main sequence stars*, The Astrophysical Journal **323** (1987), 614–628.
- [12] Willy Benz, *Applications of smooth particle hydrodynamics (sph) to astrophysical problems*, Computer Physics Communications **48** (1988), 97–105.
- [13] E. Berti, J. A. Pons, G. Miniutti, L. Gualtieri, and V. Ferrari, *Are post-newtonian templates faithful and effectual in detecting gravitational signals from neutron star binaries?*, Physical Review D **66** (2002), 064013.
- [14] G. Bertin and G. Lodato, *A class of self-gravitating accretion disks*, Astron. Astrophys. **350** (1999), 694–704.
- [15] G. V. Bicknell, *The equations of motion of particles in smoothed particle hydrodynamics*, SIAM J. Sci. Stat. Comput. **5** (1991), 1198–1206.
- [16] Nigel T. Bishop, Roberto Gomez, Sascha Husa, Luis Lehner, and Jeffrey Winicour, *A numerical relativistic model of a massive particle in orbit near a schwarzschild black hole*, Physical Review D **68** (2003), 084015.
- [17] Luc Blanchet, *Energy losses by gravitational radiation in inspiralling compact binaries to five halves post-newtonian order*, Physical Review D **54** (1996), 1417–1438.
- [18] ———, *Gravitational radiation reaction and balance equations to post-newtonian order*, Physical Review D **55** (1997), 714–732.

- [19] ———, *Gravitational radiation from post-newtonian sources and inspiralling compact binaries*, Living Rev. Relativity **5** (2002), [Online article]: cited on 3 Dec. 2004, <http://www.livingreviews.org/lrr-2002-3>.
- [20] ———, *Post-newtonian theory and its application*, gr-qc/0304014 (2003).
- [21] Luc Blanchet, Thibault Damour, and Bala R. Iyer, *Gravitational waves from inspiralling compact binaries: Energy loss and waveform to second post-newtonian order*, Physical Review D **51** (1995), 5360–5386.
- [22] Luc Blanchet, Thibault Damour, Bala R. Iyer, Clifford M. Will, and Alan G. Wiseman, *Gravitational-radiation damping of compact binary systems to second post-newtonian order*, Physical Review Letters **74** (1995), 3515–3518.
- [23] Luc Blanchet and Guillaume Faye, *On the equations of motion of point-particle binaries at the third post-newtonian order*, Physics Letters **58** (2000), A217.
- [24] Luc Blanchet, Guillaume Faye, Bala R. Iyer, and Benoit Joguet, *Gravitational-wave inspiral of compact binary systems to $7/2$ post-newtonian order*, Physical Review D **65** (2002), 061501.
- [25] Luc Blanchet, Guillaume Faye, and Benedicte Ponsot, *Gravitational field and equations of motion of compact binaries to $5/2$ post-newtonian order*, Physical Review D **58** (1998), 124002.
- [26] Luc Blanchet, Bala R. Iyer, Clifford M. Will, and Alan G. Wiseman, *Gravitational waveforms from inspiralling compact binaries to second post-newtonian order*, Classical and Quantum Gravity **13** (1996), 575–584.
- [27] Patrick R. Brady, D. E. Creighton, and Kip S. Thorne, *Computing the merger of black-hole binaries: the ibbh problem*, Physical Review D **61501** (1998).
- [28] Bernd Bruggmann, *Numerical relativity in 3+1 dimensions*, Annalen Phys. **9** (2000), 227–246.

- [29] H. A. Buchdahl, *Seventeen simple lectures on general relativity theory*, John Wiley & Sons, New York, 1981.
- [30] Herbert B. Callen, *Thermodynamics and an introduction to thermostatistics*, John Wiley & Sons, New York, 1985.
- [31] S. Chandrasekhar, *The post-newtonian equations of hydrodynamics in general relativity*, *Astrophysical Journal* **142** (1965), 1488–1513.
- [32] ———, *Conservation laws in general relativity and in the post-newtonian approximations*, *Astrophysical Journal* **158** (1969), 45–53.
- [33] S. Chandrasekhar and Donna D. Elbert, *The deformed figures of the dedekind ellipsoids in the post-newtonian approximation to general relativity*, *Astrophysical Journal* **192** (1974), 731–746.
- [34] S. Chandrasekhar and F. Paul Esposito, *The 2-1/2 post-newtonian equations of hydrodynamics and radiation reaction in general relativity*, *Astrophysical Journal* **160** (1970), 153–179.
- [35] S. Chandrasekhar and Yavuz Nutku, *The second post-newtonian equations of hydrodynamics in general relativity*, *Astrophysical Journal* **158** (1969), 55–79.
- [36] E. Chow and J. J. Monaghan, *Ultrarelativistic sph*, *Journal of Computational Physics* **134** (1997), 296–305.
- [37] Curt Cutler and Eanna E. Flanagan, *Gravitational waves from merging compact binaries: How accurately can one extract the binary’s parameters from the inspiral waveform?*, *Physical Review D* **49** (1994), 2658–2697.
- [38] Thibault Damour, Bala R. Iyer, Piotr Jaranowski, and B.S. Sathyaprakash, *Gravitational waves from black hole binary inspiral and merger: The span of third post-newtonian effective-one-body templates*, *Physical Review D* **67** (2003), 064028.

- [39] Thibault Damour, Bala R. Iyer, and B. S. Sathyaprakash, *Improved filters for gravitational waves from inspiraling compact binaries*, Physical Review D **57** (1998), 885–907.
- [40] Serge Droz, *Gravitational waves from inspiraling compact binaries: Second post-newtonian waveforms as search templates. ii*, Physical Review D **59** (1999), 064030.
- [41] Mark R. Dubal, *A particle-grid method for general relativistic hydrodynamics: I. formalism and test applications*, Class. Quantum Grav. **8** (1991), 453–475.
- [42] Albert Einstein, *Der feldgleichungen der gravitation*, Sitzungsberichte der Deutschen Akademie der Wissenschaften zu Berlin, Klasse für Mathematik, Physik, and Technik (1915), 844.
- [43] August E. Evrard, *Beyond n-body: 3d cosmological gas dynamics*, Mon. Not. R. astr. Soc. **235** (1988), 911–934.
- [44] O. Flebbe, S. Munzel, H. Herold, H. Riffert, and H. Ruder, *Smoothed particle hydrodynamics: Physical viscosity and the simulation of accretion disks*, The Astrophysical Journal **431** (1994), 754–760.
- [45] Peter Fritschel, *Second generation instruments for the laser interferometer gravitational wave observatory (ligo)*, Proceedings of the SPIE conference on Astronomical Telescopes and Instrumentations, 22–28 Aug 2002, Waikoloa, HI, USA (Mike Cruise and Peter Saulson, eds.), SPIE, 2003, pp. 282–291.
- [46] David A. Fulk and Dennis W. Quinn, *An analysis of 1-d smoothed particle hydrodynamics kernels*, Journal of Computational Physics **126** (1996), 165–180.
- [47] Jonathan R. Gair, Leor Barack, Teviet Creighton, Curt Cutler, Shane L. Larson, E. Ster Phinney, and Michele Vallisneri, *Event rate estimates for lisa extreme mass ratio capture sources*, Classical and Quantum Gravity **21** (2004), S1595–S1606.

- [48] GEO600, <http://www.geo600.uni-hannover.de>, 2004.
- [49] R. A. Gingold and J. J. Monaghan, *Smoothed particle hydrodynamics: Theory and application to non-spherical stars*, Mon. Not. R. astr. Soc. **181** (1977), 375–389.
- [50] ———, *Kernel estimates as a basis for general particle methods in hydrodynamics*, Journal of Computational Physics **46** (1982), 429–453.
- [51] Harvey Gould and Jan Tobochnik, *An introduction to computer simulation methods, applications to physical systems part 2*, Addison-Wesley, Reading, Massachusetts, 1988.
- [52] David Halliday and Robert Resnick, *Physics*, John Wiley & Sons, New York, 1978.
- [53] William O. Hamilton, *Resonant detectors of gravitational radiation*, Astrophysical Sources for Ground-Base Gravitational Wave Detectors, Philadelphia, Pennsylvania 30 October - 1 November, 2000 (Joan M. Centrella, ed.), American Institute of Physics, 2001, pp. 24–35.
- [54] F. H. Harlow, *Hydrodynamic problems involving large fluid distortions*, J. Assoc. Comput. Mach. **4** (1957), 137.
- [55] ———, *Pic and its progeny*, Computer Physics Communications **48** (1988), 1–10.
- [56] J. F. Hawley, L. L. Smarr, and J. R. Wilson, *Something hydro gr*, Astrophysical Journal **70** (1984), 419–443.
- [57] Edwin A. C. Henneken and Vincent Icke, *Sph faces emery's jump*, Computer Physics Communications **74** (1993), 239–246.
- [58] Lars Hernquist, *Some cautionary remarks about smoothed particle hydrodynamics*, The Astrophysical Journal **404** (1993), 717–722.

- [59] Lars Hernquist and Neal Katz, *Treesph: A unification of sph with the hierarchical tree method*, The Astrophysical Journal Supplement Series **70** (1989), 419–446.
- [60] William F. Hughes and John A. Brighton, *Schaum's outline of theory and problems of fluid dynamics*, McGraw-Hill, New York, 1967.
- [61] R. A. Hulse and J. H. Taylor, *A high sensitivity pulsar survey*, Astrophysical Journal **191** (1974), L59.
- [62] ———, *A deep sample of new pulsars and their spatial extent in the galaxy*, Astrophysical Journal **201** (1975), L55.
- [63] ———, *Discovery of a pulsar in a binary system*, Astrophysical Journal **195** (1975), L51.
- [64] James Isenberg and James Nester, *Canonical gravity*, General Relativity and Gravitation (A. Held, ed.), Plenum Press, 1980, pp. p 23–97.
- [65] Malvin H. Kalos and Paula A. Whitlock, *Monte carlo methods, volume 1: Basics*, John Wiley & Sons, New York, 1996.
- [66] Arkady Kheifets, Warner A. Miller, and Wojciech H. Zurek, *Covariant smoothed particle hydrodynamics on a curved background*, Physical Review D **41** (1990), 451–454.
- [67] A. M. Knapp, E. J. Walker, and T. W. Baumgarte, *Illustrating stability properties of numerical relativity in electrodynamics*, Physical Review D **65** (2002), 064031.
- [68] Steven E. Koonin, *Computational physics*, Addison-Wesley, Redwood City, California, 1986.
- [69] Pablo Laguna, Warner A. Miller, and Wojciech H. Zurek, *Smoothed particle hydrodynamics near a black hole*, The Astrophysical Journal **404** (1993), 678–685.

- [70] Pablo Laguna and Deirdre Shoemaker, *Numerical stability of a new conformal-traceless 3+1 formulation of the einstein equations*, *Class. Quantum Grav.* **19** (2002), 3679–3686.
- [71] Luis Lehner, *Numerical relativity: a review*, *Class. Quantum Grav.* **18** (2001), R25–R86.
- [72] Alan P. Lightman, William H. Press, Richard H. Price, and Saul A. Teukolsky, *Problem book in relativity and gravitation*, Princeton University Press, Princeton, New Jersey, 1975.
- [73] LIGO, <http://www.ligo.caltech.edu>, 2004.
- [74] Seymour Lipschutz and Marc Lipson, *Schaum's outline of linear algebra*, McGraw-Hill Trade, New York, 2000.
- [75] LISA, <http://lisa.jpl.nasa.gov>, 2004.
- [76] J. Alberto Lobo, *Lisa*, gr-qc/0404079 (2004).
- [77] David Lovelock and Hanno Rund, *Tensors, differential forms, and variational principles*, Dover Publications, Inc., New York, 1989.
- [78] L. Lucy, *A numerical approach to the testing of the fission hypothesis*, *The Astrophysical Journal* **82** (1977), 1013.
- [79] A. G. Lyne, M. Burgay, M. Kramer, A. Possenti, R. N. Manchester, F. Camilo, M. A. McLaughlin, D. R. Lorimer, N. D'Amic, B. C. Joshi, J. Reynolds, and P. C. C. Freire, *A double-pulsar system: A rare laboratory for relativistic gravity and plasma physics*, *Science* **303** (2004), 1153–1157.
- [80] Patrick J. Mann, *A relativistic smoothed particle hydrodynamics method tested with the shock tube*, *Computer Physics Communications* **67** (1991), 245–260.
- [81] Maplesoft, <http://www.maplesoft.com>, 2004.

- [82] Karl Martel, *Gravitational waveforms from a point particle orbiting a schwarzschild black hole*, Physical Review D **69** (2004), 44025.
- [83] Karl Martel and Eric Poisson, *Regular coordinate systems for schwarzschild and other spherical spacetimes*, Am. J. Phys. **69** (2001), 476–480.
- [84] mathsoft, <http://www.mathcad.com>, 2004.
- [85] MathWorks, <http://www.mathworks.com>, 2004.
- [86] Stephen L. W. McMillan and Simon F. Portegies Zwart, *Black hole binaries from star clusters*, Astrophysical Sources for Ground-Base Gravitational Wave Detectors, Philadelphia, Pennsylvania 30 October - 1 November, 2000 (Joan M. Centrella, ed.), American Institute of Physics, 2001, pp. 119–129.
- [87] C. W. Misner, *Smoother smoothing kernels*, unpublished, Dec. 1996.
- [88] ———, *Variational principle for lagrangian hydrodynamics*, Proceedings of the Second International A. D. Sakharov Conference of Physics 1996 (I. M. Dremin and A. M. Semikhatov, eds.), World Scientific, 1997, pp. 288–293.
- [89] Charles W. Misner, Kip S. Thorne, and John Archibald Wheeler, *Gravitation*, W.H. Freeman and Company, New York, 1973.
- [90] L. Mittag, M. J. Stephen, and W. Yourgrau, *Variational principles in hydrodynamics*, Variational Principles in Dynamics and Quantum Theory (W. Yourgrau and S. Mandelstam, eds.), Dover Publications, 1979, pp. p 142–161.
- [91] J. J. Monaghan, *Why particle methods work*, SIAM J. Sci. Stat. Comput. **3** (1982), 422–433.
- [92] ———, *Particle methods for hydrodynamics*, Computer Physics Reports **3** (1985), 71–1224.
- [93] ———, *An introduction to sph*, Computer Physics Communications **48** (1988), 89–96.

- [94] ———, *On the problem of penetration in particle methods*, Journal of Computational Physics **82** (1989), 1–15.
- [95] J. J. Monaghan and R. A. Gingold, *Shock simulation by the particle method sph*, Journal of Computational Physics **52** (1983), 374–389.
- [96] J. J. Monaghan and D. J. Price, *Variational principles for relativistic smoothed particle hydrodynamics*, Mon. Not. R. astr. Soc. **328** (2001), 381–392.
- [97] J.J. Monaghan and N. K. Lahy, *A particle method for numerical relativistic fluid dynamics*, 5th Marcel Grossman Meeting on General Relativity, Perth 1988 (D. G. Blair and M. J. Buckingham, eds.), World Scientific, 1989, pp. 1179–1183.
- [98] P. Musgrave, D. Pollney, and K Lake, GRTensorII, 1994.
- [99] Nascatech, <http://www.nascatech.com>, 2004.
- [100] Richard P. Nelson and John C. B. Papaloizou, *Three-dimensional hydrodynamic simulations of collapsing prolate clouds*, Mon. Not. R. astr. Soc. **265** (1993), 905–920.
- [101] ———, *Variable smoothing lengths and energy conservation in smoothed particle hydrodynamics*, Mon. Not. R. astr. Soc. **270** (1994), 1–20.
- [102] Michael Pati and Clifford M. Will, *Post-newtonian gravitational radiation and equations of motion via direct integration of the relaxed einstein equations. i. foundations*, Physical Review D **62** (2000), 124015.
- [103] ———, *Post-newtonian gravitational radiation and equations of motion via direct integration of the relaxed einstein equations. i. two-body equations of motion to second post-newtonian order, and radiation-reaction to 3.5 post-newtonian order*, Physical Review D **65** (2002), 104008.
- [104] P. C. Peters, *Gravitational radiation and the motion of two point masses*, Physical Review **136** (1964), B1224–B1232.

- [105] P. C. Peters and J. Mathew, *Gravitational radiation from point masses in keplerian orbits*, Physical Review **131** (1963), 435–440.
- [106] Eric Poisson, *Gravitational radiation from a particle in circular orbit around a black hole. i. analytical results for the nonrotating case.*, Physical Review D **47** (1993), 1497–1510.
- [107] ———, *A relativist’s toolkit: The mathematics of black-hole mechanics*, Cambridge University Press, Cambridge, 2004.
- [108] William H Press, Saul A. Teukolsky, William T. Vetterling, and Brian P. Flannery, *Numerical recipes in c, the art of scientific computing, second edition*, Cambridge University Press, Cambridge, 1992.
- [109] Dina Prialnik, *Stellar structure and evolution*, Cambridge University Press, Cambridge, 2000.
- [110] Bernard F. Schutz, *A first course in general relativity*, Cambridge University Press, Cambridge, 1985.
- [111] Karl Schwarzschild, *Über das gravitationsfeld eines massenpunktes nach der einstein-schen theorie*, Sitzungsberichte der Deutschen Akademie der Wissenschaften zu Berlin, Klasse für Mathematik, Physik, and Technik (1916), 189–196.
- [112] Edward Seidel, *Black hole coalescence and mergers: Review, status, and “where are we heading?”*, Progress of Theoretical Physics Supplement **136** (199), 87–105.
- [113] ———, *Numerical relativity and black-hole collisions*, Relativity and Scientific Computing (F. Hehl, ed.), Springer-Verlag, 1996, pp. p 25–68.
- [114] Edward Seidel and Wai-Mo Suen, *Numerical relativity as a tool for computational astrophysics*, Journal of Computational and Applied Mathematics **109** (1999), 493–525.

- [115] Liliana E. Simone, Stephen W. Leonard, Eric Poisson, and Clifford M. Will, *Gravitational waves from binary systems in circular orbits: Does the post-newtonian expansion converge?*, *Classical and Quantum Gravity* **14** (1997), 237–256.
- [116] James C. Simpson, *Numerical techniques for three-dimensional smoothed particle hydrodynamics simulations: Applications to accretion disks*, *The Astrophysical Journal* **48** (1995), 822–831.
- [117] L. Smarr and J. York, *Kinematical conditions in the construction of spacetime*, *Physical Review D* **17** (1978), 2529–2534.
- [118] Scott C. Smith, Janet L. Houser, and Joan Centrella, *Simulations of nonaxisymmetric instability in a rotating star: A comparison between eulerian and smooth particle hydrodynamics*, *The Astrophysical Journal* **458** (1996), 236–256.
- [119] Keith Symon, *Mechanics, third edition*, Addison-Wesley, Reading, Massachusetts, 1971.
- [120] TAMA, <http://tamago.mtk.nao.ac.jp>, 2004.
- [121] J. H. Taylor and J. M. Weisberg, *A new test of general relativity: Gravitational radiation and the binary pulsar psr 1913+16*, *Astrophysical Journal* **253** (1982), 908–920.
- [122] Kip S. Thorne, *Numerical relativity for inspiraling binaries in co-rotating coordinates: Test bed for lapse and shift equations*, gr-qc/9808024 (1998).
- [123] John P. Vinti, Gim J. Der, and Nino L. Bonavito, *Orbital and celestial mechanics*, American Institute of Aeronautics and Astronautics, New York, 1998.
- [124] VIRGO, <http://www.virgo.infn.it>, 2004.
- [125] Robert V. Wagoner and Clifford M. Will, *Post-newtonian gravitational radiation from orbiting point masses*, *Astrophysical Journal* **210** (1976), 764–775.

- [126] L. A. Wainstein and V. D. Zubakov, *Extraction of signals from noise*, Prentice-Hall, Englewood Cliffs, New Jersey, 1962.
- [127] Robert M. Wald, *General relativity*, The University of Chicago Press, Chicago, 1984.
- [128] A. P. Whitworth, A. S. Bhattal, J. A. Turner, and S. J. Watkins, *Estimating density in smoothed particle hydrodynamics*, *Astron. Astrophys.* **301** (1995), 929–932.
- [129] Clifford M. Will, *Gravitational waves from inspiralling compact binaries: A post-newtonian approach*, gr-qc/9403033 (1994).
- [130] ———, *Generation of post-newtonian gravitational radiation via direct integration of the relaxed einstein equations*, *Progress of Theoretical Physics Supplement* **136** (1999), 158–167.
- [131] Clifford M. Will and Alan G. Wiseman, *Gravitational radiation from compact binary systems: Gravitational waveforms and energy loss to second post-newtonian order*, *Physical Review D* **54** (1996), 4813–4848.
- [132] Hwei-Jang Yo, Thomas W. Baumgarter, and Stuart L. Shapiro, *Improved numerical stability of stationary black hole evolution calculations*, *Physical Review D* **66** (2002), 084026.
- [133] J. W. York, *Kinematics and dynamics of general relativity*, *Sources of Gravitational Radiation* (L. L. Smarr, ed.), Cambridge University Press, 1979, pp. 83–126.

Vita

After a past that paradoxically remains enshrouded in mystery, we join Mr. Schiff as a high school student taking physics classes at the University of Pittsburgh. It was during this experience that he developed a love for mechanics, gravity, and space. However, upon entering Pennsylvania State University, he became involved in condensed matter research and vacuum physics. Graduating with honors in Physics with a minor Mathematics, he entered into the graduate studies at Carnegie Mellon University. During his time there, Mr. Schiff worked on the theoretical models of first- and second-order phase transitions under the guidance of Prof. Robert Swendsen. It was during this period that his profound love of dynamics, space, and general relativity re-awakened.

In July of 1990, Mr. Schiff withdrew from graduate studies and began work with Computer Sciences Corporation in Greenbelt MD. His work centered on the development of new technology and algorithms to support the International Space and Terrestrial Physics (ISTP) program, which included the WIND, POLAR, and SOHO spacecraft. In particular, he began study of the dynamics of the circular and elliptical restricted three-body problems and their applications to double-lunar swingby and libration point orbits. This work would subsequently be applied to the WIND, SOHO, and ACE missions - in the latter of which he was the lead mission analyst and trajectory designer. In 1992, Mr. Schiff became part of the trajectory design team for the Clementine mission, which was sponsored and developed by the Naval Research Laboratory. In 1994, after only 16 months, the Clementine spacecraft lifted off from Vandenberg Air Force base and became the first mission, since Apollo, to return to the Moon.

After the completion of Clementine mission, Mr. Schiff enrolled in graduate study in Physics at the University of Maryland Physics. From January 1996 to February 1997, he was employed as a graduate student research assistant to Prof. Ted Einstein studying the nonequilibrium growth during molecular beam epitaxy of face-centered cubic metals. After two years as a full-time student, Mr. Schiff was forced to return to CSC and become a part-time student. In 1997 he began his present work with Prof. Misner. That year also saw the completion of his participation in the ACE mission as he oversaw the launch and early orbit operations that sent the spacecraft into a small-amplitude Lissajous about the Sun-Earth/Moon L_1 Lagrange point.

In 1998, Mr. Schiff left CSC to take a position at a.i. solutions, Inc. The intervening years saw slow but steady progress often put on hold while Mr. Schiff attended to various NASA missions. Chief amongst these was the Microwave Anisotropy Probe. Brought onto MAP in fall of 1999, Mr. Schiff was tasked with bringing a wayward mission back on course. This activity consumed almost every moment of the next two and a half years.

Currently, Mr. Schiff holds the positions of Chief Scientist and Director of Emerging Markets at a.i. solutions, Inc., a small-business aerospace company with corporate offices in Lanham, MD and offices at Goddard Space Flight Center and Kennedy Space Center. His research interests include gravity, general relativity, dynamics and optimal control, differential geometry and the restricted three-body problem, and scientific computing and visualization. After completion of his doctoral degree, he would like to continue the exploration of general relativity and gravity.

Highlights of Professional Experience

- Mission design and analysis lead and technical consultant for the James Webb Space Telescope (JWST).
- Technical lead for the Global Precipitation Measurement (GPM) Mission and lead designer and developer of the constellation coverage tool (Indra/COV).
- Microwave Anisotropy Probe (MAP) Trajectory Design and Mission Analysis Lead. Led trajectory work on the MAP mission involving a phasing-loop gravity

assist transfer to a Lissajous orbit about the L2 Sun-Earth Lagrange point. Developed algorithms for producing new launch blocks and analyzing the stability of the resulting solutions. Implemented a fuel-minimized Monte Carlo analysis of the impact of launch vehicle dispersions.

- Magnetospheric MultiScale (MMS) Mission Analysis Lead. Developed multi-parameter analysis to balance science requirements and eclipse duration constraints, inter-spacecraft ranging and communication, and formation-flying initialization and control in highly elliptical HEOs and lunar gravity assists.

- Project Lead on ACE Mission Design Designed the 3-impulse transfer trajectory from low-Earth parking orbit to Lissajous orbit. Determined optimal Lissajous orbit parameters and designed the Lissajous insertion maneuver. Analyzed coupling between orbit and attitude dynamics during the maneuver execution.

- Clementine I Mission Design lead for the encounter with the asteroid Geographos and on maneuver error analysis and recovery/redesign strategies.

- Technical consultant on solving the sun-glint interference problem on the Calipso mission via pixel modeling of sensor footprints.

- Technical consultant on fault resolution for the Aqua mission.

- Technical lead on the analysis, testing and verification of the FreeFlyer Orbit Determination system met for use on the Aura mission.

- Conceived and championed the design and development of the Constellation Coordination System (CCS) for use with the ESO PM-train.

- Led research and development into optimal methods for determining spacecraft trajectories using Primer Vector theory and the Howell-Pernicka two-level method.

- Research participant into Adaptive Kalman Filter/Neural Network technology for use in orbit determination.

- Lead designer of the engine component of the GSFC Swingby program. Engine development included mathematical models of spacecraft orbital dynamics and orbital force modeling, attitude descriptions, impulsive and finite maneuver modeling, targeting and optimization, and deep-space mission design techniques involving double lunar swingby cycles, lunar back flips, halo and Lissajous orbits.

Awards

- GSFC Customer Service Excellence Award for MAP Monte Carlo Development and Analysis
- GSFC Customer Service Excellence Award for MAP Trajectory Design
- Team Technical Excellence Award for support of the Clementine Mission
- President's Excellence Award for support of Clementine Mission

Selected Publications

- D. Rand, C. Schiff, and J. Reilly, "Operational Experiences in Planning and Reconstructing Aqua Inclination Maneuvers", ISSFD 2004 Munich Germany Oct 11-15
- L. H. Mailhe, C. Schiff, and J.L. Stadler, "Calipso's Mission Design: Sun-Glint Avoidance Strategies", AAS 04-114, 14th AAS/AIAA Space Flight Mechanics Meeting February 8-12, 2004, Maui, Hawaii
- L. Mailhe, C. Schiff, and D. Folta, "Initialization of Formation Flying using Primer Vector Theory", International Symposium on Formation Flying Missions and Technologies, 29-31 October 2002, Centre National d'Etudes Spatiales Toulouse Space Centre - France
- D. Rohrbaugh and C. Schiff, "Stationkeeping Approach for the Microwave Anisotropy Probe (MAP)", AIAA-2002-4429, AIAA/AAS Astrodynamics Specialist Conference, August 5-8, 2002, Monterey, California
- T. Tran and C. Schiff, "Implementation of an Object-Oriented Design for Orbit Determination Using FreeFlyer", 2002 Core Technologies for Space Systems Conference Nov. 19-21, Colorado Springs, Colorado
- J.J. Guzman and C. Schiff, "A Preliminary Study for a Tetrahedron Formation: Quality Factors and Visualization",
- A. Ederly and C. Schiff, "The Double Lunar Swingby of the MMS Mission", 2001 FMET Symposium Goddard Space Flight Center

- C. Schiff and L. Mailhe, “Indra/COV: A New Tool for Optimization of Constellations Coverage Statistics”, 16th International Symposium on Space Flight Dynamics, 3-7 December 2001, Pasadena, California.
- L. Mailhe, C. Schiff, and S. Hughes, “Formation Flying in Highly Elliptical Orbits: Initializing the Formation”, CNES International Symposium on Space Dynamics, Biarritz, France, June 26-30, 2000
- C. Schiff, D. Rohrbaugh, and J. Bristow, “Formation Flying in Elliptical Orbits”, 2000 IEEE Aerospace Conference, Big Sky Montana, April 18-25, 2000, paper 317
- C. Schiff, S. Good, and D. Rohrbaugh, “Risk Mitigation Using Monte Carlo”, AAS/AIAA Space Flight Mechanics Meeting, Clearwater, Florida 23-26 January 2000
- J. Carrico and C. Schiff, “Mission Analysis and Design Tool (Swingby): Mathematical Principles”, NASA Technical Document